Process design and simulation of gasification and Fischer-Tropsch process for biofuels production from lignocellulosic biomass

Master's Thesis

Matevz Mencigar

Aalborg University Esbjerg
Department of Chemical Engineering
June 2020

Department of Chemical Engineering

Aalborg university

https://www.en.aau.dk/

Title:	Process design and simulation of gasification and Fischer-Tropsch process for biofuels production from lignocellulosic biomass
Theme:	Process simulation
Project Period:	Spring Semester 2020
Project Group:	K10-K-10-F20
Author:	Matevž Mencigar
Supervisor:	Ben-Guang Rong
Page Numbers:	94
Date of hand in:	June 4, 2020

Abstract

The simulation and evaluation of several biomass-to-liquid processes using gasification and Fischer-Tropsch (FT) synthesis was conducted using Aspen Plus. Three different process were simulated based on different conditions of FT synthesis. High temperature and low temperature FT synthesis was included. Two low temperature FT synthesis based process were conducted, one using Fe-based catalyst, the other using a Co-based catalyst. Due to different FT product distributions, different final product profiles were obtained. The processes focused on diesel and gasoline like biofuels as well as methane production. Thereafter, the processes were economically evaluated and compared. Based on the results, low temperature FT synthesis using a Co-based catalyst was the most optimal one. Lastly, optimisation and design of two main processing units, the main distillation column and the fractional distillation column were performed for the Co-based catalyst low temperature FT synthesis case in order to optimise its performance. As a result, the equipment cost for the process was reduced by a total of 175.000 $.

Preface

This thesis is a result of a project carried out in the 10th semester as a part of a Master's course in chemical engineering. A big part of the project was in the comparison between the different cases. The results came as a surprise since a very high profit was obtained.

I would like to extend my thanks to my supervisor Ben-Guang Rong for taking his time for meetings whenever asked of him and for the guidance throughout the project.

Matevž Mencigar,

Aalborg University, June 4, 2020

Table of Contents

1 Introduction....3

2 Problem formulation....4

3 Process synthesis and conceptual design....5

3.1 Process overview....5

3.1.1 Lignocellulosic biomass sources....5

3.1.2 Processing of lignocellulosic biomass....6

3.1.3 Gasification and Fischer – Tropsch pathway....8

3.2 Feedstock selection and analysis....11

3.3 Thermochemical conversion....12

3.3.1 Gasification....12

3.3.2 Raw syngas clean up....19

3.3.3 Raw syngas conditioning....33

3.4 Upgrading to liquid transportation fuel....34

3.4.1 Fischer – Tropsch synthesis....34

3.4.2 Upgrading of FT products....38

3.5 Separation technologies....41

4 Process simulation....45

4.1 Co-LTFT simulation case....47

4.2 Fe-LTFT simulation case....57

4.3 HTFT simulation case....62

5 Process evaluation....70

5.1 General comparison between different cases....70

5.2 Economic comparison between cases....72

5.2.1 Product fuel profits....72

5.2.2 Fixed capital cost....73

5.2.3 Operating cost 74
5.3 Overall case comparison 75
6 Individual unit analysis and design 77
6.1 Distillation column 77
6.1.1 Sensitivity analysis 77
6.1.2 Column design 78
6.2 Fractional distillation column 82
7 Conclusions 85
8 List of abbreviations 86
9 References 87
10 Appendix 92

1 Introduction

The world's energy consumption has steadily been increasing. With the development of countries in Africa and Asia, this trend is likely to continue at a higher rate in the future. In 2018, the world's largest energy consuming country, China, also had the highest energy consumption growth rate. Additionally, the world's second largest energy consuming country, the USA, had the second highest energy consumption growth rate, which was partially caused by the increasing intensity and frequency of extreme weather conditions contributing to hotter summers and colder winters [1]. As a well-known fact, the changes in the global climate are caused mostly by emissions of the current energy producing technologies and their source mediums. The energy consumption in transport, alone, is projected to rise by 20 % until 2040 from which the majority is represented by the road sector [2]. Due to the increasing demand of road vehicles and their reliance on fossil fuels new solutions are needed to limit the amount of emissions as the world economies continue to modernise. Most of the solutions focus on the production of energy and fuels from renewable sources.

Throughout the past 20 years increasing attention has been given towards production of biofuels in gaseous, liquid and solid form from biomass sources [3]. Global production of biogas from mostly agricultural and municipal solid waste was around 35 Mtoe in 2018 and is projected to more than double to around 75 Mtoe in 2040 [4]. The commercial production of ethanol from food crops has already been well established as well as the production of biodiesel from oil seeds. However, production of biofuels from food crops is not optimal due to competition with the foods market. Therefore, increased attention has been given to the production from lignocellulosic biomass materials. The commercial production of ethanol has seen the biggest results until now while the bio-oil and drop-in biofuels production is still in its developing stage. Currently, commercial production of bio-oil and biofuel from lignocellulosic biomass is still not economically viable due inefficiencies in conversion and upgrading [3].

The focus of this thesis will be the simulation and economic evaluation of liquid biofuel production from lignocellulosic biomass. Several production processes will be simulated in Aspen Plus and evaluated in order to obtain the most optimal process for future development.

2 Problem formulation

Production of biofuels from lignocellulosic biomass consists of several sections and unit operations. Many technologies for the conversion of biomass into intermediate products and many pathways of the possible upgrading routes of intermediate products into final fuels are available. So far, optimal process configurations have not yet been established in the academic and industrial circles.

The focus of this thesis was to explore and compare possible process configurations in order to identify the one with the highest potential for future development. To this end, several routes of biomass-to-liquid processes were studied. Three separate processes cases, which differed in Fischer-Tropsch (FT) synthesis conditions, were finally chosen for further development. This included high temperature and low temperature FT synthesis and different catalyst use in low temperature FT synthesis. The thermochemical conversion, upgrading and separation sections were simulated in Aspen Plus for each case. Due to different FT synthesis product profiles, different fractions of the final fuels were obtained for each case. The simulations were then economically evaluated, and compared. Lastly, rigorous simulations and detail design of the main distillation column and fractional distillation column were performed and included in the report.

3 Process synthesis and conceptual design

3.1 Process overview

In this chapter, the content covering biomass variety, biomass processing and the different processing units used in the production of biofuels is entailed.

3.1.1 Lignocellulosic biomass sources

There are several biomass sources potentially useful for biofuel production. These include food crops, wood-derived biomass and municipal waste. First generation biofuels used food grains and vegetable oils as feedstock which provided its own set of problems like raising the prices of the food market, contributing to global warming as well as net energy losses [5], [6]. Consequently, second generation biofuel production technologies are being developed with the focus on the use of lignocellulosic biomass as feedstock. The advantages in using lignocellulosic biomass lay in using a carbon-neutral feedstock with higher availability due to less competition in comparison to food crops as well as higher security of supply due to ease of cultivation and a more consistent geographical distribution of sources when compared with fossil fuels. On the other hand, there are several disadvantages in the use of lignocellulosic biomass for instance low-yielding production, noticeable pressure on forests and nature areas or conversely the need for arable land, which could otherwise be used for growing food crops and/or urban area development. [5]

Food crops and lignocellulosic biomass are both forms of plant biomass. Plants biomass is grown through photosynthesis with the conversion of solar energy, CO_2 and H_2O into carbohydrates. Most of the carbohydrates are stored in a polymeric form i.e. cellulose, lignocellulose and starch [7]. Lignocellulosic biomass is composed mostly of cellulose, hemicellulose, lignin and traces of pectin and glycosylated proteins [8]. Cellulose and hemicellulose are chain polysaccharides which constitute the majority of lignocellulose while lignin acts as an adhesive between cellulosic and lignocellulosic polysaccharides by crosslinking the structures and giving the plant rigidity as well as resistance to rotting [8]. Lignin is comprised of organic polymers and could act as a source of chemicals, particularly aromatic compounds which are currently obtained mostly from fossil fuels [9], [10].

Lignocellulosic biomass sources used in bioenergy applications are divided into three sources. These are forest residues (forest harvest and residues, wood process residues), agricultural residues (corn stover, wheat chaff, rice husks) and energy crops (willow coppice, poplar coppice, energy dense grass species), which are specifically grown as fuel source and are designed to maximize the energy yield of the crop per land area [8], [11].

3.1.2 Processing of lignocellulosic biomass

Lignocellulosic biomass can be used to produce heat/electricity, gaseous fuels, liquid fuels and chemical feedstock. The biomass can be processed through either thermochemical or biological/biochemical pathway [5]. An outline of these processes is presented in *Figure 3.1.*

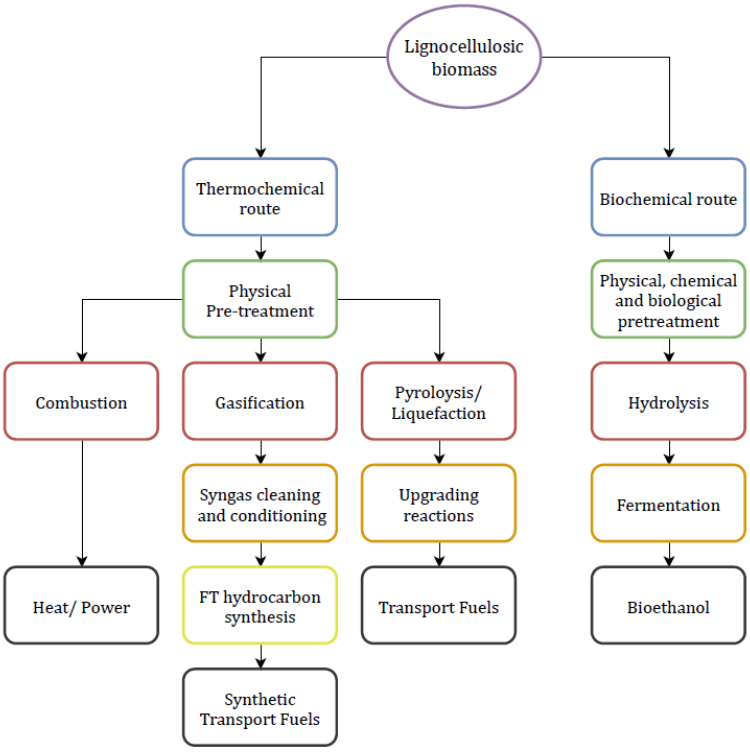

Figure 3.1 - Pathways of biofuel production

When biofuel is produced through biological/biochemical pathway, the biomass is converted with the use of enzymes and microorganisms. Essentially, the carbohydrates from hemicellulose and cellulose are converted by firstly chemically pre-treating the biomass with chemicals and microbial enzymes in separate stages in order to extract the lignin and sugars. Afterwards the sugars are fermented with the use of yeast, fungi or bacteria and the products chemically treated in order to synthesise gaseous and liquid biofuel products which are mostly comprised of different alcohols and hydrogen [8].

Thermochemical processes involve heating or burning the biomass under supervised temperature and oxygen conditions in order to produce the desired product. The lowest energy dense product is raw lignocellulosic biomass, which is combusted for heat or electricity production. Higher energy densities can be achieved through the production of gaseous or liquid fuels, which are also better suited for transportation. The highest energy dense fuel is achieved by upgrading the low-energy dense liquid and gaseous fuels into high-energy dense liquid fuels. The production of high-energy dense fuels with a composition similar to liquid fossil-derived fuels is the most effective way to displace the use of fossil fuels in the transportation sector [8]. The thermochemical conversion of biomass to synthetic fuel useable in current fuel transportation infrastructure and engines is referred to as biomass-to-liquid (BtL). BtL biofuel is superior in comparison to fossil-derived liquid fuels in the sense that it has severely lower CO_2 emissions, low NO_x emissions, no particulate matter and an adjustable quality [12].

BtL fuels can be produced by gasification, pyrolysis, direct liquefaction or supercritical fluid extraction. Depending on the different biomass type, different processes are used. From the mentioned techniques gasification, pyrolysis and liquefaction have already been extensively researched and are commercially viable while still undergoing optimization in the academia [8].

The different thermochemical production techniques vary in conversion process type as well as operating conditions. In liquefaction or supercritical fluid extraction, the conversion is carried out under near-critical water or other solvent conditions with temperatures reaching 400°C and pressures approximating to 250 bar when water is used. The higher pressure enables greater penetration of the solvent and the fragmentation of biomass molecules into bio-oil. Due to a large amount of char produced the bio-oil yield ranges from 20 wt. % to 60 wt. % based on dry feed. The bio-oil has high moisture content and a low energy density. With the use of several upgrading techniques it can be converted to synthetic fuels with properties similar to diesel, gasoline or jet fuel [8].

In pyrolysis the decomposition of biomass is achieved under anaerobic conditions with temperatures ranging from 350 to 700°C under atmospheric pressure with treatment time of a couple of seconds. Based on the temperature used two main types of pyrolysis techniques can be used: slow pyrolysis or fast pyrolysis. In slow pyrolysis, temperatures range around 400°C. The main products are small gaseous molecules like carbon dioxide, carbon monoxide, hydrogen, methane and light hydrocarbons. This mixture of gaseous molecules is referred to as syngas. The syngas can be further upgraded to liquid transportation fuels or combusted for power and heat generation. In fast pyrolysis, temperatures range around 500°C with mainly bio-oil being produced with a yield of 75 wt. % based on dry feed and minor amount of char and syngas. The bio-oil is a mixture of oxygen compounds which can be deoxygenated in order to form synthetic fuel similar to diesel and gasoline [8].

Gasification is the thermochemical decomposition of biomass under high temperatures ranging from 600°C – 1000°C with the presence of an oxidizing agent like air, steam, carbon dioxide, nitrogen, oxygen or a mixture of these. The products obtained include syngas, char, tar and minor contaminants like ammonia. The syngas can be combusted for the conversion into heat or electricity or upgraded into liquid biofuels via Fischer – Tropsch (FT) reactions. The focus of this thesis will be on biomass conversion using gasification and FT reactions, therefore, this pathway will be further described in the next chapter [8].

In comparison with biochemical/biological conversion pathway, thermochemical conversion uses much higher temperatures, faster processing time and higher conversion rates at lower operation cost. As feedstock the thermochemical are well suited for both wet and dry lignocellulosic biomass and in comparison to biological/biochemical processes require no chemical pre-treatment but solely the reduction in size and drying if necessary [8].

3.1.3 Gasification and Fischer – Tropsch pathway

In this thesis, the conversion of biomass using gasification and FT reaction synthesis is used. A summary of the entire process is described in this section while the individual process sections are described in the subsequent sections.

3.1.3.1 Feedstock pre-treatment

Since thermochemical conversion is used, the only pre-treatment necessary is physical. This includes size reduction and drying. Size reduction is employed in order to obtain specific particle size distribution, shape of particles, compressibility and compact ratio. The techniques employed are chopping, milling or grinding. For drying, the main purpose is to obtain a desired moisture content of the biomass particles. The techniques employed are natural drying, mechanical drying and thermal drying [8].

3.1.3.2 Thermochemical conversion and raw gas cleaning

After pre-treatment the feedstock is led to a gasifier at temperatures around 800°C, where the biomass reacts with the chosen oxidizing agent and forms raw gas. Raw gas is a mixture of carbon monoxide, carbon dioxide, hydrogen, methane, nitrogen, small hydrocarbon chains, char particles, ash and other impurities depending on the different feedstock source (nitrogen compounds, sulphur compounds and trace metals). The retention time in the gasifier is from 3 to 4 seconds. Afterwards, the gas is cooled in a heat exchanger and led to a set of cyclones where the solid particles are removed from the gas. If impurities are present in the gas stream, they can pose problems to the catalysts used further downstream and therefore need to be removed. The type of technique used for the removal of impurities depends on the nature of the impurities. Usually, a packed bed with an absorbent or water scrubbing is used. If the content of impurities is low and only sulphur and nitrogen compounds are present water scrubbing is sufficient treatment. When the gas stream has been cleaned, a H_2/CO ratio of 2 is needed for optimal FT hydrocarbon synthesis in the next step. Therefore, before the gas can be converted to liquid fuel it is conditioned through a water gas shift reaction (WGSR) to produce syngas. In the WGSR reactor the carbon monoxide reacts with water vapour over a catalyst in order to produce carbon dioxide and hydrogen [8].

3.1.3.3 Fischer – Tropsch reaction and upgrade to liquid fuels

The syngas is led to a reactor to undergo the FT process where the gas molecules are converted to longer chain hydrocarbon molecules, which constitute gasoline and diesel oil along with wax, olefins and alcohols.

Several catalysts can be used in the reaction ranging from compounds based on iron, cobalt, ruthenium and potassium. The type of catalyst used, the temperature and pressure of the system influence the distribution of products in the exit stream. Low temperature Fischer – Tropsch (LTFT) with temperature from 200 °C – 250 °C produces long chain molecules while a high temperature Fischer – Tropsch (HTFT) where the temperature ranges from 320 °C – 375 °C produces short chain molecules. The product stream after FT reaction is called syncrude since it contains a range of linear hydrocarbons also found in crude oil. The syncrude is present in a multiphase mixture with up to 4 different phases, which all need to be separated in order to recover the fractions. To this end, a series of separators is used. After separation into individual fraction, each fraction is upgraded in order to produce a single-phase syncrude composed of hydrocarbon compounds present in petroleum fuels [8].

Depending on the distribution of products in the crude oil, different combinations between the separation units and the upgrading reaction units are possible. The separations can be achieved using several separation technologies like 2-phase, 3-phase separators and distillation columns. Likewise, for the upgrading reaction units, there is variety of technologies to choose from depending on the carbon number of the fraction being upgraded and the type of the product desired. The gaseous mixture (C_1 – C_4) can be upgraded through alkylation and/or oligomerization producing gasoline like components and gases or through oligomerization and olefin hydrogenation and so returning gasoline and jet fuel like components. The light oil fraction (C_5 – C_{10}) can be managed using naphtha hydrotreating and catalytic reforming to produce components in the range of gasoline. For the distillate fraction (C_{11} – C_{22}) can be converted to either diesel like fuel through hydrogenation or jet fuel like components through hydroisomerization. The heaviest wax like fraction (C_{23}+) can be upgraded to gasoline, diesel and jet fuel like components through hydrocracking [8].

3.1.3.4 Syncrude separation

After all the fractions have been separated and upgraded the streams can be blended together for easier transport and at a later stage separated in single fractionation column likened to one used in petroleum refineries in order to obtain synthetic gas, gasoline, diesel and unconverted wax [8].

3.2 Feedstock selection and analysis

As feedstock, lignocellulosic biomass is chosen due to its availability, renewability and ease of cultivation. Depending on the type of lignocellulosic biomass chosen the feedstock chemical composition changes which affects the processing further downstream [8].

As already mentioned the contents of lignocellulosic biomass are mostly cellulose, hemicellulose and lignin. The amount of each constituent varies based on the type of lignocellulosic biomass, whether it is agriculture or forestry residue or obtained from energy crops [13].

In order to calculate the material balances in the treatment processes the contents of the lignocellulosic biomass need to be analysed and qualified. Among the most important quality parameters are the moisture content, calorific value and the amount of fixed carbon and volatile compounds. These parameters are measured through proximate and ultimate analysis. Proximate analysis is used to measure moisture (M), ash (A), volatile matter (VM) and to calculate the fixed carbon (FC) content. Ultimate analysis is used to determine the calorific value and the main chemical elements in the biomass (C, O, H, N and S) on a moisture free basis [14]. During feedstock selection preferably, low moisture content biomass is desired, due to lower pre-treatment cost since less drying is needed [8].

When choosing the type of lignocellulosic biomass to use as feedstock several other factors need to be taken into account. Some of these are the availability of raw material, the geographical conditions, feedstock cost, effects on soil, water, biodiversity, and others [15]. In Europe, wood-derived biomass feedstock is particularly well suited since wood has historically been the most popular choice for energy production and is still finding uses elsewhere today [16]. Consequently, as reported by Mantau and Eurostat the combined lumber industry in Europe produced approximately 200 million tonnes of wood waste in 2012; making forestry based lignocellulosic biomass a good feedstock choice [17]. Therefore, the biomass type used in this project will be limited to wood based biomass. Among which, some species of wood or a mixture of many will be evaluated in Section 4.

3.3 Thermochemical conversion

3.3.1 Gasification

As described in section 3.1.3 the purpose of gasification is to react biomass with an oxidizing agent in order to produce raw gas. The composition of the raw gas mostly depends on the feedstock used and the design of the gasifier. During the design of the gasifier, the most important aspects taken into consideration are obtaining the highest yield of gaseous products, minimizing the amount of char and condensable hydrocarbons and minimizing the cost of production [18]. In order to choose the most optimal route the engineer must evaluate several parts of the whole process separately and combine them into a harmonised whole. The most important process parts in the case of gasifier design are the selection of a gasifying medium and the type of gasifier used [19]. Therefore, an overview of the most optimal examples for lignocellulosic biomass is presented in this section.

3.3.1.1 Gasifying mediums

The role of gasifying mediums is to react with the carbon and heavy hydrocarbons in biomass in order to convert them into gases like CO and H_2. Gasifying agents used for this purpose can be air, oxygen or steam. Selection of a certain gasifying agent reflects highly in the composition and the heating value of the gas produced [19]. The formation of different products in a gasifier and the heating values of the gas produced depending on the choice of the medium are presented in *Figure 3.2* and *Table 3.1,* respectively.

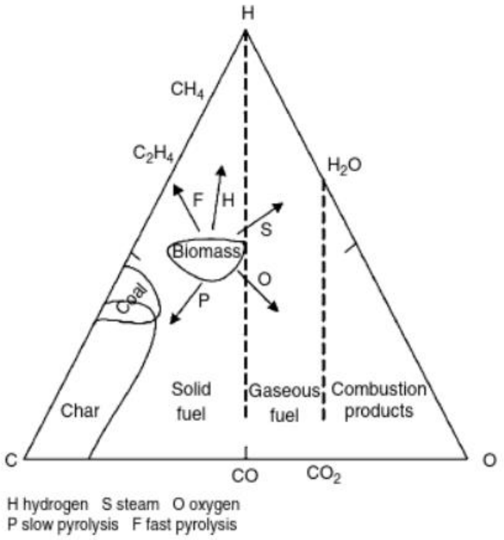

Figure 3.2 - C-H-O diagram of the gasification process [19].

As can be seen from *Figure 3.2* if oxygen is used as a gasifying medium the conversion products move toward the oxygen corner, therefore more CO and CO_2 products are released, depending on lower or higher oxygen content, respectively. If steam is used, the outlet gas contains more hydrogen per unit of carbon, resulting in a higher H/C ratio [19].

The heating value of the product gas is the highest for pure oxygen as the medium, followed by steam and air as can be seen in *Table 3.1*. The reason for the much lower heating value for air as the medium is due to the presence of nitrogen which dilutes the product gas [19].

Table 3.1 - Heating values for product gas based on gasifying medium[19].

Medium	**Heating Value (MJ/Nm^3)**
Air	4 - 7
Steam	10 - 18
Oxygen	12 - 28

For the further FT synthesis, the most important factor is the H_2/CO ratio of 2. For this purpose, the heating value of the product gas is of little interest and the composition of the gas has the most importance. Additionally, using oxygen as a medium induces the additional cost out of all other options since the oxygen needs to be extracted from air or ordered separately. Therefore, either the use of steam or air seems the most suitable choice. In order to determine which uses would be best a comparison between the cost of using steam to achieve a H_2/CO ratio closer to 2 and therefore saving cost in the WGSR unit versus the use of air as the cheaper gasifying agent but with higher costs in the WGSR unit should be examined closer, preferably through experimental work [19].

3.3.1.2 Gasifier type

Typically, a gasification process pursues a series of steps, which occur inside the gasifier. In order to better understand the different gasifier types the gasification process is briefly described next.

A typical gasification process starts by leading the already pre-dried biomass into the gasifier at which point the heat inside the gasifier dries the remaining water from the feed. Afterwards, a slow or fast pyrolysis process occurs in the reactor part with no oxidizing agent. In pyrolysis, larger hydrocarbon molecules are thermally broken down into smaller gas molecules. Due to a lack of oxygen, the process products move towards the carbon area of the diagram in *Figure 3.2*. In slow pyrolysis the products move towards the carbon corner and more solid char is formed. In fast pyrolysis the process products move closer to the C-H axis of the ternary diagram opposite of the oxygen corner. Due to a lack of oxygen, more liquid hydrocarbons are formed in fast pyrolysis reactions. Additionally, the condensable gases form tar that can greatly affect the optimal operating of the gasifier. Therefore, additional steps are taken in order to crack or reform the tar into non-condensable gases [19].

The gasification step takes place after pyrolysis. The hydrocarbons in fuel, steam, carbon dioxide, oxygen, hydrogen and the evolved gases react forming the gaseous products constituting raw gas. Most of these reactions are endothermic so heat needs to be externally supplied. The reactions with hydrogen/oxygen and carbon are exothermic however, and therefore provide some internal heat to the reactor environment. Following gasification, the combustion of unreacted char takes place. During combustion, the carbon from char exothermically reacts with oxygen in order to form carbon dioxide and carbon monoxide. An important part of combustion is the appropriate amount of oxygen so that mostly carbon monoxide is formed. If there is an excess of oxygen more carbon dioxide and heat is formed, diluting the product gas as well as raising the temperature of the gasifier [19].

Depending on the gasifier type different process conditions, product composition and suitable feed type are specified. In *Table 3.2* an overview of some commercial gasifiers is given.

Table 3.2 – Overview of commercial gasifiers as adapted from P.Basu [20]

Parameters	**Fixed/Moving bed**	**Fluidized bed**	**Entrained bed**
Feed size [mm]	< 51 mm	< 6 mm	< 0,15 mm
Tolerance for fines	Limited	Good	Very good
Tolerance for coarse	Very good	Good	Limited
Exit gas temperature [°C]	450 - 650	800 - 1000	> 1260
Oxidant requirements	Low	Moderate	High
Operating temperature [°C]	1090	800 - 1000	1990
Steam requirement	High	Moderate	Low
Ash produced	Dry	Dry	Slagging
Cold gas efficiency [%]	80	89	80
Capacity	Small	Medium	Large
Problems	Tar production and utilization of	Carbon conversion	Raw gas cooling

As seen from *Table 3.2* there are three main types of gasifiers, which are largely distinguished by the gas-solid contacting mode, power usage and capacity. Moving bed reactors require the least power for heating (10 kW – 10 MW) and can process small amounts of feed, which makes them optimal for pilot plants, smaller productions or parallel gasification with multiple reactors. Fluidized bed reactors are medium sized and demand the thermal input ranging from 5 to 100 MW. They are optimal for biomass processing due to excellent mixing, temperature uniformity and low tar production. The biggest production gasifiers that use the most power input (above 50 MW) are the entrained-flow gasifiers. They are the most widely used for large-scale coal gasification. They are unsuited for biomass use due to two main reasons. Firstly, due to short residence time the feed needs to be finely grinded which is hard to achieve with fibrous biomass.

Secondly, the molten biomass ash, due to its alkali compounds, corrodes the gasifier's refractory lining and greatly shortens its operating lifespan. On the other hand, entrained-flow gasifiers can easily destroy tar, which in other gasifiers causes problems [19].

Due to large shortcomings for biomass gasification, entrained-flow reactors will not be further discussed and more focus will be given onto moving and fluidized bed reactors.

There are several subtypes of the three main gasifier reactors. The subtypes for moving bed and fluidized bed reactors are presented in *Figure 3.3* bellow.

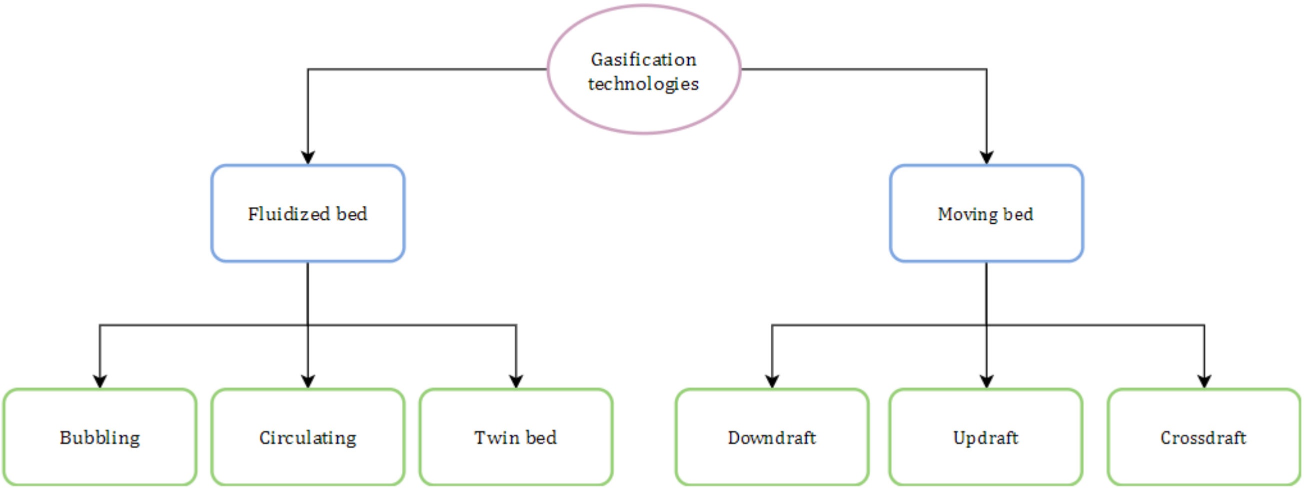

Figure 3.3 - Division of gasifiier subtypes.

The moving bed reactors are divided into three subdivisions based on the direction of the feed and product streams. In an updraft gasifier, the feed is led in at the top with the product gas exiting from the top as well. The preheated oxidizing agent is fed from the bottom as can be seen in *Figure 3.4*. As the gasifying agent rises it reacts with the descending fuel, heating up to 1000 °C in the combustion/gasification zone, where most of the oxygen gets used up while forming CO_2 during char combustion. As the gas rises the oxygen quantity in it is reduced and more CO is formed. The hot gas with a mixture of CO_2, CO and water vapour from either the feed or gasifying agent then rises further up where the upper bed char is gasified. The carbon from the char reacts with water and carbon dioxide to form carbon monoxide and hydrogen. These reactions are endothermic so the gas cools down in this section. As the gas rises further up it heats up the dried biomass. Pyrolysis of biomass occurs. The biomass is decomposed into non-condensable gases, condensable gases and char. In the top layer, the leftover heat dries the fresh biomass and exits the gasifier with a mixture of pyrolysis and gasification products [19].

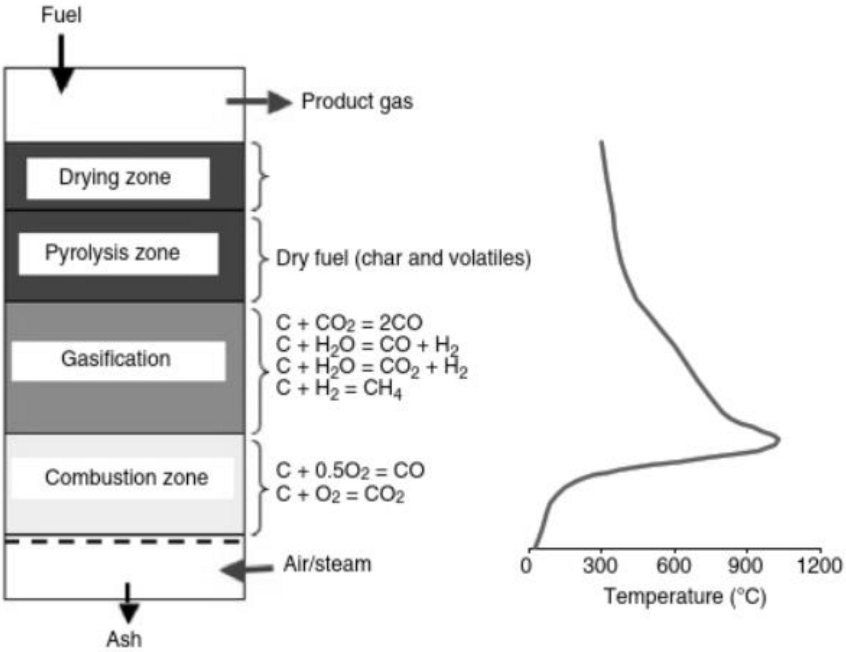

Figure 3.4 – Gasification stages in an updraft gasifier

In a downdraft gasifier the oxidizing medium is fed into the lower section of the gasifier while the biomass is fed from the top as can be seen in *Figure 3.5.* The pyrolysis and combustion products move downward. The hot gas moves in the same direction and reacts with char, where gasification occurs. This configuration produces tar-free, low-energy content gases [19].

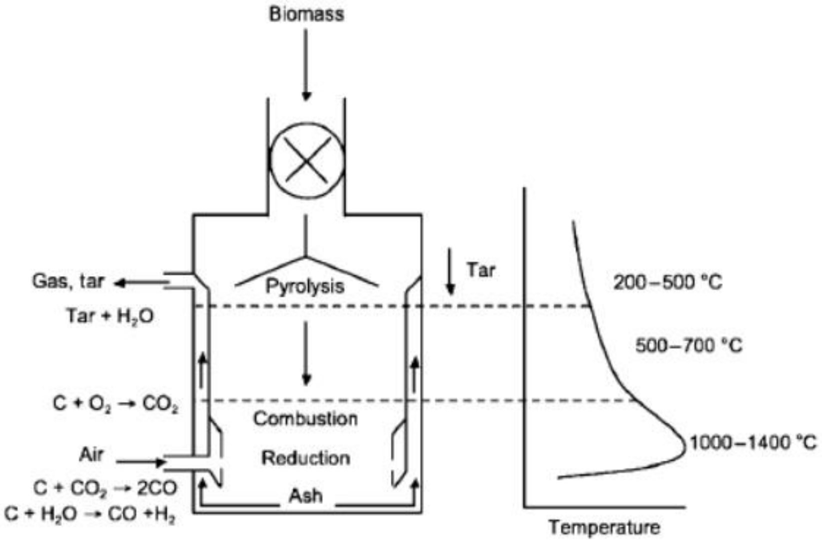

Figure 3.5 - Downdraft gasification reactions

Fluidized bed reactors are well suited for gasification of agricultural residues and wood-derived biomass. Due to the large thermal inertia and rapid mixing a wide range of feeds and their mixtures can be treated at a time. This property makes them suitable for gasification of different lignocellulosic biomass depending on its availability. Moreover, the temperature in fluidized bed reactors typically ranges from 800 – 1000 °C, which is below the ash agglomeration temperature. Therefore, high-ash fuels like wood-derived biomass can be gasified without ash sintering and agglomeration. Due to the reasons mentioned above fluidized bed reactors are popular among large-scale biomass gasification processes [19].

In fluidized-bed reactors, the fresh feed particles heat up through contact with hot bed solids (sand) and undergo rapid drying and pyrolysis. The oxidizing agent (fluidizing gas) enters the reactor from the bottom and leaves through the top. As the oxygen meets char mixed with bed materials it exothermically reacts, transferring heat onto the bed materials, which disperse it to whole of the fluidized bed. Depending on the concentration of oxygen in the fluidizing gas and the amount of char, a certain amount of heat is released [19].

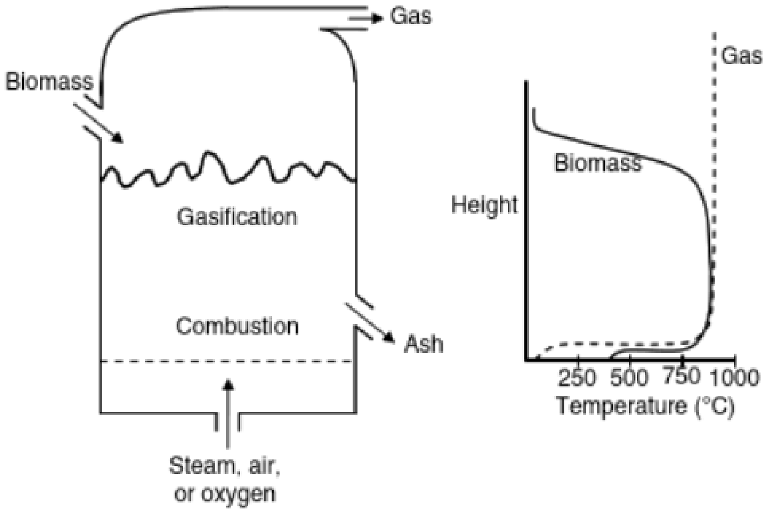

Figure 3.6 - Fluidized bed gasifier

In a bubbling fluidized bed gasifier presented in *Figure 3.6,* the feed is led in from the top or the sides. The gaseous products formed in the fluidized bed rise up in bubbles and leave the gasifier through the top where they are cooled down. Problems arise if the bubbles, as they rise, bypass the solids without undergoing gasification reactions in which case the pyrolysis products break down into non-condensable gases due to the heat in the bed. As the non-condensable gases are led through the top exit of the gasifier, they get cooled and form tar and char. Another problem facing bubbling fluidized bed gasifiers are the partially gasified char particles, which arise due to high degree of solid mixing. Furthermore, the slow diffusion of oxygen inside the bubbles to the particles in the fluidized bed encourages combustion reactions in the bubble which decreases the gasification efficiency [19].

In circulating fluidized bed (CFB) gasifiers the feed is circulating in a loop. Inside the loop the feed is intensely mixed. These kind of gasifiers have longer residence times and do not face issues related to bubble formations.

3.3.2 Raw syngas clean up

When producing syngas for biofuel synthesis severe requirements regarding the levels of impurities are specified. Impurities present in raw syngas range from char, ash, condensable organic compounds (tar), nitrogenous compounds, sulphur compounds, hydrogen halides, halogens and trace metals. These impurities severely compromise the production process further downstream by causing catalyst poisoning, corrosion and fouling in downstream processing equipment. Therefore, the removal of impurities in raw syngas before FT synthesis is of crucial importance [21].

The impurity removal technologies can be divided based on the outlet temperature of the gas leaving the cleaning unit. Based on the temperature these technologies are classified as cold, warm and hot. Cold clean up units operate at ambient temperatures, warm at temperatures of 100 – 300 °C and hot 400 °C – 1300 °C. The employment of removal units at different temperatures is beneficial since different impurities have different condensation temperatures at which they can be removed. For instance, ammonium chloride condensation occurs at 300 °C, while many alkali compounds condense at higher temperatures [22].

On the other hand, using cold clean up units lowers the total process efficiency due to the need of reheating the clean gas before FT synthesis. Therefore, applying high and warm temperature cleaning processes that can provide effective cleaning without previous gas cooling could be economically more optimal as long as the alternative cleaning unit operations do not require large operating costs [23].

In *Table 3.3* the typical raw syngas impurity concentration is presented as well as the level of purification required in the raw syngas to be suitable for FT synthesis. The exact level of purification for each impurity is dependent on each plant, since it can use different catalysts that have different allowed levels of impurities. Additionally, each plant operator can decide to tolerate a certain amount of catalyst poisoning and the consequent decreasing production if they deem the investment costs for additional clean up units to be too great. Therefore, the removal levels specified serve more as a rule-of-thumb that is derived from data based on FT synthesis [24].

Table 3.3 Impurity concentration and the required removal level for a typical raw syngas obtained from gasification of wood with 15% moisture content at 850 °C in an atmospheric air-blown CFB gasifier [21].

Impurity	**Impurity level [mg/m^3]**	**Removal level**
Particulates	2000	Completely
Tar	7000	Below dew point
Nitrogenous compounds	2200 (NH_3)	< 1 ppmV

Sulphur compounds	150 (H_2S)	< 1 ppmV
Halogens and halogen halides	130 (HCl)	< 10 ppbV
Trace metals	n/a	< 10 ppbV

3.3.2.1 Particulates

Particulates include the ash, dust, unconverted carbon formed in low temperature gasification, soot formed in high temperature oxygen blown gasifiers and solid bed material carried over from fluidized bed gasifiers [21].

Particulates can be removed using multiple technologies where some are more suitable for rough clean up of mostly large particles and other for fine particulate removal. The following systems can be used: cyclones, barrier filters, solvent scrubbers and electrostatic precipitators (ESP) [21]. In *Table 3.4* and *Figure 3.7* below an overview of the separation technologies, their temperature range, general removal percentages as well as removal percentages depending on the particle size is summed up.

Table 3.4 - Comparison of particle separators [25].

Separator	**Operating temperature range [°C]**	**Particle reduction [%]**
Cyclone	20 – 900	45 - 70
Dynamic granular bed filter	20 – 900	80 – 95
Candle filter/ bag filter	150 – 750	90 – 99
Scrubber	20 – 200	40 – 65
Wet electrostatic precipitator (ESP)	40 – 50	95 – 99

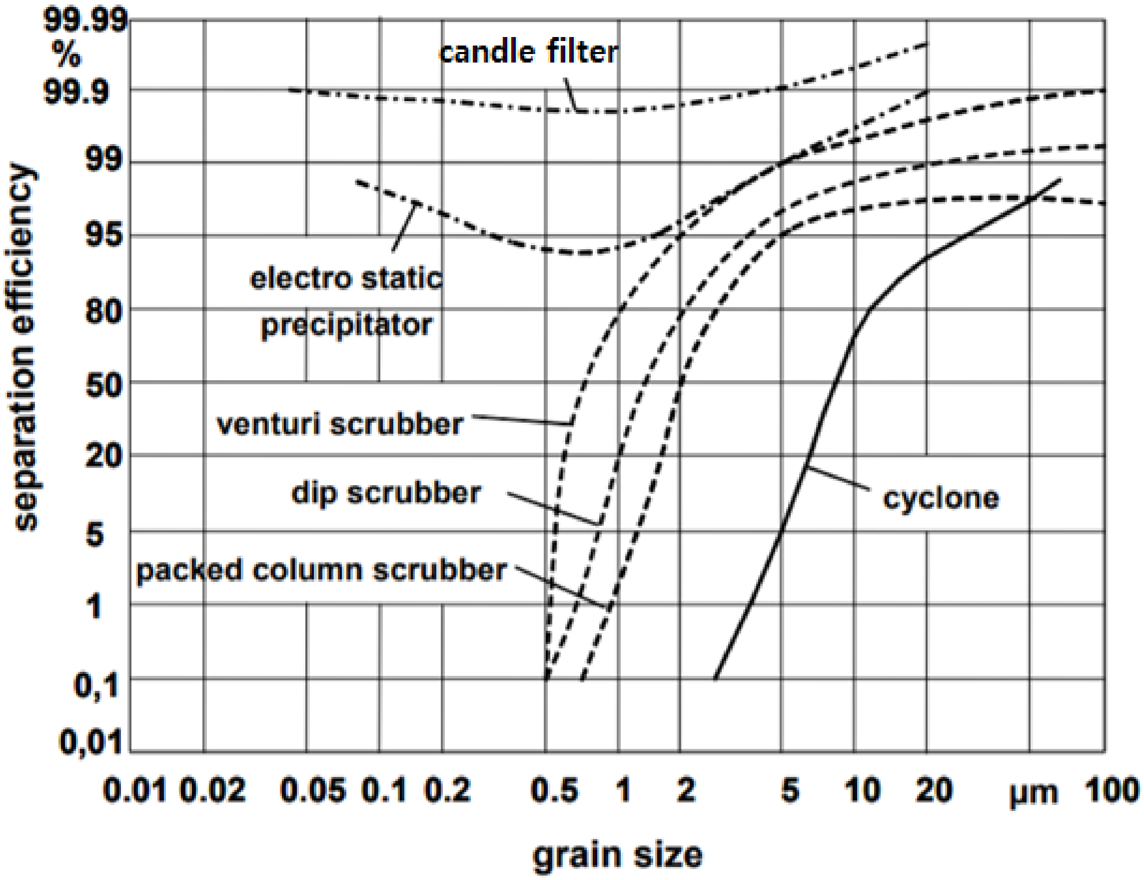

Figure 3.7 – Typical separation efficiencies for different sized particles by several gas cleaning systems [26].

Particle removal is achieved in several steps ranging from rough to fine particle removal. For first stage particle removal cyclones are normally used, which operate by making use of particle's mass moment of inertia to remove mostly larger particulate matter from the gas. There are two main groups of cyclones based on the direction of the gas flow: reverse-flow and axial flow. In a reverse flow cyclone, the flow of the gas is reversed at the bottom and flows back upwards whereas in the axial flow cyclone the gas flows straight through. Since the reverse flow cyclones are the most commonly used their principle of operation is described further. The particle-contaminated gas enters the cyclone at a tangent and flows downward in a circular spiral vortex (outer vortex) towards the lower end of the cyclone. Larger particles with a high moment of inertia flow outwards toward the cyclone body, slow down upon impact and fall down to the dust chamber at the bottom. Meanwhile, smaller particles with low mass moment of inertia are swept along by the gas stream and lifted up through the inner vortex and out of the cyclone at the top. A graphical representation of a reverse flow cyclone separator as well as the outer and inner vortices is shown in *Figure 3.8* [27].

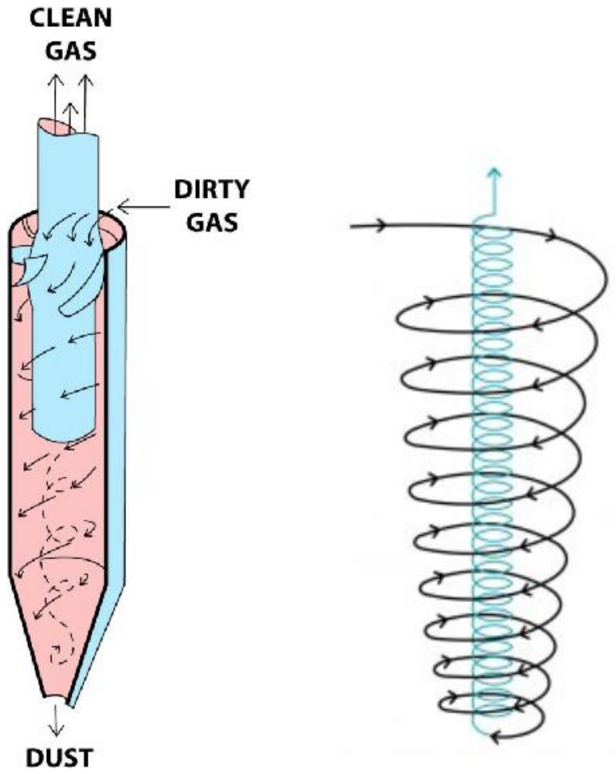

Figure 3.8 – Reverse flow cyclone representation (left) and inner and outer vortices formation (right) [27].

Cyclones are normally used for rough particle clean up since they can also operate at high temperatures. Subsequent removal steps are necessary, however, to remove the leftover particulate matter [21].

High temperature removal units suitable for fine particle removal are dynamic granular bed filters and candle filters [25].

Dynamic granular bed filters operate by capturing the particles from the raw gas stream in-between the crevices of the granular material while the gas passes through. The use of fixed bed granular filters raises problems with the dust cake build up which results in a high-pressure drop and requires back pulsing for continued operation. However, the dynamic granular bed filters evade this problem since the granular material is moving against the coming gas flow, which can keep the dust cake at a certain thickness. In this way, the operating pressure drop remains constant and the collection efficiency is continuously guaranteed. On the other hand, the formation of high-speed zones with over 10 times faster gas velocity near the inlet and outlet of the vertical granular bed allows the gas and dust particulates to pass through the filter bed directly [28].

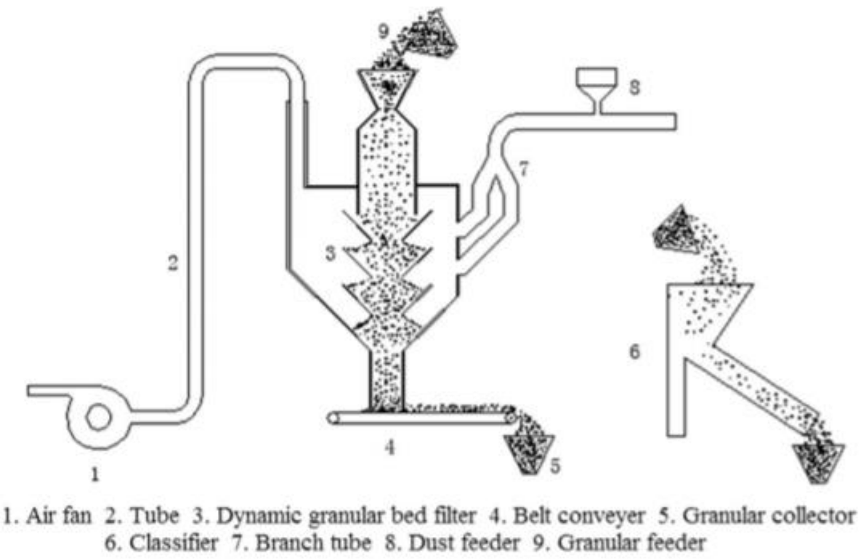

Figure 3.9 - High temperature dynamic granular bed filter representation [28].

Candle filters operate by leading the raw gas through large ceramic or metal rods of high porosity (candles). The raw gas with dust particulates moves from the outside of the candle inward building up a dust cake layer on the outside of the candle. A back pulse with clean gas from a gas tank or a blowback system regenerates the candle by pushing the dust cake off the candle surface. The candles are arranged in groups and installed in a tubesheet by vertically hanging with one end in the clean gas vessel room and the other in the raw gas vessel room. The raw gas enters the vessel from the bottom, enters the hanging candles from the outside, travels inwards, through to the other end of the candle and out through the surface of the candle in the clean gas vessel room[29].

The candle length can range from 1 to 3 metres with a width of 6 to 15 centimetres. The filter system can be a single tubesheet design, a multi-stage filter system, cross flow filtration and more which all have their own advantages and disadvantages. The most commonly used design is the single tubesheet. More information about the individual design advantages and disadvantages can be found in reference [29].

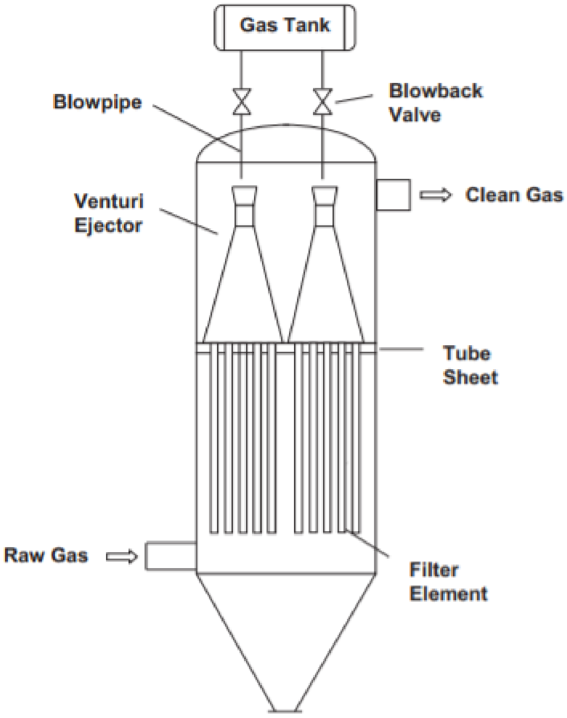

Figure 3.10 - Scheme of a single tubesheet candle filtration design [29].

Ceramic candles made from alumina silicates or silicon carbide with 40% porosity have a reported removal rate of nearly 100%, including for submicron particles. The porosities for ceramic can range from up to 40% for high-density ceramics and up to 90% for low density ceramics. The low-density ceramic candles operate at lower pressure drops, although they are more prone to breakage and require carefully controlled pressure of the back pulse. High density ceramic candles have a higher life time, due to being less prone to breakage but require higher operating pressures of more than 5 MPa. Ceramic candle can handle operating temperatures of 1000 °C and more [29].

The main advantages for this type of filtrations are high particular removal rate and operation at high temperatures. The main disadvantages are the need for back pulsing, and high pressure drop. Additionally, as already mentioned many advantages and disadvantages arise while choosing specific candle materials or reactor design [29].

When employing hot gas filtration an important parameter to consider is the operating temperature. In order to insure efficient filtration the temperature must remain above the tar condensation temperature so that tar does not form and clog the filters [26].

Following the cyclone separation the remaining particulates can be separated with low temperature separators like fabric filters, ESPs or scrubbers. These separation units should be employed after the hot, dry gas filtration in order to reduce unnecessary costs for subsequent gas reheating [26].

Fabric filters operate in the same manner as candle filters, except at lower temperatures, which vary depending on the filter material used [26].

In ESPs particulates are separated through attractive electrostatic forces. Firstly, the particulates are given and electrical charge. Secondly, the charged particles are attracted to the surface of electrodes in an electrostatic field. Lastly, the separated particles are removed from the collecting electrodes [26].

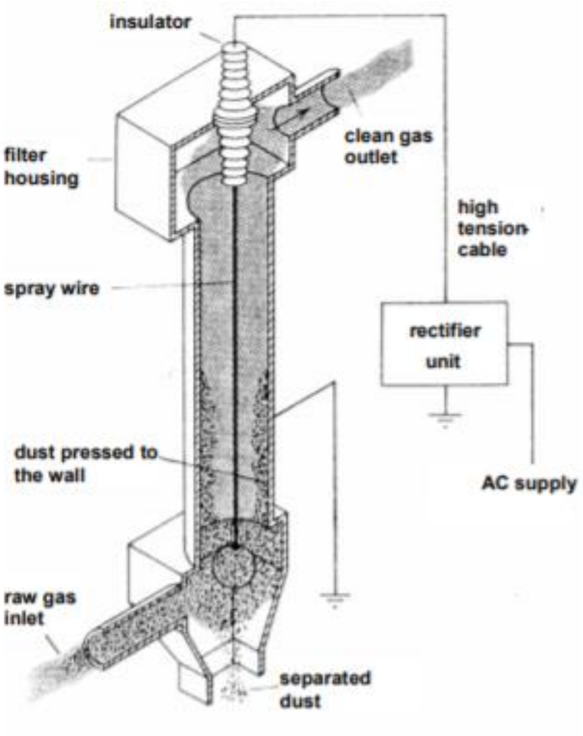

Figure 3.11 – Representation of a 1-step pipe ESP [26]

As shown in *Figure 3.11* the particles enter the ESP pipe filter at the bottom where they are charged. The particles are pressed to the pipe wall due to the ensuing electrical field and the clean gas leaves through the top. There are several different types of ESPs like plate or tubular types as well as dry or wet ESPs [30]. Wet ESPs can be used after water scrubbing for additional fine particle and tar removal [26].

The advantages of ESPs are high efficiency, reliability and ease of operation. The disadvantages include higher running costs compared to other devices and a large area requirement for effective removal on a large scale [30].

Solvent scrubbers or spray towers in particular are a popular choice for fine particle removal due to multiple types of impurities removed by them. Since scrubbers are used for cleaning of tar, ammonia and other compounds as well, they will be described in detail in the following sections.

3.3.2.2 Tar

Tar is made up of condensable organic compounds with molecular weight higher than benzene. Among these compounds are oxygenates, phenolic compounds and olefins as well as aromatic and polyaromatic hydrocarbons. Tars are usually removed by wet scrubbing through a liquid absorbent. Alternatively, tar combustion or catalytic tar treatment is possible for tar removal [8]. When regarding the level of tar removal the tar dew-point is considered the main parameters, since it represents the temperature at which tar starts condensing and agglomerating which causes fouling. Tar compounds have boiling temperatures between 80 – 350 °C, below which the tars start to condense and cause clogging of equipment [21].

Tar cracking is a method under which heavy tar compounds are broken down into lighter hydrocarbons under high temperatures (~ 1300 °C). Due to high energy costs this method is not preferred. However, tar cracking does convert a portion of tar products into methane, hydrogen, carbon monoxide, and smaller hydrocarbons which can be used up later either as power generation gas, reactants for FT reactions further downstream and contribute to the amount of liquid biofuel [31]. For the purpose of maximized green diesel production, tar combustion through the use of an entrained flow gasifier was considered by ECN and Shell in 2003. The results of the study can be viewed in references [32], [33].

In order to avoid high temperature conditions, alternatively catalytic tar cracking is possible. Typically, this step is performed immediately after biomass gasification at temperatures of 400 – 900 °C. Transition-metal-based catalysts such as Ni are used. The advantage of this method is the lower energy cost while still obtaining the desired tar conversion products mentioned earlier. The biggest disadvantage of this method is catalyst poisoning, caused by the inorganic impurities in the raw syngas [25].

Wet scrubbers operate by absorption of compounds in the liquid solvent, by capturing solid particles through inertial or diffusional impact with liquid droplets or by dissolution of compounds in the absorbent [34].

Using water as a solvent has benefits of using the cheapest solvent as well as simultaneous removal of water-soluble impurities like NH_3 and HCl. Likewise, the hydrophilic components in tar can easily be removed with water as well. However, the majority of compounds in tar are hydrophobic for which the removal rate using water ranges only at 22.1 – 38.9% according to a study by Phuphuakrat et. al. [35]. Due to the low removal, the tar condenses and clogs the scrubber apparatuses, which prevents continued operation. Moreover, problems arise in effective solvent regeneration due to the comparatively costly expense of tar-filled water processing [22], [26].

To achieve higher tar removal, especially for non-polar and heterocyclic compounds, oil-based solvents or oil-water mixtures are used. Removal efficiency of at least 60% or higher were reported for each tar component when using oil based solvents in the study by Phuphuakrat et. al. [35]. The use of scrubbing solvent emulsions has the advantage of removing tarry compounds and avoiding clogging of apparatuses. The scrubbing emulsion is enriched with tar as well as water condensed from the raw gas as it passes through the scrubber. The water and oil phase need to be later separated and the contaminated water either processed or properly disposed. The oil phase can be continually used until full saturation with tarry compounds at which point it must be recycled or properly disposed [8], [26].

In another case an OLGA removal unit was developed by ECN [21] which operated under higher temperature conditions (> 300 °C) and only used an oil based solvent. This led to high tar removal down, resulting in tar condensation temperature below 0 °C. Additionally, since no liquid water was present, the processing of contaminated water and coinciding treatment costs were avoided [21].

Wet scrubbers can be classified into four groups of scrubbers suitable for biomass gasifier plants. The schematic configurations, operating conditions as well as the energy requirements for each group are presented in *Table 3.5* [26].

Table 3.5 – Overview of wet scrubber types and their characteristics [25].

Type	**Packed column scrubber**	**Jet scrubber**	**Dip scrubber**	**Venturi - scrubber**
	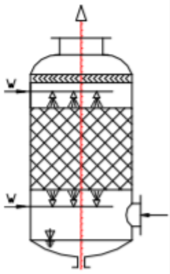	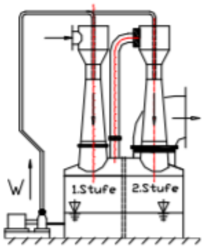	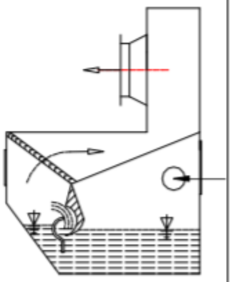	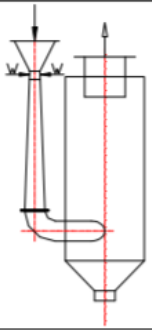
Critical grain size at ρ = 2.42 g/cm^3 in [µm]	0.7 – 1.5	0.8 – 0.9	0.6 – 0.9	0.05 – 0.2
Mean relative speed [m/s]	1	10 – 25	8 – 20	40 – 150
Pressure loss [mbar]	2 – 25	-	15 – 28	30 – 200
Washing medium/gas $\left[\frac{l*(h)}{(h)*m^3}\right]$	0.05 – 5	5 – 20	-	0.5 – 5
Energy requirement [kWh/1000m^3]	0.2 - 1.5	1.2 - 3	1 – 2	1.5 - 6

Packed column scrubbers are one of the more popular categories of wet scrubbers. The packed bed is filled with solid, packing material, which is wetted with the solvent. Multiple jets, installed in the scrubber vessel spray the solvent on the packed bed to achieve sufficient wetness. The purpose of the packing material is to increase the surface area for liquid-particle and liquid-gas contact. The packing material is kept in place by wire mesh retainers and supported by a plate near the bottom of the scrubber. The gas travels through a vertically or horizontally designed scrubber in a counter or cross flow to the solvent, respectively. The clean gas leaving the packed bed is passed through a demister where the impurity filled solvent condenses and falls to the bottom of the chamber [26], [34].

The main characterization of jet scrubbers is the spraying of the washing solvent with overpressure. This way, the solvent liquid disperses into 1-3 mm sized drops, which increases the surface area between the gaseous and liquid phase [26].

The dip scrubber design comprises a pool filled with scrubbing solvent, which the raw gas is forced to bubble through. This method provides good gas-liquid surface area for the transfer of mass, due to high turbulent mixing in the pool [26].

The venturi scrubber is especially effective for separation of solid particles. It has a venturi tube design, which has a narrowing cross section. When the gas passes through the narrowing section it greatly accelerates, at which point it collides with the scrubbing solvent. Due to the high shearing forces between the gas and liquid very fine droplets form which capture particles in the gas through impaction and by agglomeration around the solid particles. The droplets are separated further downstream through impact separation. Due the high mass moment of inertia the tar filled drops are forced out of the gas stream into a barrier, while the solvent-free gas escapes through an opening at the top [26], [34].

3.3.2.3 Nitrogenous compounds

Among nitrogenous compounds NH_3 and N_2 are usually present in large amounts and NO and HCN in smaller amounts. NH_3 causes FT synthesis catalyst poisoning and forms NOx compounds upon combustion, which is why it has a high need for removal. NO_x compounds contribute to acid rain and smog formation as well as impact the ozone layer which is why their emissions are under strict regulations. HCN compounds are poisonous to humans and therefore represent a safety hazard [8], [36]. Water-based wet scrubbing is normally used for their removal, due to high solubility of NH_3 and HCN in water. Alternatively, catalytic decomposition of NH_3 is possible [37].

Since wet scrubbing is a cold clean up method and also requires waste water treatment, alternative methods of nitrogenous compounds removal need to be explored.

Catalytic decomposition of NH_3 can be achieved through two routes, decomposition and selective oxidation:

Decomposition: $2\ NH_3 \rightarrow N_2 + 3\ H_2$

Selective oxidation: $4\ NH_3 + 3\ O_2 \rightarrow 2\ N_2 + 6\ H_2O$

Decomposition occurs with the use of a catalyst, usually under higher temperatures, in order to decompose ammonia to nitrogen and hydrogen. This reaction is desirable since it introduces a higher amount of hydrogen into the gas stream, while no additional contaminants are generated. For the use of a catalyst, mostly calcined dolomite, nickel and iron catalysts are used.

Main problems arise due to the presence of other compounds found in raw syngas. These compounds compete with NH_3 for the catalyst adsorption sites, reducing the catalysts efficiency, react with NH_3 decomposition intermediates to form other impurities as well as negatively affect the catalyst performance. One example reported the use of a calcined dolomite catalyst with which the NH_3 removal reached 100% at 850 °C in an inert atmosphere. However, when 8% of steam was present, under 900 °C, the decomposition of NH_3 was almost negligible. Additionally, it is possible for CO and methane to react with NH_3 and produce HCN, leading to higher concentrations of impurities [37].

For selective oxidation route, a controlled addition of an oxidizer is injected to the gasification gas to selectively convert NH_3 into N_2. Applicable oxidizers are O_2, NO or their mixture. The main advantage of this approach is that the oxidation reaction is thermodynamically favourable at all temperatures, leading to lower temperature conditions than those needed for the decomposition route. On the other hand, the main disadvantage is that O_2 and NO may react with H_2 and lead to increasing H_2O and NH3 concentrations. Moreover, O_2 and NO may react to form NO_2, which needs to be removed. Therefore, the main challenge for this route to become more widely adopted is to find a suitable catalyst and conditions under which a more selective ammonia oxidation could be achieved [37].

3.3.2.4 Sulphur compounds

Sulphur compounds are mostly present in the form of H_2S and smaller amounts of COS. Together with CO_2 they are regarded as acid gases. Their concentration in raw syngas varies greatly depending on the feedstock source; woody biomass was found to contain approximately half the amount of sulphides than agricultural or energy crops [38]. The sulphur compounds need to be removed to the range of parts per billion, since even in small amounts they present a threat for catalyst poisoning further downstream and metal surface corrosion. Typically, sulphur is recovered as a saleable by-product with the use of a solvent in a counter current absorber and filters as a fine cleaning step [22].

There are different types of solvents to be used for the removal of acid gases. These range from chemical solvents and physical solvents to hybrid solvents, which are a mixture of both. Chemical solvents include primary, secondary and tertiary amines. The advantages of using amine-based solvents are low capital and solvent cost and a low absorption of syngas main components. The main disadvantages are that they require high temperatures for solvent regeneration, have problems with amine degradation and corrosion, as well as offer poor COS removal [39].

Physical solvents absorb acid gas based on the difference in the partial pressure between the gaseous and liquid phase. The absorption performs better under higher pressures. Main advantages of physical solvents are high selectivity for H_2S and COS, high loadings under high acid gas partial pressures, which result in low circulating rates, and low heat requirements for regeneration as it can be performed in part by pressure let-down. Main disadvantages of using a physical solvent are complex process schemes, high capital costs, low operating temperatures, leading to thermal performance losses and high operating costs [39].

After primary removal, the level of sulphur compounds is usually not low enough for the sensitive FT synthesis catalysts and therefore a secondary cleaning units needs to be set up. Usually this comes in the form of guard beds made from materials like ZnO or activated carbon. Metal oxides, have an exceptionally high selectivity for H_2S removal among which zinc oxide is the most commonly used, due to its high efficiency and lower costs. ZnO performance for other sulphur compounds is limited which is why it is best to either convert them to H_2S upstream or use a different absorbent, like a layer of Cu-ZnO at the bottom of the ZnO bed [39].

3.3.2.5 Halogens and trace metals

Hydrogen halides, halogens and trace metals are often removed by wet scrubbing with caustic solution or water. The NaOH in caustic solution reacts with HCl in order to form NaCl, which is later precipitated out of the solution. Using caustic solution instead of water is an economically preferable option, since the use of water requires an ionic exchanger for the removal of chlorine. The removal of trace metals is accomplished to a sufficient extent by water scrubbing and physical absorption by employment of active carbon guard beds [22].

3.3.3 Raw syngas conditioning

After gas clean up, conditioning of syngas is performed. For the case of FT synthesis this means increasing the H_2/CO ratio to reach a ratio of 2 by converting CO and H_2O into H_2 and CO_2 through the water-gas-shift reaction:

$$CO + H_2O \rightarrow CO_2 + H_2$$

The equilibrium between the products and the reactants depends on the temperature, but is independent of pressure up to 70 bar. The equilibrium is established naturally without a catalyst in the temperature range of 950 – 1000 °C. However, typically, a catalyst at lower temperature is used so that the equilibrium towards H_2 can be reached. With respect to different temperature ranges two catalysts are used commercially; iron based catalysts for high temperature shift at 300 – 510 °C or copper – zinc – aluminium oxide based catalysts for low temperature shift at 180 – 270 °C [25].

3.4 Upgrading to liquid transportation fuel

3.4.1 Fischer – Tropsch synthesis

Fischer – Tropsch synthesis is a catalytic reaction of CO and H_2 (syngas) into hydrocarbons (syncrude), which was developed by F. Fischer and H. Tropsch as a part of a coal utilization research in the early 1920s in Germany. The biggest appeal of the synthesis process is the clean fuel produced, which if correctly processed contains no sulphur and aromatic compounds [21].

The reaction is operated under temperatures of 200 – 350 °C and pressures of 25 – 60 bar. Syngas is converted to a mixture of hydrocarbons of different molecular weight such as gasoline and diesel oil constituents, waxes and olefins as well as alcohols. To the biggest extent straight–chain paraffin (saturated) hydrocarbons (C_xH_{2x}) are formed and to a lesser extent branched and olefin (unsaturated) hydrocarbons. FT synthesis reaction is an exothermic reaction with approximately 20% of the chemical energy being released as heat. It can be regarded as a carbon chain-building reaction where methylene ($-CH_2-$) groups are sequentially attached in a carbon chain [21], [40]:

$$nCO + (n + m/2)H_2 \rightarrow C_nH_m + nH_2O$$

Based on the chain length the FT synthesis products can be divided into groups presented in *Table 3.6.*

Table 3.6- Carbon chain groups produced as FT products [40].

Carbon number	Group Name
C1 – C2	SNG (synthetic natural gas)
C3 – C4	LPG (liquefied petroleum gas)
C5 – C7	Light petroleum
C8 – C10	Heavy petroleum
C11 – C20	Middle distillate
C11 – C12	Kerosene
C13 – C20	Diesel
C22 +	Wax

The catalysts used are based on iron (Fe), cobalt (Co), ruthenium (Ru) and potassium (K), depending on the desired product distribution. Iron and cobalt based catalysts are the most commonly used [40].

Iron catalysts are cheaper and have a higher tolerance to sulphur than the other catalysts. They have a wide range of tolerable temperatures, a high water-gas-shift affinity and produce more olefin products and alcohols. Due to the high water-gas-shift affinity the H_2/CO ratio can be adjusted in the synthesis reactor. The catalyst lifetime is generally limited to eight weeks [40].

Cobalt catalysts are applicable at lower temperatures of around 200 – 250 °C, have a lower water-gas-shift affinity and produce more high molecular weight hydrocarbons than the iron based catalyst at similar conditions as well as less olefins and alcohols. They have higher conversion rates and a lifetime of over 5 years [21], [40].

An important aspect of every FT synthesis production plant is the distribution ratio of the FT products. The product distribution is mostly determined by the temperature of the synthesis reactor. Therefore, it is of great importance to avoid an increase in temperature, which can easily arise, as all of the FT reactions are exothermic. By keeping the temperature constant optimal product selectivity can be maintained and longer catalyst lifetime can be reached by preventing catalyst sintering, which reduces activity [40].

The FT synthesis process can be operated under two temperature regimes; low-temperature Fischer-Tropsch (LTFT, 200 – 240 °C) and high-temperature Fischer-Tropsch (HTFT, 300 – 350 °C). Higher temperatures shift the reaction selectivity to more lower carbon number products (especially CH_4), more hydrogenated products, more branched products and more by-products such as oxygenates (ketones, alcohols, aldehydes, carboxylic acid) and aromatic compounds. Therefore, LTFT synthesis, which results in more higher carbon chain products, seems to be better in terms of fuel production, since less upgrading units need to be used for conversion to liquid fuel. The obtained long carbon chains can be hydrocracked to produce high-quality gasoline and diesel in desired fractions, depending on the market needs [40]. An overview of the two temperature regimes, their operating conditions as well as preferred products is summed up in *Table 3.7.*

Table 3.7 – Process conditions for Fischer-Tropsch synthesis [25], [40].

Parameter	**Low-temperature FT**	**High-temperature FT**
Products	Waxes and diesel fuels	Gasoline, light olefins
Temperature range [°C]	200 - 240	300 - 350
Pressure [bar]	20 - 60	25

Due to the exothermic nature of the reactions, the reactor designs have mainly focused on heat dissipation out of the reactor and temperature control. The four major reactor types are the tubular fixed-bed reactor (TFBR, Arge reactor), the fixed slurry-bed reactor, the circulating fluidized-bed reactor (Synthol reactor) and the fixed fluidized-bed reactor (Sasol advanced Synthol reactor, SASR) [41].

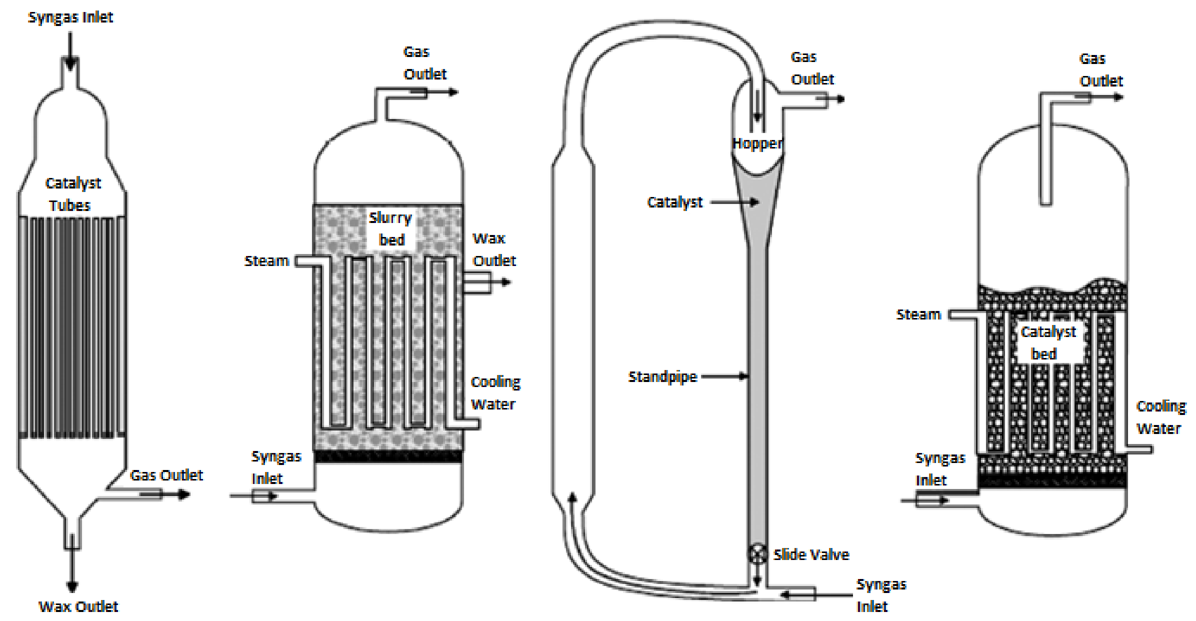

Tubular (ARGE) Fixed-bed

Fixed Slurry-bed

Circulating (Synthol) Fluidized-bed

Fixed (Sasol Advanced Synthol) Fluidized-bed

Figure 3.12 – The four major types of FT reactor designs [41].

The TFBR, Arge reactor is an older model, which was popular for LTFT synthesis from natural gas between 1955 and 1993. It comprises 2050 tubes of 12 metres in length and 5 centimetres in diameter, packed with an iron based catalyst, inside a shell. The LTFT reactions occurred inside the tubes, while steam was raised through the shell side for heat removal. A big advantage of the TFBR was that the produced wax was separated from the catalysts naturally. On the other hand, it required large capital costs, was complex to operate, difficult to scale-up, had heavy tube sheet resulting in costly structure, had to replace the catalyst periodically, which required labor intensive, complex procedures leading to longer downtimes and issues with uneven temperature distribution. Due to these difficulties, the TFBR reactor was largely replaced by Sasol's fixed slurry-bed reactor in 1995 [41].

The fixed slurry-bed reactor developed by Sasol, South Africa, 1995, was designed for converting natural gas to FT fuels, mainly middle distillates. It comprised a bed of Fe-based catalyst particles through which syngas was blown from the bottom up. As the syngas reacts with the catalyst the liquid FT products, mainly wax, form a slurry bed with the catalyst particles. This raises difficulty regarding the separation of the wax product from the catalyst. To combat this issue Sasol developed a wax-separation process as well as a Co-based catalyst which was much more resistant to degradation and allowed for excellent solids separation [41].

The SASR and the CFB Synthol reactor were both developed for HTFT synthesis. Between the two, the SASR is more popular, since it is far simpler and allows for a larger FT product production of 20000 barrels/day in comparison to CFBs 7500 barrels/day. The production difference largely amounts to the larger catalysts/feed gas ratio in the reaction zone of the SASR, which almost twice as large as in the CFB. Moreover, the SASR is also more thermally efficient, since it allows for greater cooling area of the reactor, which enables increased high-pressure steam production, for energy efficiency and more control of the process, leading to a more stable production. On the other hand, the SASR does have some difficulties regarding problematic shutdowns, where it can sometime stand idle for periods up to two weeks [41].

3.4.2 Upgrading of FT products

In this section the upgrading reactions used in the simulations are described regarding their conditions and catalysts use.

As described in *Table 3.6* the FT synthesis products can be divided into gas, naphtha (light and heavy petroleum), middle distillate, wax and aqueous fractions. After the fractions are separated they are upgraded depending on the type of fraction, the amount of it and the desired end product profile. In this project gasoline and diesel fuel are produced therefore the upgrading sections are designed with the intention of obtaining gasoline and diesel like liquid fuel, which satisfies the fuel specifications set by the EU.

The general description concerning the conversion technology for each fraction is given below.

3.4.2.1 Gaseous components

The gaseous fraction includes the options of upgrading into higher carbon number compounds, which are included, in different forms, in the end product or alternatively SNG or LPG gas generation and isolation for the purpose of generating heat or electricity in the processing plant. The gaseous products (C_1 – C_4) can be upgraded to branched aromatic compounds through *aromatic alkylation* and added to gasoline for higher octane content or diesel for lower cetane number and higher density. Alternatively, the gases can be upgraded to higher carbon number compounds through *oligomerization* for an increased amount of compounds in the gasoline to jet fuel range. In order to obtain paraffin compounds of higher carbon number *olefin oligomerization* is performed and *olefin hydrogenation* in order to convert the olefin hydrocarbons into paraffin compounds [8].

Aromatic alkylation is the reaction of olefin hydrocarbons with an aromatic compound like benzene or toluene. Usually this reaction is catalysed with solid phosphoric acid (SPA) under temperatures of around 100 °C [8].

Olefin oligomerization is the coupling of two or more olefins to produce mainly C_5 – C_{12} iso-olefins. If gasoline range products are wanted SPA catalyst is a typical choice [8].

Olefin hydrotreating is performed to convert olefins into paraffins. Specifically, this step is useful to convert the C_5 – C_{12} iso-olefins from olefin oligomerization into iso-alkanes, which are typical components of gasoline [8].

3.4.2.2 Naphtha components

Naphtha range compounds can be upgraded through *naphtha hydrotreating* followed by *catalytic reforming* to increase the amount of branched and aromatic compounds resulting in a higher octane number in the gasoline end product. Additionally *isomerization* techniques are employed to improve the octane number of paraffin compounds.

Naphtha hydrotreating and isomerization is the transformation of naphtha-ranged olefins into paraffins and branched paraffins. Typically, bifunctional catalysts that contain metallic sites for hydrogenation and acid sites for skeletal isomerization are used. Such catalysts are metal catalysts like NiMo which are supported over an acidic support like zeolites (ZSM-5) or amorphous oxides (Al_2O_3) [42].

Catalytic reforming is the term for transforming paraffin compounds into aromatics to improve the octane number of gasoline. This conversion is usually carried out in fixed bed or moving reactors with the use of multifunctional precious metal catalysts under high temperatures of 500 °C and atmospheric pressure. For instance a metal promoted H-ZMS-5 catalysts was reported to promote benzene, toluene as well as ortho-, meta-, para-xylene formation [8].

3.4.2.3 Middle d*istillate components*

Middle distillate composition is different depending on the FT synthesis type. If HTFT is done, the distillate is comprised of mainly olefins, which need to be treated in a *hydrotreating* unit in order to produce paraffins in the diesel range. When LTFT is performed, the distillate is mainly comprised of paraffins and thus does not need any additional treatment.

3.4.2.4 Wax components

The wax fraction is composed of components with boiling points above 370 °C. This wax fraction, (C_{22+}) can be converted to shorter chain components via wax *hydrocracking* technology. Wax hydrocracking is a common term for two types of reactions taking place in the reactor simultaneously: *hydroisomerization* and *catalytic hydrocracking*.

Catalytic hydrocracking converts the wax range compound into smaller chain compounds in the gasoline and diesel range. The reactions are catalysed with the use of bifunctional catalysts with the same functions as the catalysts used for *naphtha hydrotreating/isomerization*. The catalysts with acidic sites promote the isomerization/cracking reactions while the catalysts with metal sites promote hydrogenation/dehydrogenation reactions. Conversion takes place under high temperatures and pressures. In this project, pressures of 34 bars and temperatures of 340 °C were chosen. The catalysts used can be many metallic catalysts supported over an acidic amorphous support, for instance a NiMo or CoMo catalyst supported over amorphous silica-alumina or aluminium oxide [8].

3.4.2.5 Aqueous components

The aqueous fraction is composed of polar components like short chain alcohols, carbonyl components, carboxylic acids, which dissolve in the water fraction. In order to recover the organic compounds the alcohols are catalytically dehydrated into olefins for easier separation. Aldehydes and ketones can be hydrogenated into alcohols and thereafter transformed into olefins [8].

3.5 Separation technologies

Separation technologies are used in the overall process in order to separate the FT products before they can be upgraded and to separate the final upgraded syncrude blend into final product fuels. For the FT products, distillation columns and three phase separators are used to separate the mixture into separate fractions, determined by their carbon number.

The final upgraded fractions are blended together and need to be separated in a fractionation column. The individual components are recovered based on the difference in their boiling temperatures. The products obtained from the fractionation column can include gases, aqueous products, gasoline, diesel and heavy residues.

3.5.1.1 Three phase separator

A three-phase separator is a pressurized vessel used to separate the gaseous, aqueous and organic phase of the inlet stream. It can be designed horizontally or vertically. A schematic design of a horizontal separator is included in F*igure 3.13* [43].

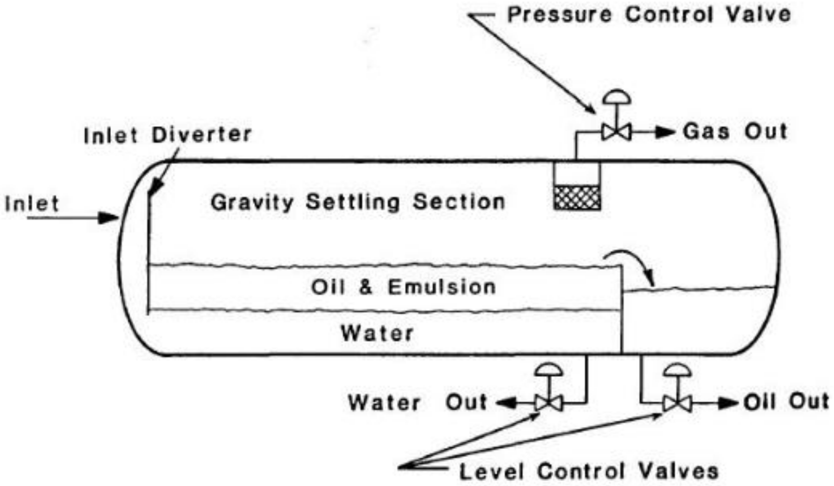

Figure 3.13 A schematic representation of a three phase separator [43].

After the stream enters the separator it is directed to an inlet diverter, which forces the liquid phases to enter the separator below the oil/water interface and gas to rise above. By doing so the mixing of water and oil at the top of the oil-water interface is avoided and easier oil-water interface control is achieved. The second part of the separator is the liquid collecting section where the heavier water settles to the bottom and the oil & oil-water emulsion rises to the top. The collecting section is closed off by a weir, which serves as a barrier for the contained liquid as well as to control the oil level inside the collecting section. The oil is skimmed over the weir into a separate part of the separator in which the separated oil phase is collected and released through a level control valve at the bottom. A second level controller valve at the bottom of the collecting section keeps the level of the water-oil interface at an appropriate height. Once the water-oil interface level rises, the valve releases the separated water from the bottom of the collecting section. The gas travels through the top of the separator and exits the separator through a mist extractor into a pressure control valve so that constant pressure inside the vessel is maintained [43].

3.5.1.2 Distillation column

A distillation column is a unit operation, which utilizes the difference in boiling points between components in order to separate them from the original mixed inlet stream. It is a simple design, which allows for the recovery of two product streams. The lighter product with a lower boiling point is recovered at the top while the heavier product, with a higher boiling point is recovered at the bottom [44].

Essentially a distillation column is a vertical vessel with trays or packings inside. The trays are filled with holes or bubble caps, to allow the passing and promote the condensation of vapour. Trays additionally provide a platform for the liquid in order to have more contact between the liquid and vapour phase. Packings are used to provide additional contact surface between vapour and liquid in order to promote the condensation of vapour and thus enhance the separation [44].

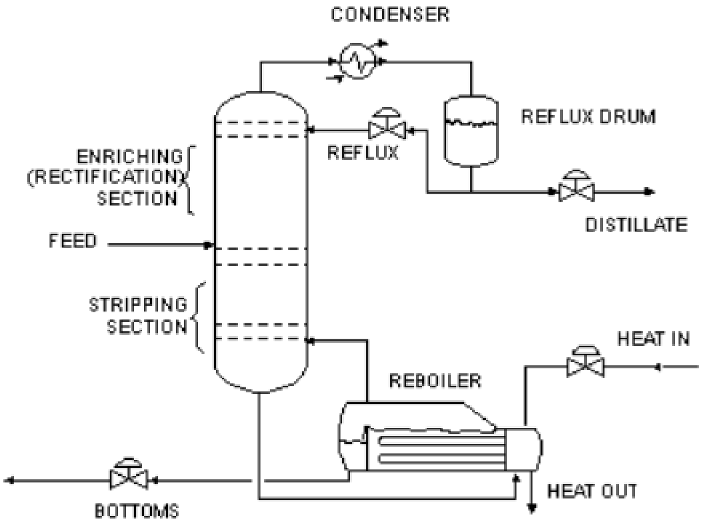

Figure 3.14 A schematic representation of a distillation column [44].

Additionally, a condenser, a reflux drum and a reboiler are included in the distillation column setup on the outside of the vertical vessel. The condenser is used to cool and condense the vapour that is leaving from the top of the column. The reflux drum is a vessel, which holds the condensed liquid. From the reflux drum, a part of the liquid is recycled back to the top of the distillation column. This stream is called the reflux. The condensed liquid that does not get recycled back is removed from the system as the distillate or top product [44].

The function of the reboiler is to generate vapour by heating up the liquid removed from the bottom and reintroducing it into the column at the bottom. A part of the liquid at the bottom is removed and is known as the bottom product [44].

The feed enters the distillation vessel at the middle of the column into what is known as the feed tray. The column is divided into a top, rectifying, section and the bottom, stripping section by the feed tray. The feed then flows down to the bottom column, is collected and heater in the reboiler [44].

3.5.1.3 Fractional distillation column

Fractional distillation column uses the same principle for the separation of components as the distillation column described above, except that it allows for recovery of multiple components. The difference is in the design of the vessel, which includes large collecting trays for the collection of the condensed liquids at different heights of the column. A compound is collected where the temperature in the column is at the collected component's boiling temperature. As with the distillation column, the temperature in the vessel is highest at the bottom and lowest at the top. Therefore, components with the highest boiling point condense lower in the column, while components with higher boiling points rise towards the top [45].

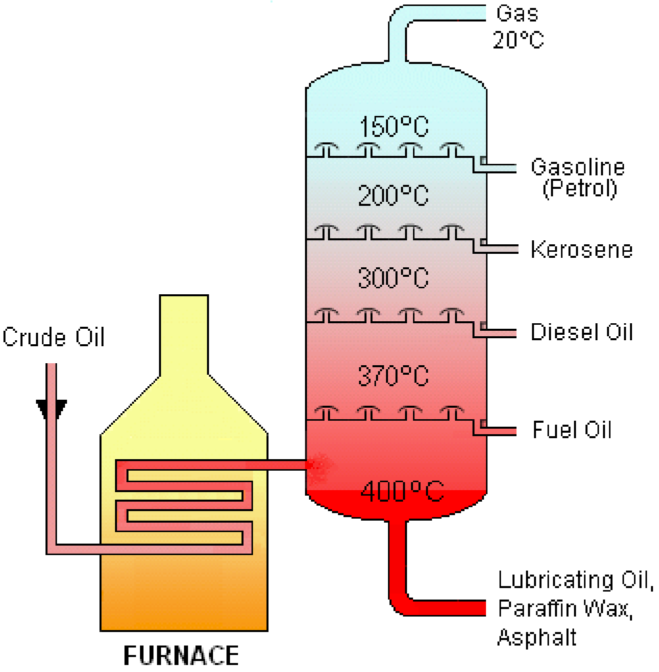

Figure 3.15 Schematic representation of a typical atmospheric pressure crude oil fractionation column used in oil refineries [46].

4 Process simulation

In this chapter the concepts, design and decisions leading to the final process setups are described. The base and alternative cases for the evaluation of different process setups are presented as set up in Aspen Plus simulation program. The complete BtL processes are described in terms of unit operations selected for the representation of actual unit operations that could be used for a conversion of biomass into liquid biofuel products with the focus on gasoline and diesel generation.

The goal of creating different processes is to obtain the most economically viable BtL process setup. Therefore, part of the simulation is focused on the cost of the feed stream, supportive streams, heat generation as well as end product quality and price. In order to obtain a sellable product the process design needs to be oriented towards obtaining liquid biofuels that satisfy the specifications for the respected biofuel type. Since gasoline and diesel production is emphasised the specifications for those fuels have to be met. The EU specifications for gasoline and diesel fuels are presented in *Table 4.1* and *Table 4.2,* respectively.

Table 4.1 - Gasoline fuel requirements in the EU – EN 228 [8], [47].

Parameter	Minimum limit	Maximum limit
Motor octane number	85	-
Reid vapour pressure [kPa]	-	60
Density at 15 °C [kg/m^3]	720	775
Final boiling point [°C]	-	370
Olefin content [vol %]	-	18
Aromatics content [vol %]	-	35
Benzene content [vol %]	-	1
Oxygenate content [vol %]	-	15
Oxygen content [wt %]	-	3,7

Table 4.2 – Diesel fuel requirements in the EU – EN 590 [8], [47].

Parameter	Minimum limit	Maximum limit
Cetane number	51	-
Density at 15 °C [kg/m^3]	-	860
Final boiling point [°C]	-	370
Flash point [°C]	55	-
Water content [mg/kg]	-	200
Viscosity at 40 °C [mm^2/s]	2	4,5

The main difference between the base and alternative processes is in the FT synthesis conditions. The FT synthesis was chosen as the differentiating step due to having the biggest impact on the product profile distribution of syncrude. HTFT and LTFT-based processes as well as LTFT processes based on different catalyst usage are simulated and compared. From the comparison of the three cases, the most economically viable case is obtained. Further optimisation of the most economical case is performed via numerical analysis of selected unit operations with the tools provided in the simulation program (sensitivity analysis).

The simulation reactor yields and feed composition are based on experimental results obtained by Paola Ibarra Gonzalez as part of her PhD research [8].

The basic thermodynamic model used for the simulation of the process cases is the Soave-Redlich-Kwong equation of state with Kabadi-Danner mixing rules (SRK-KD), since it is well suited for hydrocarbon-water mixtures [8]. For the separation units, which include the RadFrac (absorption tower, distillation column), DSTWU (distillation columns), Flash (phase separator) and Sep (phase separator) unit, the Non-Random Two-Liquid Redlich-Kwong (NRTL-RK) model was used.

4.1 Co-LTFT simulation case

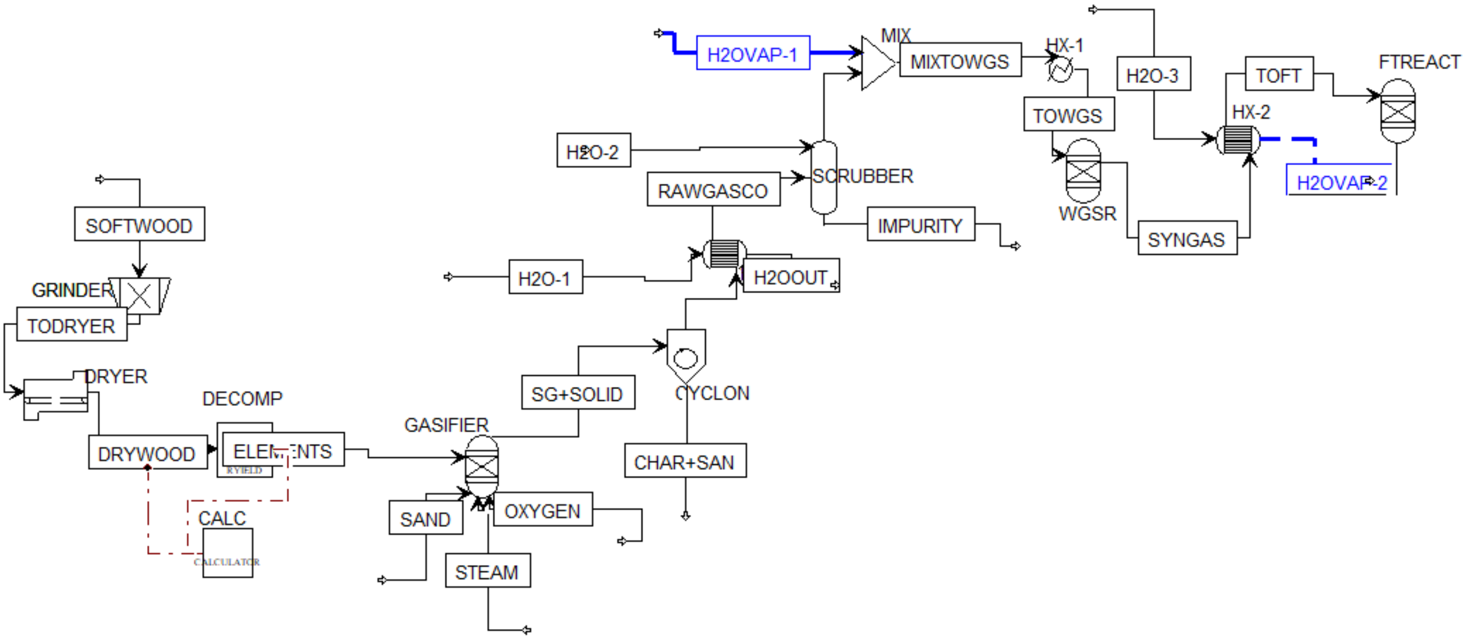

Figure 4.1 - Co-LTFT case simulation flowsheet – thermochemical conversion section

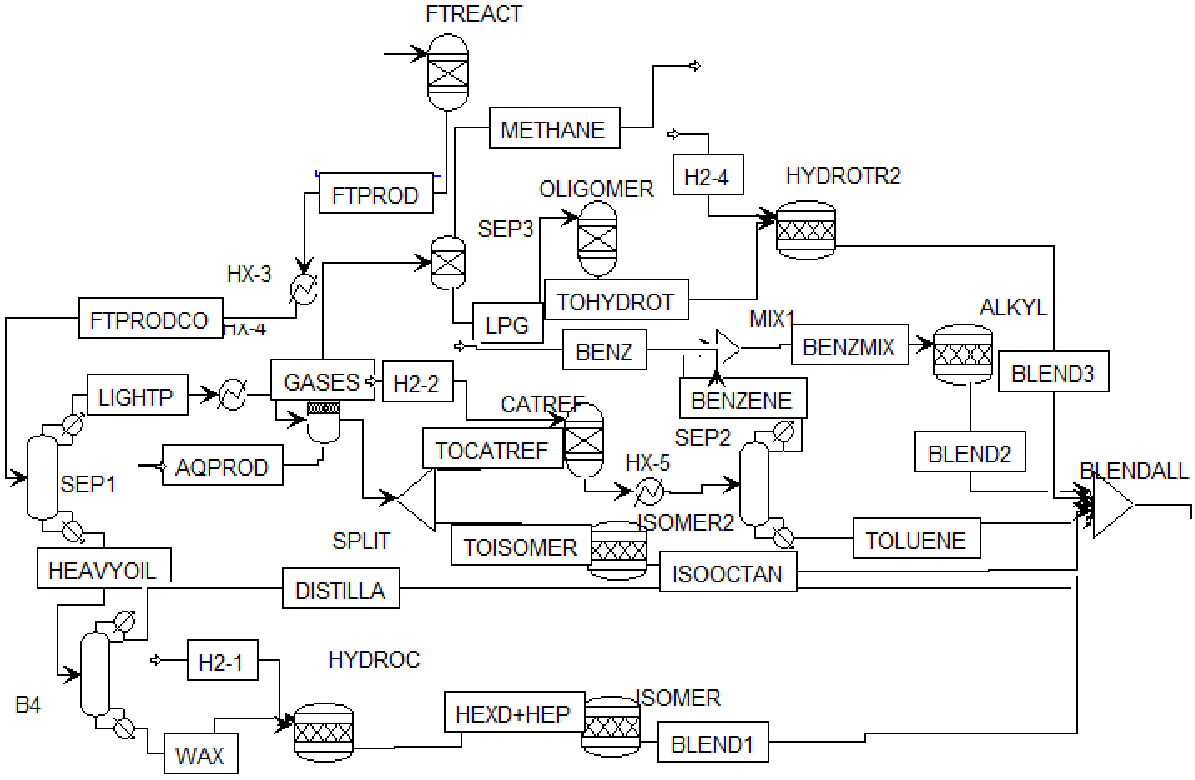

Figure 4.2 - Co-LTFT case simulation flowsheet – upgrading section

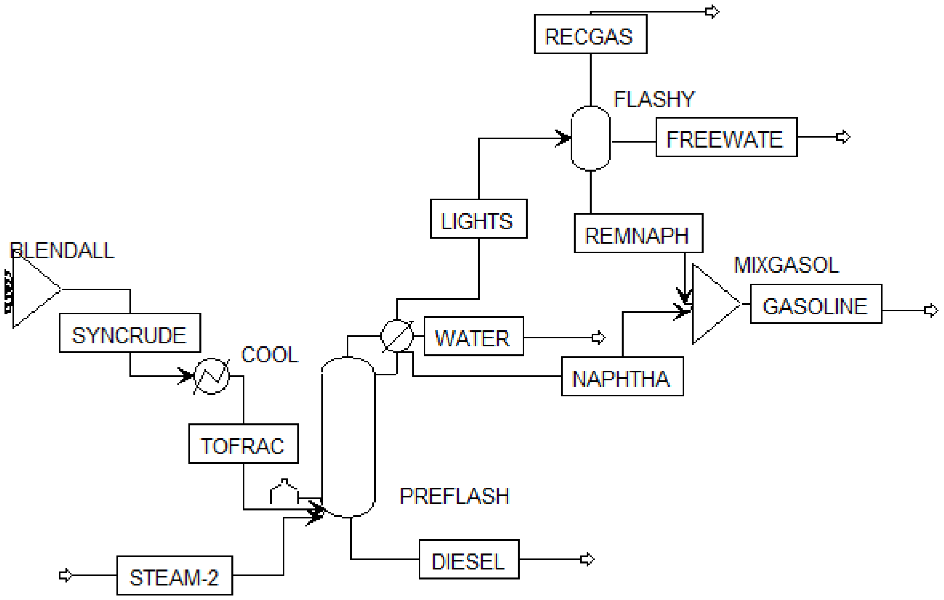

Figure 4.3 - Co-LTFT case simulation flowsheet – separation section

Table 4.3 – Overview of the Aspen unit blocks used for each unit operation in the Co-LTFT process simulation.

Unit ID	Aspen Unit block
GRINDER	Crusher
DRYER	Drier
CYCLON	Cyclone
DECOMP, GASIFIER, WGSR, FTREAC, CATREF, OLIGOMER	Ryield
SCRUBBER, SEP-1	RadFrac
B4, SEP-2	DSTWU
HYDROC, ISOMER, ISOMER2, HYDROTR2, ALKYL	Rstoic
B3	Flash3
SEP3	Sep
PREFLASH	PetroFrac
FLASHY	Flash2

The feedstock selected for the process was spruce, which is a commonly found wood in northern Europe. It is suitable for BtL purpose due to its availability and low sulphur content so the need for sulphur clean up is avoided as water scrubbing is sufficient for its removal [8].

The wood is first grinded to particle size between 2 and 6 mm, which is represented in the simulation as the GRINDER unit. Afterwards the grinded feed is dried in a dryer and led to a DECOMP unit, which is represented as a RYield reactor in Aspen Plus. The DECOMP unit serves to input the elemental composition of the non-conventional solid DRYWOOD stream in the simulation, the ELEMENTS stream so that it can be included as part of the simulation.

The stream is led to an atmospheric fluidized bed gasifier unit represented by a RYield reactor for which the yield was adapted from the yield in P. Ibarra Gonzalez's research [8]. The gasifier uses steam and oxygen as the gasifying mediums, which means the product composition is moved towards higher CO, CO_2 content as well as a higher H/C ratio as depicted in *Figure 3.2.* Sand is used as a heat transferring material (hot bed solids) and is heated to temperatures approximating 1000 °C that lead to final temperatures of around 800 °C in the gasifier. It is selected as an inert component in the reactor simulation.

The product raw gas is led to a series of cyclones, which are represented in the simulation as a single cyclone unit with complete solid/gas separation. The solid-free raw gas stream is cooled to approximately 250 °C and led to a water scrubber unit, represented as a RadFrac unit, where the majority of ammonia is removed. In the scrubber, the temperature ranges from 70 °to 50 °C. The outlet stream at 50 °C is then mixed with pressurized water vapour under 2 bars and at 230 °C. The mix is heated to temperatures of around 360 °C and led to a WGSR unit for H_2/CO ratio adjustment.

The WGSR unit is represented as a RYield reactor operating at 400 °C. The conditions reflect a high temperature shift WGSR process using an iron-based catalyst. The unit yield was again taken from P. Ibarra Gonzalez's research [8] with only CO, CO_2, H_2 and H_2O as the components participating in the reaction.

After the H_2/CO ratio adjustment the syngas stream is cooled to around 250 °C and led to a FT synthesis reactor operating at 220 °C and pressures of 20 bar. The FT reactor is represented by an RYield reactor unit with yields adapted from a generic FT synthesis syncrude composition included in *Table 10.1* in Appendix [48]. The yield used in the simulation is simplified by using certain components to represent a specific product fraction. For this case, it is based on a low temperature FT synthesis using Co-based catalyst. The compounds used for each fraction and their yields are represented in T*able 4.4,* below.

Table 4.4 – Model compounds for representation of LTFT products using Co-based catalyst adapted from [48].

Product fraction	Component	Yield [wt %]
SNG	Methane	8,4
LPG	Propylene	3,5
Naphtha	Octane	19,9
Distillate	Pentadecane	21,9
Wax	Tricosane	44,6
Aqueous Products	Propanol	1,6

The FT product stream is cooled to 100 °C and led to a distillation column represented by a RadFrac unit. The column includes 20 stages with the feed being introduced above the 10th stage. The reflux ratio and distillate mass flow rate is set to 2 and 600 kg/hr, respectively. This configuration was obtained by running a sensitivity analysis for the mass reflux ratio and distillate mass flow rate as the manipulated variables and water mass fraction in the liquid phase (HEAVYOIL stream) as the tabulated variable. Water fraction was chosen due to being the only component present in both streams and for which maximized separation was desired. A plot of the analysis results is shown in *Figure 4.4.* The reflux ratio is not included in the figure since it was found to have no effect on the tabulated variable.

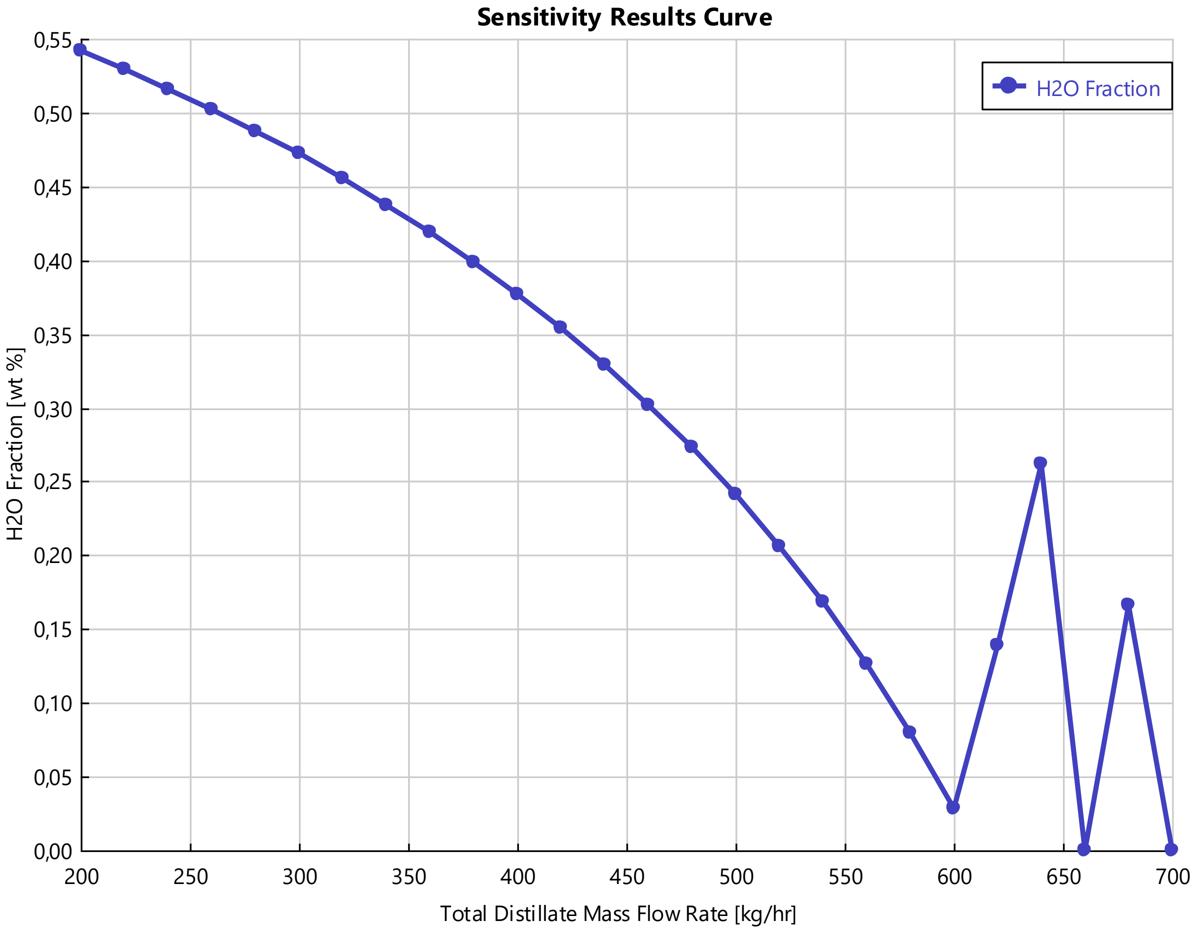

Figure 4.4 – Sensitivity analysis result regarding distillate mass flow rate vs H_2O fraction in the bottom stream.

The heavy oil stream that is mostly composed of distillate and wax range components is sent to a distillation column represented by a DSTWU unit in order to separate the distillate and wax fractions. The WAX stream is hydrocracked in an RStoic reactor operating at 34 bars and 330 °C. In the hydrocracker the tricosane compound together with an additional pressurized H_2 stream reacts to form a mixture of hexadecane and heptane. Complete conversion of wax is assumed. After that a HEXD+HEP stream is sent to an isomerization unit represented by another RStoic rector unit operating at 34 bar and 330 °C. In the reactor, all of heptane is converted into isoheptane. These two reactors are modelled separately although in reality both reactions would occur in one reactor. The final upgraded stream BLEND1 is then mixed with other upgraded stream in a mixing unit.

The DISTILLA stream, which is the distillate stream from the wax/distillate distillation column, does not need further upgrade since it is already composed of linear hydrocarbons, in this case pentadecane and is lead to the mixing unit together with other upgraded streams.

The light products stream (LIGHTP) leaving SEP1 is a vapour stream containing SNG, LPG, naphtha and aqueous product fractions. It is first cooled to 25 °C and led to a Flash3 unit, which represents a 3-phase separator operating at 25 °C and 1 bar. Separation into gaseous, light oil and aqueous product stream is achieved.

The aqueous product stream is discarded since it mostly contains water.

The light oil stream is split so that 40% of the stream is sent to a catalytic reformer represented by a RYield reactor unit and 60% of the stream is sent to an isomerization reactor represented by a RStoic reactor. The separation was done so that the gasoline like fuel produced in the end will suit the EU gasoline specification. In the RStoic reactor complete conversion of octane into isooctane (2,2,4-trimethylpentane) is modelled and the stream mixed together with the rest of the upgraded blends. In the RYield reactor (catalytic reformer), the octane is mixed with additional H_2 and converted into benzene, toluene and methane. The yield is composed of equal amount of methane, benzene and toluene and was used from P. Ibarra Gonzalez's research [8] with H_2 and octane being the only components to react. The NAPHT stream obtained is cooled to 300°C and sent to a distillation column represented by a DSTWU unit for the separation of toluene and benzene. The toluene stream is the final upgraded version of the light oil fraction and is sent to the mixer with the other upgraded stream while the benzene stream is mixed with additional benzene and led into an alkylation unit. In the alkylation unit, which is a RStoic reactor all of the methane and benzene are converted into toluene and mixed with the other rest of the upgraded streams.

The GASES stream from the 3-phase separator is mostly composed of methane and propylene. The two gases are separated into their own individual stream in a cryogenic distillation unit modelled by a SEP unit, where the methane gas is completely separated into its own stream (METHANE). The LPG stream composed mostly of propylene (60% wt.) is sent to an oligomerization unit represented by a RYield reactor at 200 °C and 40 bars pressure. 80% of propylene is modelled to convert into 2-methyl-1-pentene while other components pass as inert gases. The obtained stream is sent to a hydrotreating unit

(RStoic reactor) where 2-methyl-1-pentene is converted into 2-methyl-1-pentane (isohexane) and the BLEND3 stream is sent to the mixer with the other upgraded streams.

The METHANE stream composed entirely of methane is left as tail gas.

The upgraded streams are blended into a SYNCRUDE stream, which is further cooled to 80 °C before entering a fractional distillation unit represented by a PetroFrac unit. The RadFrac unit is composed of 10 stages, with the feed entering at the bottom stage. The temperatures from the top to bottom stage range from 15 to 150 °C. The bottoms mass flow rate was set to 300 kg/hr as satisfactory separation of the main heavy and light fractions was achieved under these conditions. Therefore, 300 kg/hr of the final diesel stream is obtained. The specifications for the obtained diesel fuel were calculated in Aspen Plus and are presented in *Table 4.5.*

The gases stream leaving the fractional distillation at the top (LIGHTS) is a mixture of gaseous and naphtha ranged components, which need to be separated. For this reason, the stream is sent to a 2-phase separator modelled by a Flash2 unit under 30 bars of pressure and 15 °C. Under the specified conditions, the liquid naphtha ranged component can be separated from the gas in the bottom liquid stream (REMNAPH). The gases are recovered as RECGAS stream, which is mostly composed of H_2 and methane.

The NAPHTHA stream from the fractional distillation unit is composed mostly of toluene, isooctane and isoheptane. It is mixed together with the REMNAPH stream into a final gasoline blend for which the calculated specifications can be seen in *Table 4.5* below.

For the vol% content of gasoline, manual calculations from the mass fractions of the stream were computed in excel. Moreover, the research and motor octane numbers were approximated by manually adding up the octane values times the mass fraction of each individual unit together. The rest of the gasoline specifications were calculated in Aspen Plus.

The stream properties for the simulation and the heat exchanger details are presented in *Table 4.6* and *Table 4.7*, respectively.

Table 4.5 – Specifications calculated from the obtained gasoline and diesel fuel streams.

Parameter	Diesel	Gasoline
Cetane number	102	-
Flash point [°C]	50,5	-
Water content [mg/kg]	1885	-
Viscosity at 40 °C [mm^2/s]	2,2	-
Final boiling point [°C]	259	102,5
Density at 15 °C [kg/m^3]	760	750
Motor octane number	-	83
Research octane number	-	88
Reid vapour pressure [kPa]	-	19,0
Olefin content [vol %]	-	0
Aromatics content [vol %]	-	32,4
Benzene content [vol %]	-	0,1
Oxygenate content [vol %]	-	1
Oxygen content [wt %]	-	0,02

Table 4.6 – Stream properties table for Co-LTFT

Stream Name	SOFTWOOD	SG+SOLID	CHAR+SAN	IMPURITY	TOWGS	SYNGAS	FTPROD	HEAVYOIL	LIGHTP	AQPROD	BLEND1	DISTILLA	ISOOCTAN	TOLUENE	BLEND2	BLEND3	METHANE	SYNCRUDE	DIESEL	GASOLINE	RECGAS
Temperature [°C]	20	800	800	69,7	357	400	220	137	95	25	340	120	340	110	110	340	25	205	150	14	15
Pressure [bar]	1	1	1	1,06	1	1	20	1	1	1	34	1	34	1	1	34	1	1	1	1	30
Mass Vapor Fraction	0	0,11	0	0	1	1	0,678	0	1	0	0	0	1	0	1	1	1	0,726	0	0	1
Mass Liquid Fraction	0	0	0	1	0	0	0,322	1	0	1	1	1	0	1	0	0	0	0,274	1	1	0
Mass Solid Fraction	1	0,89	1	0	0	0	0	0	0	0	0	0	0	0	0	0	0	0	0	0	0
Enthalpy flow rate[GJ/hr]	-3,138	-110,4	-106,3	-151,5	-7,46	-6,46	-6,57	-0,74	-6,06	-6,80	-0,279	-0,361	-0,076	0,004	0,052	-0,035	-0,176	-0,695	-0,497	-0,302	-0,001
Mass flow rate [kg/hr]	500,0	8355,0	7466,0	9732,0	957,0	957,0	957,0	356,9	600,0	456,0	232,6	125,7	59,2	12,8	80,0	17,3	37,8	527,7	300,0	213,2	3,7
Component mass flow rate [kg/hr]																					
Spruce	500	0	0	0	0	0	0	0	0	0	0	0	0	0	0	0	0	0	0	0	0
O_2	0	0	0	0	0	0	0	0	0	0	0	0	0	0	0	0	0	0	0	0	0
CO	0	116	0	1	115	111	0	0	0	0	0	0	0	0	0	0	0	0	0	0	0
CO_2	0	169	0	6	163	162	0	0	0	0	0	0	0	0	0	0	0	0	0	0	0
H_2	0	133	0	Trace	133	182	0	0	0	0	Trace	0	0	0	1,7	Trace	0	1,7	Trace	Trace	1,7
N_2	0	Trace	0	Trace	Trace	Trace	Trace	Trace	Trace	Trace	0	0	Trace	Trace	Trace	Trace	0	Trace	Trace	Trace	Trace
C_2H_2	0	Trace	0	Trace	Trace	Trace	0	0	0	0	0	0	0	0	0	0	0	0	0	0	0
C_2H_4	0	13	0	2	11	11	0	0	0	0	0	0	0	0	0	0	0	0	0	0	0
C_2H_6	0	4	0	1	4	4	0	0	0	0	0	0	0	0	0	0	0	0	0	0	0
H2O	0	320	0	9639	481	435,6	436,0	9,9	425,7	424,2	Trace	9,9	Trace	Trace	Trace	1,5	0	11,5	0,6	Trace	Trace
SAND	0	7450	7450	0	0	0	0	0	0	0	0	0	0	0	0	0	0	0	0	0	0
CHAR	0	16	16	0	0	0	0	0	0	0	0	0	0	0	0	0	0	0	0	0	0
NH_3	0	89	0	81	7	7	0	0	0	0	0	0	0	0	0	0	0	0	0	0	0
CH_4	0	46	0	2	42	42	43,8	Trace	43,8	5,7	0	0	Trace	Trace	0	0	37,8	Trace	Trace	Trace	Trace
C_3H_6	0	0	0	0	0	0	18,2	Trace	18,2	8,7	0	0	Trace	Trace	Trace	1,8	0	2,2	Trace	0,8	1,4
Octane	0	0	0	0	0	0	103,7	Trace	103,7	Trace	0	0	0	0	0	5,8	0	5,8	3,8	2,1	Trace
Isohexane	0	0	0	0	0	0	0	0	0	0	0	0	0	0	0	7,5	0	7,5	Trace	7,4	Trace
Isoheptane	0	0	0	0	0	0	0	0	0	0	71	0	0	0	0	0	0	71,0	2,8	68,2	Trace
Isooctane	0	0	0	0	0	0	0	0	0	0	0	0	58,7	0	0	0	0	58,7	2,8	55,9	Trace
Pentadecane	0	0	0	0	0	0	114,6	114,6	Trace	0	1,1	113,5	0	0	0	0	0	115,0	114,6	Trace	0
Hexadecane	0	0	0	0	0	0	0	0	0	0	160,5	0	0	0	0	0	0	160,5	160,5	Trace	0
Tricosane	0	0	0	0	0	0	232,4	232,4	Trace	0	0	2,3	0	0	0	0	0	2,3	2,3	Trace	0
Benzene	0	0	0	0	0	0	0	0	0	0	0	0	0	Trace	Trace	0	0	Trace	Trace	Trace	Trace
Toluene	0	0	0	0	0	0	0	0	0	0	0	0	0	12,6	78,0	0	0	90,7	12,5	78,1	Trace
Propanol	0	0	0	0	0	0	8,3	Trace	8,3	7,7	0	0	Trace	Trace	Trace	Trace	0	0,7	Trace	0,7	Trace

Table 4.7 – Heat exchanger details for Co-LTFT

Heat Exchanger	Type	Base Duty [Gcal/hr]	Hot Inlet Temperature [°C]	Hot Outlet Temperature [°C]	Cold Inlet Temperature [°C]	Cold Outlet Temperature [°C]	Base Area [m^2]	Hot Side Fluid	Cold Side Fluid	Heat Transfer Coefficient [kcal/hr*m^2*K]
GASIFIER_heat_Exchanger	Cooler	0,5047	800	799,5	249	250	5,512	GASIFIER_heat	HP Steam Generation	166,4
HX	Process Exchanger	0,4337	800	278,6	20	100,7	36,44	RAWGAS_To_RAWGASCO	H2O-1_To_H2OOUT	29
HX-3	Cooler	0,1262	220	100	30	35	13,04	FTPROD_To_FTPRODCO	Air	81,6
COOL	Cooler	0,05775	205,3	80	30	35	7,143	SYNCRUDE_To_TOFRAC	Air	83,6
Condenser@B4	Cooler	0,01701	120,7	120,2	30	35	3,154	To Condenser@B4_TO_DISTILLA	Air	61,4
HYDROC_heat_Exchanger	Cooler	0,01277	340	339,5	249	250	0,8499	HYDROC_heat	HP Steam Generation	166,4
HX-2	Process Exchanger	0,1339	400	260,8	20	218,8	31,45	SYNGAS_To_TOFT	H2O-3_To_H2OVAP-2	23,1
ALKYL_heat_Exchanger	Heater	0,01618	125	124	31,4	110	2,3	LP Steam	ALKYL_heat	166,4
HX-1	Heater	0,2203	1000	400	80,7	357	77,73	Fired Heat (1000)	MIXTOWGS_To_TOWGS	7,2
HX-5	Cooler	0,005146	500	300	249	250	1,269	NAPHT_To_TOSEP2	HP Steam Generation	31,8
CATREF_heat_Exchanger	Heater	0,02098	1000	400	20	500	0,9806	Fired Heat (1000)	CATREF_heat	61,4
Reboiler@PREFLASH	Heater	0,06624	175	174	86,8	150	1,36	MP Steam	To Reboiler@PREFLASH_TO_DIESEL	775,6
ISOMER2_heat_Exchanger	Heater	0,01296	1000	400	25,2	340	0,4883	Fired Heat (1000)	ISOMER2_heat	61,4
ISOMER_heat_Exchanger	Cooler	0,000886	340	339,5	249	250	0,05897	ISOMER_heat	HP Steam Generation	166,4
HYDROTR2_heat_Exchanger	Cooler	0,000427	340	339,5	249	250	0,02841	HYDROTR2_heat	HP Steam Generation	166,4
OLIGOMER_heat_Exchanger	Heater	0,000198	250	249	25	200	0,01028	HP Steam	OLIGOMER_heat	166,4
Condenser@SEP1	Cooler	0,652	98,3	95,1	30	35	106,9	To Condenser@SEP1_TO_LIGHTPDuplicate	Air	94,1
Condenser@SEP2	Cooler	0,06423	32,4	31,9	20	25	41,84	To Condenser@SEP2_TO_BENZENE	Cooling Water	163,3
Condenser@PREFLASH	Cooler	0,08975	75,5	15	-25	-24	1,872	To Condenser@PREFLASH_TO_WATER	Refrigerant 1	615,7
FLASHY_heat_Exchanger	Cooler	0,00052	15	14,5	-25	-24	0,08888	FLASHY_heat	Refrigerant 1	149
B3_heat_Exchanger	Cooler	0,01389	25	24,5	-25	-24	1,892	B3_heat	Refrigerant 1	149
Reboiler@B4	Heater	0,05523	3000	2999	376,8	377,3	0,3431	Very High Temperature	To Reboiler@B4_TO_WAX	61,4
HX-4	Cooler	0,2635	95,1	25	-25	-24	2,714	LIGHTP_To_TOFL2	Refrigerant 1	952,4
Reboiler@SEP1	Heater	0,7227	175	174	100,3	137,1	7,171	MP Steam	To Reboiler@SEP1_TO_HEAVYOIL	1458,8
Reboiler@SEP2	Heater	0,05835	125	124	109,1	109,6	23,22	LP Steam	To Reboiler@SEP2_TO_TOLUENE	166,4
WGSR_heat_Exchanger	Heater	0,2399	1000	400	357	400	19,44	Fired Heat (1000)	WGSR_heat	61,4
FTREACT_heat_Exchanger	Heater	0,1086	250	249	220	220,5	22,3	HP Steam	FTREACT_heat	166,4

4.2 Fe-LTFT simulation case

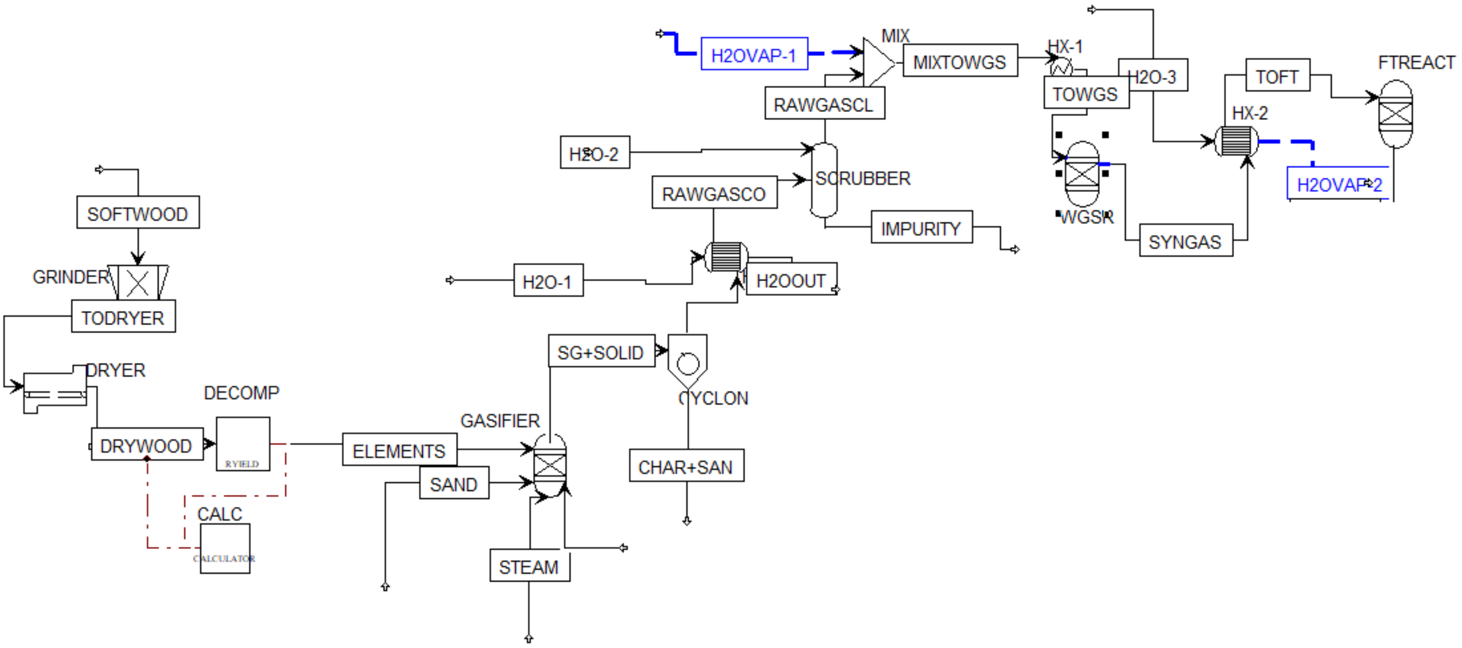

Figure 4.5 – Fe-LTFT simulation flowsheet – thermochemical conversion section

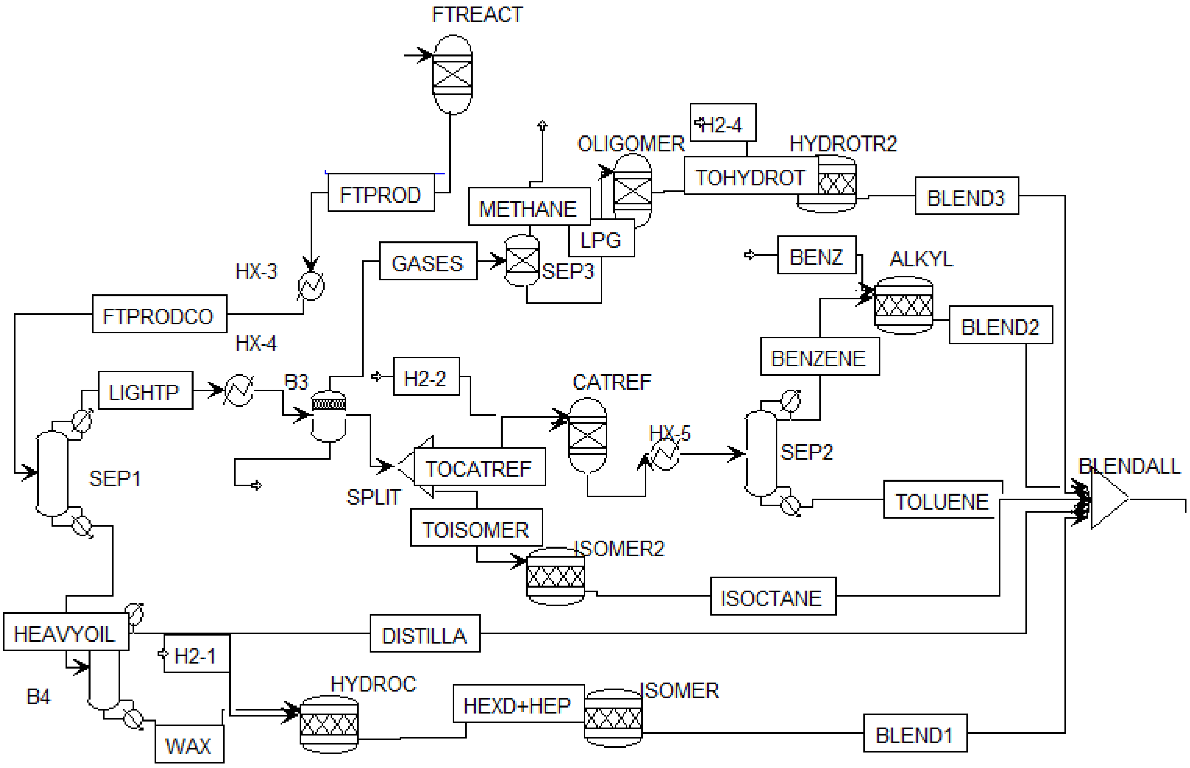

Figure 4.6 – Fe-LTFT simulation flowsheet – upgrading section

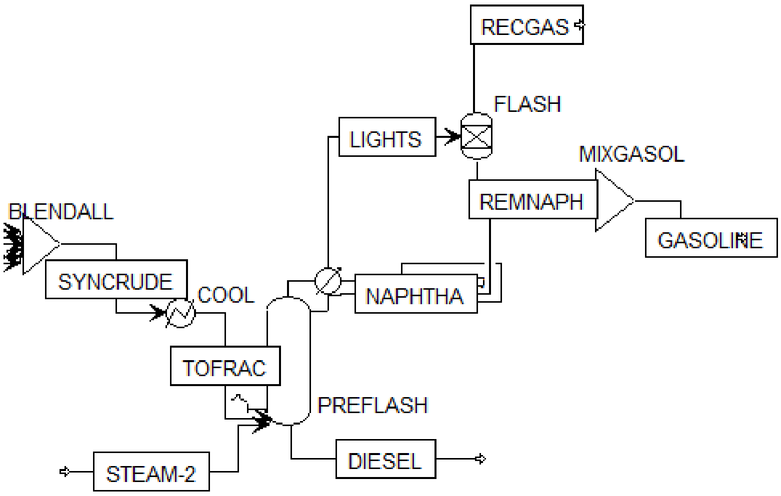

Figure 4.7 - Fe-LTFT simulation flowsheet – separation section

In this alternative case, LTFT synthesis using Fe-based catalyst is modelled by using a yield specific for this kind of catalyst.

Table 4.8 - Model compounds for representation of LTFT products using Fe-based catalyst adapted from [48].

Product fraction	Component	Yield [wt %]
SNG	Methane	6,3
LPG	Propylene	7,8
Naphtha	Octane	12,3
Distillate	Pentadecane	19,5
Wax	Tricosane	49,9
Aqueous Products	Propanol	4,2

As can be seen by comparing *Table 4.4* and *Table 4.8* the only difference in the LTFT products is the product distribution due to the use of a different catalyst. Therefore, for this case the operating units remain the same and were modelled the same as in the Co-LTFT case. The difference between this case and the previous is the mass flow rates of the individual streams. For instance, the distillate flow rate in SEP-1 distillation column was set to 580 kg/hr, which was 20 kg/hr less than in Co-LTFT case, due to a higher amount of the distillate and wax fraction. The differences amount to a difference in the gasoline and diesel fuel stream for which the specifications are presented in *Table 4.9.*The stream properties and exchanger detail information are presented in *Table 4.10* and *Table 4.11, respectively.*

Table 4.9 - Specifications calculated from the obtained gasoline and diesel fuel streams.

Parameter	Diesel	Gasoline
Cetane number	106	-
Flash point [°C]	87,3	-
Water content [mg/kg]	2655	-
Viscosity at 40 °C [mm^2/s]	2,5	-
Final boiling point [°C]	270	99,8
Density at 15 °C [kg/m^3]	766	739
Motor octane number	-	75
Research octane number	-	79
Reid vapour pressure [kPa]	-	34,6
Final boiling point [°C]	-	99,8
Olefin content [vol %]	-	0
Aromatics content [vol %]	-	28,8
Benzene content [vol %]	-	0,05
Oxygenate content [vol %]	-	1
Oxygen content [wt %]	-	0,02

Table 4.10 – Stream properties table for Fe-LTFT

Stream Name	SOFTWOOD	SG+SOLID	CHAR+SAN	MPURITY	TOWGS	SYNGAS	FTPROD	HEAVYOIL	LIGHTP	AQPROD	BLEND1	DISTILLA	ISOOCTAN	TOLUENE	BLEND2	BLEND3	METHANE	SYNCRUDE	DIESEL	GASOLINE	RECGAS
Temperature [°C]	20	800	800	69,7	357	400	220	127,7998	95,4	25	340	112,8	340	109,6	110	340	24,99999	204,8	150	13,9	15
Pressure [bar]	1	1	1	1,06	1	1	20	1	1	1	34	1	34	1	1	34	1	1	1	1	30
Mass Vapor Fraction	0	0,11	0	0	1	1	0,66	0	1	0	0	0	1	0	1	1	1	0,68	0	0	1
Mass Liquid Fraction	0	0	0	1	0	0	0,34	1	0	1	1	1	0	1	0	0	0	0,32	1	1	0
Mass Solid Fraction	1	0,89	1	0	0	0	0	0	0	0	0	0	0	0	0	0	0	0	0	0	0
Enthalpy flow rate[GJ/hr]	-3,138	-110,4	-106,3	-151,5	-7,46	-6,46	-6,5202	-0,8599	-5,91	-6,78	-0,3122	-0,424	-0,0389	0,00286	0,03897	-0,0395	-0,128	-0,773	-0,4995	-0,292	0,0003
Mass flow rate [kg/hr]	500,0	8355,0	7466,0	9732,0	957,0	957	957	376,9	580,0	466,9	260,0	118,5	30,2	9,7	60,9	25,6	27,5	504,8	290,0	194,8	4,2
Component mass flow rate [kg/hr]																					
Spruce	500	0	0	0	0	0	0	0	0	0	0	0	0	0	0	0	0	0	0	0	0
O_2	0	0	0	0	0	0	0	0	0	0	0	0	0	0	0	0	0	0	0	0	0
CO	0	116	0	1	115	111	0	0	0	0	0	0	0	0	0	0	0	0	0	0	0
CO_2	0	169	0	6	163	162	0	0	0	0	0	0	0	0	0	0	0	0	0	0	0
H_2	0	133	0	Trace	133	182	0	0	0	0	Trace	0	0	0	1,3	Trace	0	1,3	Trace	Trace	1,3
N_2	0	Trace	0	Trace	Trace	Trace	Trace	Trace	Trace	Trace	0	0	Trace	Trace	Trace	Trace	0	Trace	Trace	Trace	Trace
C_2H_2	0	Trace	0	Trace	Trace	Trace	0	0	0	0	0	0	0	0	0	0	0	0	0	0	0
C_2H_4	0	13	0	2	11	11	0	0	0	0	0	0	0	0	0	0	0	0	0	0	0
C_2H_6	0	4	0	1	4	4	435,6	0	0	0	0	0	0	0	0	0	0	0	0	0	0
H2O	0	320	0	9639	481	435,6	0	15	420	419	Trace	15	Trace	Trace	Trace	1	0	16	0,9	Trace	Trace
SAND	0	7450	7450	0	0	0	0	0	0	0	0	0	0	0	0	0	0	0	0	0	0
CHAR	0	16	16	0	0	0	0	0	0	0	0	0	0	0	0	0	0	0	0	0	0
NH_3	0	89	0	81	7	7	0	0	0	0	0	0	0	0	0	0	0	0	0	0	0
CH_4	0	46	0	2	42	42	32,8	Trace	32,8	5,2	0	0	Trace	Trace	0	0	27,5	Trace	Trace	Trace	Trace
C_3H_6	0	0	0	0	0	0	40,6	Trace	40,6	21,8	0	0	Trace	Trace	Trace	3,7	0	4,2	Trace	1,7	2,5
Octane	0	0	0	0	0	0	64,1	Trace	64,1	Trace	0	0	0	0	0	4,8	0	4,8	Trace	4,5	Trace
Isohexane	0	0	0	0	0	0	0	0	0	0	0	0	0	0	0	15	0	15,0	Trace	14,6	Trace
Isoheptane	0	0	0	0	0	0	0	0	0	0	79,4	0	0	0	0	0	0	79,4	2,7	76,7	Trace
Isooctane	0	0	0	0	0	0	0	0	0	0	0	0	29,6	0	0	0	0	29,6	1,1	28,4	Trace
Pentadecane	0	0	0	0	0	0	101,6	101,6	Trace	0	1,0	100,6	0	0	0	0	0	101,6	99,5	2,1	Trace
Hexadecane	0	0	0	0	0	0	0	0	0	0	179,54	0	0	0	0	0	0	179,5	179,1	Trace	Trace
Tricosane	0	0	0	0	0	0	260	260	Trace	0	0	2,6	0	0	0	0	0	2,6	2,6	Trace	0
Benzene	0	0	0	0	0	0	0	0	0	0	0	0	0	Trace	Trace	0	0	Trace	Trace	Trace	Trace
Toluene	0	0	0	0	0	0	0	0	0	0	0	0	0	9,6	59	0	0	68,5	3,6	64,9	Trace
Propanol	0	0	0	0	0	0	21,9	Trace	21,9	20,7	0	0	Trace	Trace	Trace	0,6	0	1	Trace	1,1	Trace

Table 4.11 – Heat exchanger details for Fe-LTFT

Heat Exchanger	Type	Base Duty [Gcal/hr]	Hot Inlet Temperature [°C]	Hot Outlet Temperature [°C]	Cold Inlet Temperature [°C]	Cold Outlet Temperature [°C]	Base Area [m^2]	Hot Side Fluid	Cold Side Fluid	Heat Transfer Coefficient [kcal/hr*m^2*K]
Reboiler@SEP1	Heater	4,621	175	174	100,2	127,8	21,32	MP Steam	To Reboiler@SEP1_TO_HEAVYOIL	2964,4
GASIFIER_heat_Exchanger	Cooler	0,5047	800	799,5	249	250	5,512	GASIFIER_heat	HP Steam Generation	166,4
HX	Process Exchanger	0,4337	800	278,6	20	100,7	36,44	RAWGAS_To_RAWGASCO	H2O-1_To_H2OOUT	29
COOL	Cooler	0,05284	204,8	80	30	24,8	6,067	SYNCRUDE_To_TOFRAC	Air	83,6
Condenser@B4	Cooler	0,01931	113,3	112,8	30	24,8	3,676	To Condenser@B4_TO_DISTILLA	Air	61,4
HYDROC_heat_Exchanger	Cooler	0,01435	340	339,5	249	250	0,9552	HYDROC_heat	HP Steam Generation	166,4
HX-2	Process Exchanger	0,1339	400	260,8	20	218,8	31,45	SYNGAS_To_TOFT	H2O-3_To_H2OVAP-2	23,1
ALKYL_heat_Exchanger	Heater	0,01211	125	124	40	110	1,831	LP Steam	ALKYL_heat	166,4
HX-1	Heater	0,2556	1000	400	80,7	400	98,31	Fired Heat (1000)	MIXTOWGS_To_TOWGS	7,2
HX-5	Cooler	0,003934	500	300	250	250	0,9736	NAPHT_To_TOSEP2	HP Steam Generation	31,8
CATREF_heat_Exchanger	Heater	0,01599	1000	400	20	500	0,7474	Fired Heat (1000)	CATREF_heat	61,4
HYDROTR2_heat_Exchanger	Cooler	0,001886	340	339,5	249	250	0,1256	HYDROTR2_heat	HP Steam Generation	166,4
OLIGOMER_heat_Exchanger	Cooler	0,001832	200	199,5	174	175	0,436	OLIGOMER_heat	MP Steam Generation	166,4
ISOMER2_heat_Exchanger	Heater	0,006633	1000	400	24,9	340	0,2499	Fired Heat (1000)	ISOMER2_heat	61,4
ISOMER_heat_Exchanger	Cooler	0,000991	340	339,5	249	250	0,06597	ISOMER_heat	HP Steam Generation	166,4
Reboiler@PREFLASH	Heater	1,19E-05	175	175	149,5	150	0,000617	MP Steam	To Reboiler@PREFLASH_TO_DIESEL	765,2
B3_heat_Exchanger	Cooler	0,01429	25	24,5	-25	-25,5	1,918	B3_heat	Refrigerant 1	149
WGSR_heat_Exchanger	Heater	0,2045	3000	2999	400	400,5	1,282	Very High Temperature	WGSR_heat	61,4
Condenser@SEP2	Cooler	0,04851	32,4	31,9	20	25	31,34	To Condenser@SEP2_TO_BENZENE	Cooling Water	163,3
Reboiler@B4	Heater	0,06391	3000	2999	377,1	377,6	0,3971	Very High Temperature	To Reboiler@B4_TO_WAX	61,4
HX-4	Cooler	0,2597	95,4	25	-25,5	-24	2,646	LIGHTP_To_TOFL2	Refrigerant 1	956,9
FTREACT_heat_Exchanger	Heater	0,1198	250	249	220	220,5	24,61	HP Steam	FTREACT_heat	166,4
Reboiler@SEP2	Heater	0,04402	125	124	109,1	109,6	17,49	LP Steam	To Reboiler@SEP2_TO_TOLUENE	166,4
FLASH_heat_Exchanger	Cooler	0,000502	15	14,5	-25	-25,5	0,08428	FLASH_heat	Refrigerant 1	149
Condenser@SEP1	Cooler	-4,289	98,4	95,4	30	24,8	-635,5	To Condenser@SEP1_TO_LIGHTPDuplicate	Air	94,1
Condenser@PREFLASH	Cooler	-0,09737	106,6	15	-25	-25,5	-1,767	To Condenser@PREFLASH_TO_WATER	Refrigerant 1	615,9
HX-3	Cooler	0,1247	220	100	24,8		-32770	FTPROD_To_FTPRODCO	Air	-28174548,6

4.3 HTFT simulation case

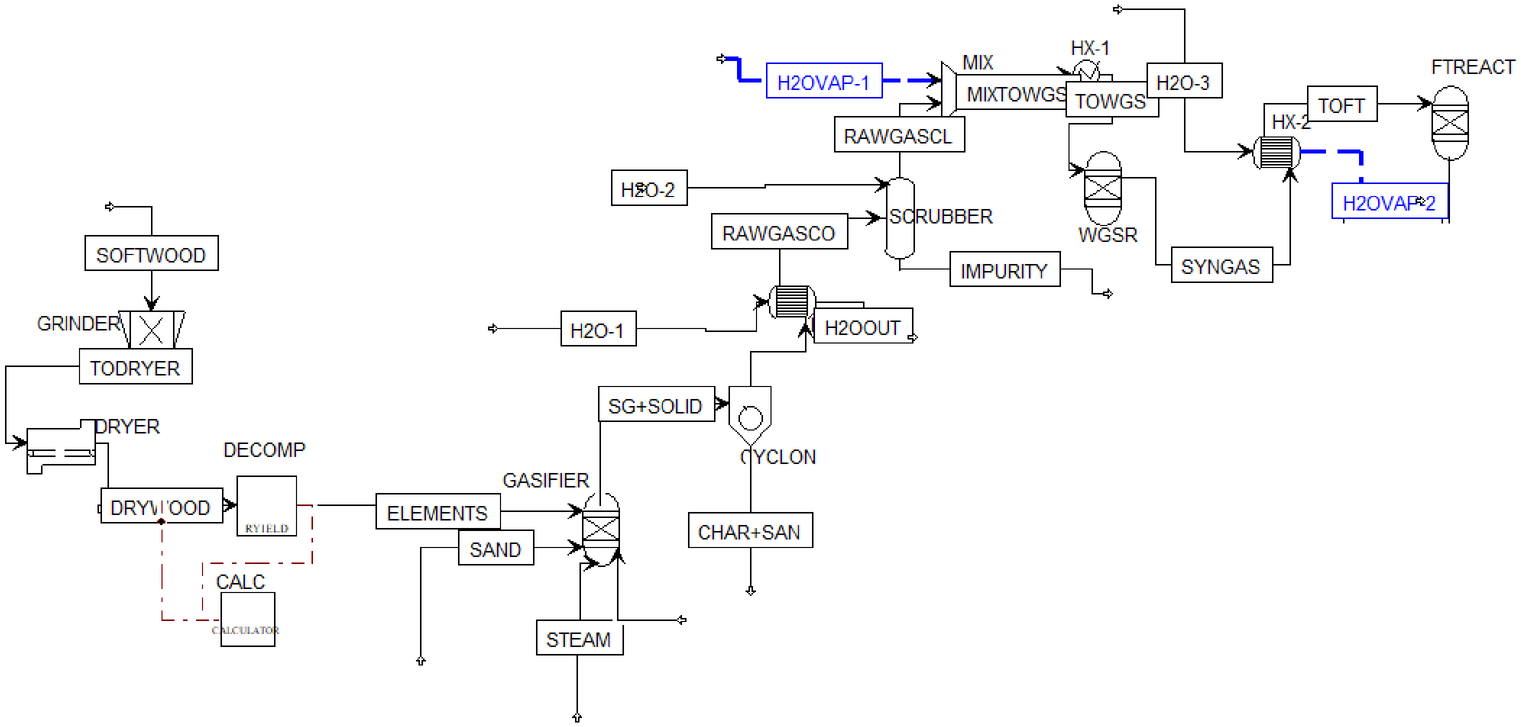

Figure 4.8 - HTFT case simulation flowsheet – thermochemical conversion section

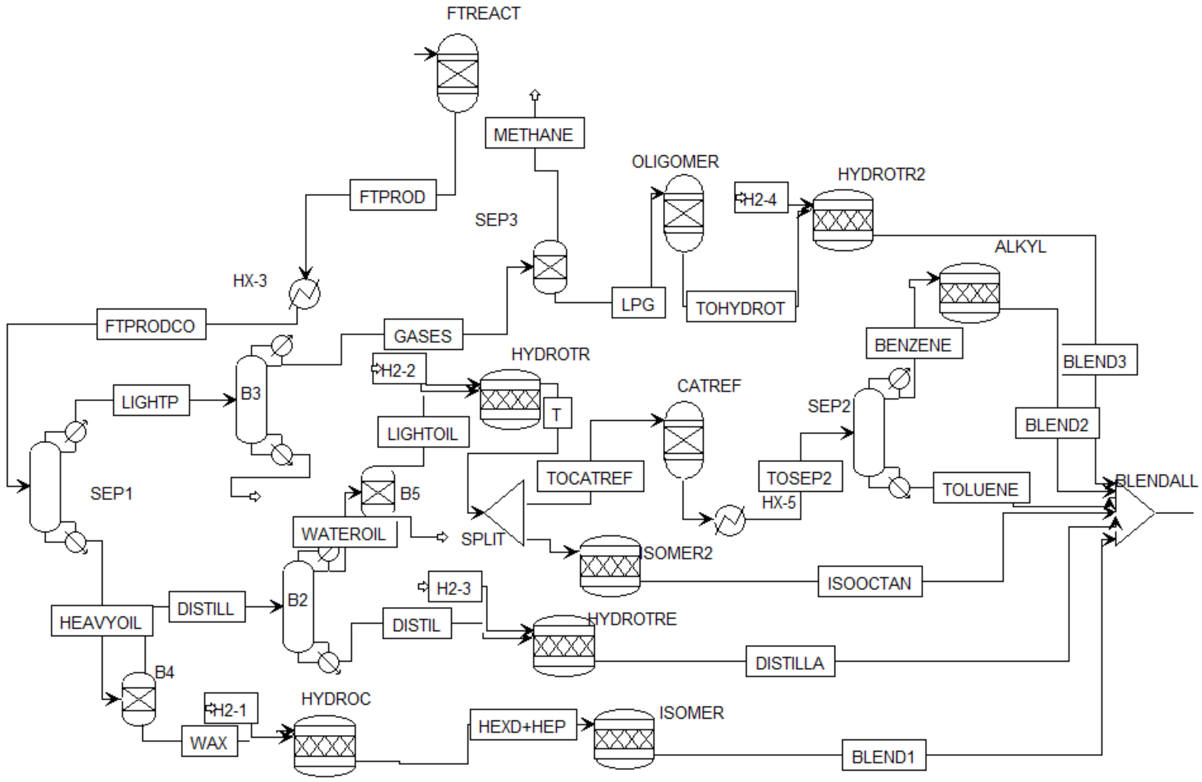

Figure 4.9 - HTFT case simulation flowsheet – upgrading section

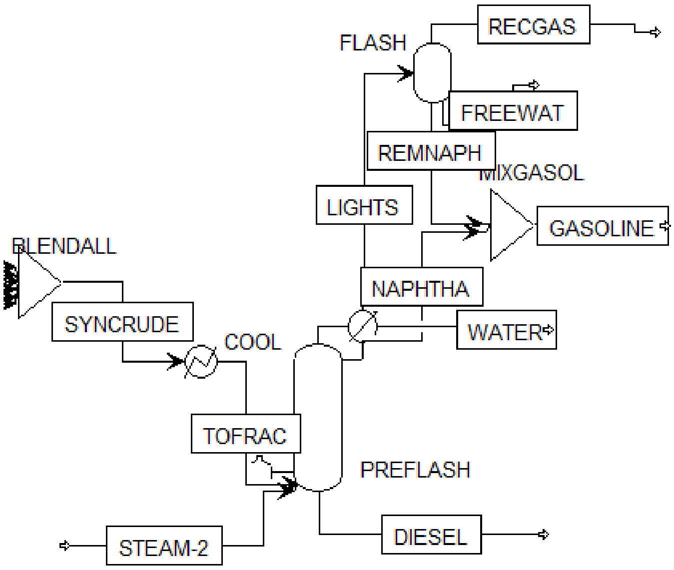

Figure 4.10 - HTFT case simulation flowsheet – separation section

Table 4.12 – Overview of the Aspen unit blocks used for each unit operation in the HTFT process simulation.

Unit ID	Aspen Unit block
GRINDER	Crusher
DRYER	Drier
CYCLON	Cyclone
DECOMP, GASIFIER, WGSR, FTREAC, CATREF, OLIGOMER	Ryield
SCRUBBER, SEP-1	RadFrac
B2, B3, SEP-2	DSTWU
HYDROC, ISOMER, HYDROTRE, ISOMER2, HYDROTR, ALKYL, HYDROTR2	Rstoic
B4, B5, SEP3	Sep
PREFLASH	PetroFrac
FLASH	Flash2

The last case is done with FT synthesis under high temperature conditions with Fe-based catalyst. The product distribution of the synthesis is modelled as presented in *Table 4.13*.

Table 4.13 - Model compounds for representation of HTFT products using Fe-based catalyst adapted from [48].

Product fraction	Component	Yield [wt %]
SNG	Methane	22,8
LPG	Propylene	24,2
Naphtha	Octene	33,4
Distillate	Pentadecene	7,0
Wax	Tricosane	2,9
Aqueous Products	Ethanol	9,7

The major difference in the FT products in comparison with the LTFT cases is that the majority of the products are made of the smaller carbon chain molecules (methane, propylene, octene). Secondly, higher contents of olefin compounds are produced such as octene and pentadecene instead of their paraffin counterparts. Finally, the propanol is replaced with the smaller carbon number ethanol.

Due to the changes in the product distribution the upgrading section is comprised of different operating units for the product separation. Therefore, the cooled FT product stream is sent to the distillation column (SEP1) modelled as a RadFrac unit with 20 stages. In this case, the distillate rate was increased to 720 kg/hr compared to the other cases since there are more products with lower boiling points in the feed stream. The distillate rate was obtained so that the biggest possible split was achieved for the octene compound, so that most of it (98,6%) is split into the HEAVYOIL stream. The light stream (LIGHTP) mostly contains water, methane and propylene.

The HEAVYOIL stream composed of water, octene, pentadecene and tricosane is sent to a distillation column modelled by a Sep unit where the wax stream gets separated together with a small amount of pentadecene in the bottom stream. The wax stream is treated in the same manner, as in the LTFT case, it is hydrocracked and isomerized to convert the wax fraction into hexadecane and isoheptane.

The lighter DISTILL stream, containing water, octene and pentadecene is sent to a second distillation tower modelled by a RadFrac unit with 20 stages and 180 kg/hr distillate rate. Under these conditions, almost a complete split between water and octene in the lighter stream (WATEROIL) and pentadecene and traces of tricosane in the heavier stream (DISTIL) is achieved.

The heavier stream, containing mostly pentadecene is sent to a hydrotreater where conversion of pentadecene into pentadecane under temperatures of 34 °C and 34 bars is achieved. Afterwards the mostly pentadecane stream (DISTILLA) is mixed together with the other upgraded streams.

The lighter stream (WATEROIL) is sent to a separator unit, modelled by a Sep unit, to separate the water from octene. Complete separation was assumed. The octene stream (LIGHTOIL) is further sent to a hydrotreater unit to convert the octene into octane. The conversion is modelled at 340 °C and pressures of 34 bars. Afterwards the octane stream is split into two equal mass flow streams. One stream is led to an isomerization unit to form isooctane while the other is catalytically reformed to form aromatic compounds (benzene, toluene) and some methane as in the previous cases. The stream leaving the catalytic reformer is processed in the same manner as in previous cases, it is cooled after which the benzene and methane are separated from toluene by distillation and sent to an alkylation unit while the toluene stream is mixed with the other upgraded streams. In this case, no additional benzene was added before the alkylation unit, since enough benzene was already produced due to there being a higher amount of naphtha-ranged compounds in HTFT synthesis. Therefore, in the RStoic ALKYL reactor a 20% conversion of methane into toluene was set as the limiting factor. The product stream (BLEND2) is mixed with the other upgraded streams.

The LIGHTP stream, which is the gaseous stream leaving SEP1 is first cooled to room temperature and afterwards sent to a distillation column (DSTWU) to separate the aqueous products from the gases. A 99.9% separation of methane with 0,1% content of water is modelled to be separated. The AQPROD stream is discarded as waste stream.

The GASES stream is treated in the same manner as with the previous cases. It is sent to a SEP unit, representing cryogenic distillation, where methane and propylene are divided into their own stream. Afterwards methane is used for energy purposes while the propylene stream is upgraded through oligomerization to form 2-methyl-1-pentene into isomerization for the formation of 2-methyl-1-pentane. After which the stream (BLEND3) is mixed with the other upgraded streams.

The upgraded streams are blended into a SYNCRUDE stream, which is then separated similarly to the previous cases. The biggest difference is the bottoms flow rate is set to 45 kg/hr since there are much less diesel-ranged compounds in this case.

The gases stream leaving the fractionation column at the top (LIGHTS) is a mixture of gaseous and naphtha ranged components, which need to again be separated. The separation is achieved in a 2 phase separator, modelled by a Flash2 unit operating at 15 °C and 20 bars. The bottom liquid stream (REMNAPH) is mixed with the rest of the NAPHTHA stream to form the final gasoline blend while the gases are recovered as RECGAS stream.

The calculations for the final gasoline and diesel streams were completed in the same manner as for the previous cases and are presented in *Table 4.14*, below. The streams properties and the heat exchanger details are presented in *Table 4.15* and *Table 4.16*, respectively.

A comparison between the product profiles for each case is included in the next chapter.

Table 4.14 - Specifications calculated from the obtained gasoline and diesel fuel streams.

Parameter	Diesel	Gasoline
Cetane number	102,5	-
Flash point [°C]	107,9	-
Water content [mg/kg]	6000	-
Viscosity at 40 °C [mm^2/s]	2,9	-
Final boiling point [°C]	261	110
Density at 15 °C [kg/m^3]	765	714
Motor octane number	-	88
Research octane number	-	91
Reid vapour pressure [kPa]	-	12,9
Olefin content [vol %]	-	1,5
Aromatics content [vol %]	-	20,2
Benzene content [vol %]	-	0,2
Oxygenate content [vol %]	-	0
Oxygen content [wt %]	-	0,02

Table 4.15 – Stream properties table for HTFT

Stream Name	SOFTWOOD	SG+SOLID	CHAR+SAN	IMPURITY	TOWGS	SYNGAS	FTPROD	HEAVYOIL	LIGHTP	AQPROD	BLEND1	DISTILLA	ISOOCTAN	TOLUENE	BLEND2	BLEND3	METHANE	SYNCRUDE	DIESEL	GASOLINE	RECGAS
Temperature [°C]	20	800	800	69,7	357	400	325,0	114,2	89	84,1	340	340	340	109,6	110	340	-11,9	258,1	150	14,9	15
Pressure [bar]	1	1	1	1,06	1	1	25	1	1	1	34	34	34	1	1	34	1	1	1	1	20
Mass Vapor Fraction	0	0,11	0	0	1	1	1	0	1	0	0	0	1	0	1	1	1	1	0	0	1
Mass Liquid Fraction	0	0	0	1	0	0	0	1	0	1	1	1	0	1	0	0	0	0	1	1	0
Mass Solid Fraction	1	0,89	1	0	0	0	0	0	0	0	0	0	0	0	0	0	0	0	0	0	0
Enthalpy flow rate[GJ/hr]	-3,138	-110,4	-106,3	-151,5	-7,46	-6,46	-6,21	-0,435	-6,33	-6,878	-0,0183	-0,0365	-0,113	0,0085	-0,084	-0,106	-0,561	-0,349	-0,079	-0,4335	-0,107
Mass flow rate [kg/hr]	500,0	8355,0	7466,0	9732,0	957,0	957,0	957	236,9	720,0	484,2	15,4	31,9	89,7	28,7	61,0	119,4	118,7	346,0	45,0	259,3	41,7
Component mass flow rate [kg/hr]																					
Spruce	500	0	0	0	0	0	0	0	0	0	0	0	0	0	0	0	0	0	0	0	0
O_2	0	0	0	0	0	0	0	0	0	0	0	0	0	0	0	0	0	0	0	0	0
CO	0	116	0	1	115	111	0	0	0	0	0	0	0	0	0	0	0	0	0	0	0
CO_2	0	169	0	6	163	162	0	0	0	0	0	0	0	0	0	0	0	0	0	0	0
H_2	0	133	0	Trace	133	182	0	0	0	0	Trace	Trace	Trace	0	0,8	Trace	0	0,8	Trace	Trace	0,8
N_2	0	Trace	0	Trace	Trace	Trace	Trace	Trace	Trace	Trace	0	0	0	0	0	Trace	0	Trace	Trace	Trace	Trace
C_2H_2	0	Trace	0	Trace	Trace	Trace	0	0	0	0	0	0	0	0	0	0	0	0	0	0	0
C_2H_4	0	13	0	2	11	11	0	0	0	0	0	0	0	0	0	0	0	0	0	0	0
C_2H_6	0	4	0	1	4	4	0	0	0	0	0	0	0	0	0	0	0	0	0	0	0
H2O	0	320	0	9639	481	435,6	435,6	13,7	421,9	421,5	0	0	0	0	0	Trace	0	Trace	Trace	Trace	Trace
SAND	0	7450	7450	0	0	0	0	0	0	0	0	0	0	0	0	0	0	0	0	0	0
CHAR	0	16	16	0	0	0	0	0	0	0	0	0	0	0	0	0	0	0	0	0	0
NH_3	0	89	0	81	7	7	0	0	0	0	0	0	0	0	0	0	0	0	0	0	0
CH_4	0	46	0	2	42	42	118,8	Trace	118,8	0,1	0	0	0	Trace	24,4	0	118,7	24,4	Trace	0,8	23,5
C_3H_6	0	0	0	0	0	0	126,1	Trace	126,1	9,6	0	0	0	0	0	23,3	0	23,3	Trace	7,7	15,6
Octene	0	0	0	0	0	0	174,0	171,6	2,4	2,4	0	0	0	0	0	0	0	0	0	0	0
Isohexane	0	0	0	0	0	0	0	0	0	0	0	0	0	0	0	95,4	0	95,4	Trace	93,8	1,4
Isoheptane	0	0	0	0	0	0	0	0	0	0	4,6	0	0	0	0	0	0	4,6	Trace	4,6	Trace
Isooctane	0	0	0	0	0	0	0	0	0	0	0	0	87,3	0	0	0	0	87,3	Trace	86,8	Trace
Pentadecane	0	0	0	0	0	0	0	0	0	0	0	31,7	0	0	0	0	0	31,7	30,6	1,1	Trace
Pentadecene	0	0	0	0	0	0	36,5	36,5	Trace	0	Trace	0	2,3	0	0	0	0	2,7	2,5	Trace	Trace
Hexadecane	0	0	0	0	0	0	0	0	0	0	10,4	0	0	0	0	0	0	10,4	10,4	Trace	Trace
Tricosane	0	0	0	0	0	0	15,1	15,1	Trace	0	0	Trace	0	0	0	0	0	Trace	Trace	Trace	0,0
Benzene	0	0	0	0	0	0	0	0	0	0	0	0	0	Trace	0,5	0	0	0,8	Trace	0,8	Trace
Toluene	0	0	0	0	0	0	0	0	0	0	0	0	0	28,4	35,3	0	0	63,7	Trace	63,3	Trace
Ethanol	0	0	0	0	0	0	50,5	Trace	50,5	50,5	0	0	0	0	0	0	0	0	0	0	0,0

Table 4.16 – Heat exchanger details for HTFT

Heat Exchanger	Type	Base Duty [Gcal/hr]	Hot Inlet Temperature [°C]	Hot Outlet Temperature [°C]	Cold Inlet Temperature [°C]	Cold Outlet Temperature [°C]	Base Area [m^2]	Hot Side Fluid	Cold Side Fluid	Heat Transfer Coefficient [kcal/hr*m^2*K]
GASIFIER_heat_Exchanger	Cooler	0,5047	800	799,5	249	250	5,512	GASIFIER_heat	HP Steam Generation	166,4
HX	Process Exchanger	0,4337	800	278,6	20	100,7	36,44	RAWGAS_To_RAWGASCO	H2O-1_To_H2OOUT	29
Condenser@B2	Cooler	0,1206	140	111,5	30	35	15,97	To Condenser@B2_TO_WATEROIL	Air	85,5
HX-3	Cooler	0,1091	325	100	30	35	12,72	FTPROD_To_FTPRODCO	Air	54,5
Reboiler@B3	Heater	0,1024	125	124	85,7	86,2	15,98	LP Steam	To Reboiler@B3_TO_AQPROD	166,4
COOL	Cooler	0,03885	258,1	80	30	35	7,151	SYNCRUDE_To_TOFRAC	Air	48,9
OLIGOMER_heat_Exchanger	Cooler	0,01889	200	199,5	174	175	4,496	OLIGOMER_heat	MP Steam Generation	166,4
HYDROTR2_heat_Exchanger	Cooler	0,01687	340	339,5	249	250	1,123	HYDROTR2_heat	HP Steam Generation	166,4
HYDROTR_heat_Exchanger	Cooler	0,01253	340	339,5	249	250	0,8342	HYDROTR_heat	HP Steam Generation	166,4
HX-2	Process Exchanger	0,1339	400	260,8	20	218,8	31,45	SYNGAS_To_TOFT	H2O-3_To_H2OVAP-2	23,1
HX-5	Cooler	0,01149	500	300	249	250	2,837	NAPHT_To_TOSEP2	HP Steam Generation	31,7
HX-1	Heater	0,2556	1000	400	80,7	400	98,31	Fired Heat (1000)	MIXTOWGS_To_TOWGS	7,2
ALKYL_heat_Exchanger	Heater	0,005971	125	124	31,9	110	0,8515	LP Steam	ALKYL_heat	166,4
HYDROTRE_heat_Exchanger	Cooler	0,002661	340	339,5	249	250	0,1772	HYDROTRE_heat	HP Steam Generation	166,4
ISOMER2_heat_Exchanger	Cooler	0,00179	340	339,5	249	250	0,1192	ISOMER2_heat	HP Steam Generation	166,4
HYDROC_heat_Exchanger	Heater	0,001996	1000	400	65	340	0,07869	Fired Heat (1000)	HYDROC_heat	61,4
Condenser@PREFLASH	Cooler	0,09022	96,7	15	-25	-24	2,234	To Condenser@PREFLASH_TO_WATER	Refrigerant 1	523,6
Condenser@SEP1	Cooler	0,6893	96,5	89	30	35	119,8	To Condenser@SEP1_TO_LIGHTP	Air	93,8
Condenser@B3	Cooler	0,3611	-11,4	-11,9	-25	-24	26,14	To Condenser@B3_TO_GASES	Refrigerant 1	1072,7
Condenser@SEP2	Cooler	0,1751	32,4	31,9	20	25	114,3	To Condenser@SEP2_TO_BENZENE	Cooling Water	163,3
FLASH_heat_Exchanger	Cooler	0,002861	15	14,5	-25	-24	0,4891	FLASH_heat	Refrigerant 1	149
Reboiler@PREFLASH	Heater	9,68E-06	175	174	149,7	150	0,000499	MP Steam	To Reboiler@PREFLASH_TO_DIESEL	787
Reboiler@SEP1	Heater	0,7529	125	124	107,9	114,2	45,77	LP Steam	To Reboiler@SEP1_TO_HEAVYOIL	1138,2
Reboiler@SEP2	Heater	0,1619	125	124	109,1	109,6	64,42	LP Steam	To Reboiler@SEP2_TO_TOLUENE	166,4
Reboiler@B2	Heater	0,06959	1000	400	267,9	268	2,116	Fired Heat (1000)	To Reboiler@B2_TO_DISTIL	93,9
WGSR_heat_Exchanger	Heater	0,2045	3000	2999	400	400,5	1,282	Very High Temperature	WGSR_heat	61,4
FTREACT_heat_Exchanger	Heater	0,1933	1000	400	260,1	325	9,936	Fired Heat (1000)	FTREACT_heat	61,4
CATREF_heat_Exchanger	Heater	0,02587	1000	400	340	500	2,341	Fired Heat (1000)	CATREF_heat	61,4

5 Process evaluation

In general, the design goal behind each of the three cases above was the same, to produce diesel and gasoline fuels fit to EU specifications while producing excess methane for energy generation inside the plant.

The differences between the three cases were in the FT synthesis product distribution, which led to different amounts of final upgraded fuels produced as well as different upgrading units employed. In this chapter, the differences between the three cases are highlighted as well as translated into economic terms, such as investment and production costs as well as product profits.

5.1 General comparison between different cases

The major differences between the different cases are summed up in this section. They are divided into product profiles and unit operations employed for each case.

In *Figure 5.1* the different product profiles for each case are presented. It was approximated the value of the diesel and gasoline fuel is the same, so that the mass flow is the only differentiating factor between the different cases.

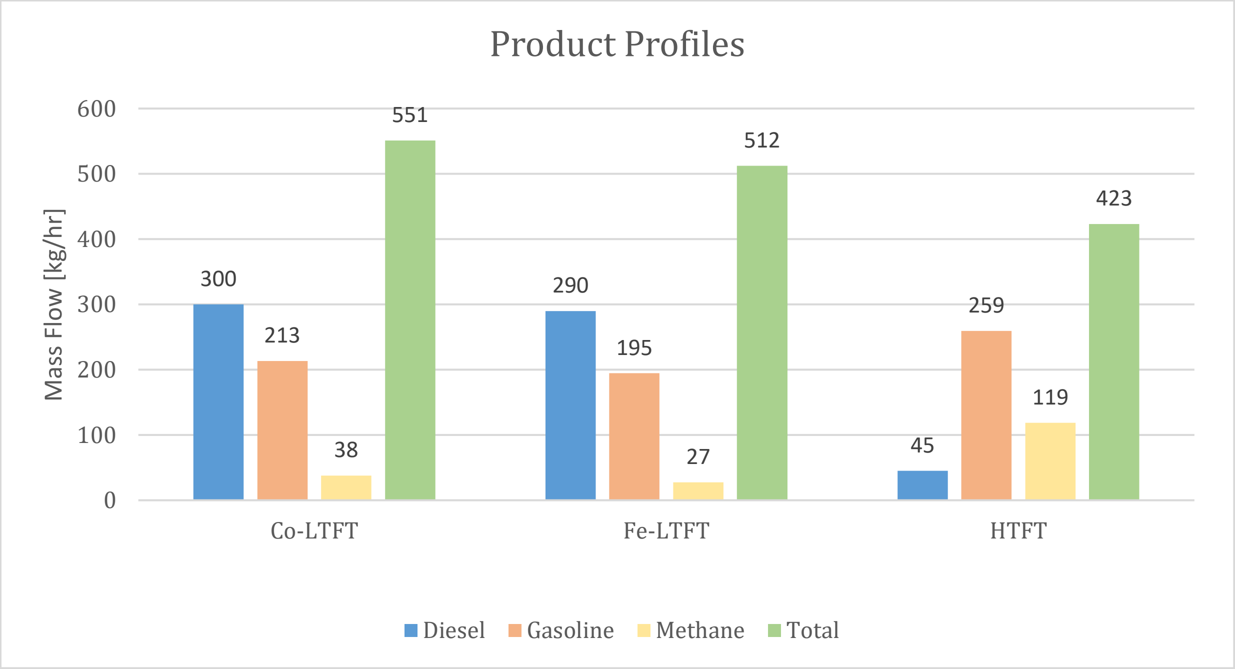

Figure 5.1 – Comparison of the product profiles for the different cases.

The carbon number distribution of FT synthesis operating at different conditions and under different catalysts reflects the final product distribution. Therefore, by reflecting on the results from *Figure 5.1* it can be noted that HTFT synthesis converts to the highest amount of methane and gasoline produced, while LTFT synthesis has the highest diesel production. Moreover, it is seen that Co-based catalyst has an increased production of all the fuels, which is mostly a result of better separation between the aqueous and gaseous products in the three-phase separator.

From *Table 5.1* the comparison between the different unit operations can be seen, For the Co- and Fe-LTFT cases the same amount of unit operations is employed with the only difference being the mass flow of reactants for the units, which is not significantly different. In the HTFT case however, more unit operations are used. However, the size and therefore the cost of most of the units is smaller than in the previous two cases.

Table 5.1 – Overview of the amount of unit operations for each case.

Unit operation	Co-LTFT	Fe-LTFT	HTFT
Reactors	10	10	12
Distillation columns	5	5	7
Separators	2	2	2
Heat Exchangers	7	7	7
Grinder	1	1	1
Dryer	1	1	1
Scrubber	1	1	1
Cyclone	1	1	1

With the general overview accomplished, the economic analysis will be conducted in the next section.

5.2 Economic comparison between cases

In order to compare the different cases the evaluation will be done in different groups divided between the product profits, fixed capital costs and operating costs. For the product profits, each product is expressed in terms of gasoline gallon equivalent (GGE), for precise comparison. For the fixed capital cost, the price and the instalment cost for each unit is obtained through Aspen Process Economic Analyzer. The operating cost involves the maintenance cost, personnel salary, raw materials (together with catalyst and intermediate chemicals) as well as utility cost.

5.2.1 Product fuel profits

In order to express the total profits obtained from a produced final fuel profile for each case the productivity is calculated. Productivity is the yearly profit obtained from selling the produced gasoline and diesel fuels. It is calculated through Equation 1, by summing up the product of the fuel flow rates in gallons per hour at standard conditions and the GGE factor. The summed value is multiplied by the number of hours in an operational year (OY) and the gasoline price (GP). The term GGE describes a factor by which the volumetric flow rate of an alternative fuel in gallons needs to be adjusted in order to obtain the volumetric flow rate of gasoline equivalent in energy.

$$\text{Productivity} = \Sigma\,(\text{fuel flow rate} * \text{GGE}) * \text{OY} * \text{GP} \qquad (1)$$

Where the GGE for diesel is 1,14, for gasoline 1 and methane 0,001024, the operational year consists of 8000 hours and the gasoline price is set to 5,2 $/gal [8], [49].

The profits for each case are presented in *Table 5.2*, below.

Table 5.2 – Table of product fuel profits for each case.

Product fuel profits	Co-LTFT	Fe-LTFT	HTFT
Diesel [$/year]	4.985.353	4.779.628	743.167
Gasoline [$/year]	3.119.830	2.865.836	3.949.228
Methane [$/year]	562.819	461.512	2.059.919
Total [$/year]	8.668.002	8.106.976	6.752.314

From Table 5.2 the highest profits for Co-LTFT case can be observed. Since Co-LTFT also has the highest total product flow rate this was to be expected. It can also be observed that the Fe-LTFT has the second highest total profit and the second highest amount of fuel while HTFT has the lowest production as well as the profits. Additionally, the flow rates for each fuel are not equal in comparison, which can be seen from the GGE factor from Equation 1. The highest value provides the diesel fuel, due to the highest energy content second highest is gasoline and the gaseous methane having the lowest energy density at standard conditions.

5.2.2 Fixed capital cost

For the fixed capital cost, the price for each unit is obtained from approximations given by Aspen Plus. The summed fixed capital costs for each case are presented in *Table 5.3*, below. The prices for individual units for each case are presented in *Table 10.2* in Appendix.

Table 5.3 – Table of fixed capital costs for each case.

Fixed capital cost	Co-LTFT	Fe-LTFT	HTFT
Equipment cost [$]	1.020.300	986.700	1.108.900
Instalment cost [$]	5.007.400	4.924.700	5.872.700
Total cost [$]	6.027.700	5.911.400	6.981.600

The fixed capital cost is the highest for HTFT case due to having the highest amount of unit operations. Even if the flow rates being upgraded in the additional units are smaller than for the LTFT cases, due to increased methane fraction, the amount of material needed to build does units does not change significantly. Therefore, the equipment cost remains highest for HTFT. The small difference between the cost of Co- versus Fe-based LTFT results from the smaller units needed in Fe-LTFT due to low fraction flow rates as seen when comparing the main stream flow rates between those two cases from *Table 4.6* and *Table 4.10*.

5.2.3 Operating cost

The annual maintenance cost for each unit was approximated to be 2% of the equipment cost price.

The personnel salary cost was calculated through Equation 2.

$$\text{Personnel salary} = \text{NP}^{*}\ \text{Annual salary} \qquad (2)$$

Where NP represents the number of personnel working, which was estimated to be 25 people per shift, which is approximately 1 per unit operation, working in 3 shifts per day. The Annual salary was calculated based on a 25 $ hourly wage and a 2000 hour working year per person.

Utility and raw material cost was obtained from Aspen Process Economic Analyzer and is presented for each case in *Table 5.4* below. The prices for each material and utility are presented in *Table 10.3* and *Table 10.4* in Appendix.

Table 5.4 – Table of operating costs for each case.

Operating cost	Co-LTFT	Fe-LTFT	HTFT
Maintenance cost [$/year]	20.406	19.734	22.178
Personnel Salary [$/year]	150.000	150.000	150.000
Raw materials cost [$/year]	2.604.030	2.088.310	2.152.810
Utility cost [$/year]	334.685	306.110	318.904
Total cost [$/year]	3.109.121	2.564.154	2.643.892

From *Table 5.4* it is seen that the biggest operating cost is attributed to Co-LTFT case, which largely amounts to the highest raw material cost. The maintenance cost is highest for the HTFT case since it has the most unit operations involved in the process. The utility cost is highest for Co-LTFT case mostly due to larger flow rates for most units. When compared to Fe-LTFT it is due to the better 3-phase separator, which excludes more aqueous products in Fe-LTFT than Co-LTFT. In turn, this leads to higher flow rates for the upgrading sections of naphtha and gaseous products and larger energy consumption for the unit operation used for treating those streams. The comparison versus HTFT is a bit more complex since the amount of unit operations is greater than in the other two cases. In HTFT the higher unit operation count leads to increased cost of the total utility cost due to having more power consuming units, however since the flow rates for those unit operations are smaller, the units themselves are smaller in size with lesser power consumption. Additionally, the higher methane production from HTFT leads to an even lesser flow rates for the FT fractions to be upgraded.

5.3 Overall case comparison

The overall comparison presented in *Table 5.5* takes into account the economic aspect as well as the effective conversion of raw materials into final products for each case. As the deciding factor for the determination of the most profitable case the overall profit, which is the result of the deduction of the operating cost from the profitability.

The total fuel produced wt. % was calculated using the biomass flow rate as well as other input feeds like oxygen, hydrogen and benzene streams. The steam streams and water streams were cancelled out since most of the water left the system separately to the fuels.

Table 5.5 – Table of overall comparison between each cases.

	Co-LTFT	**Fe-LTFT**	**HTFT**
Total fuel produced wt.%	78	73	59
Diesel wt.%	43	41	6
Gasoline wt. %	30	28	36
Methane wt. %	5	4	17
Fixed capital cost [$]	6.027.700	5.911.400	6.981.600
Operating cost [$/year]	3.109.121	2.564.154	2.643.892
Product profit [$/year]	8.668.002	8.106.976	6.752.314
Overall profit [$/year]	5.558.881	5.542.822	4.108.422

From T*able 5.5* it is evident that Co-LTFT is the most optimal case for conversion of biomass into biofuels. The Co-LTFT case has the highest conversion of biomass into end products, which is the reason it is the most optimal case. The second best case is Fe-LTFT with HTFT being the least optimal. Since Co-LTFT has the highest raw material cost and the highest conversion, which in turn relates to the highest amount of end products the result is not surprising.

It has to be said that the calculations in many ways did not reflect reality partially since a lot of units were not realistically simulated and evaluated. For instance, the units processing solids could not be evaluated by Aspen Process Economic Analyzer so the prices for the equipment cost and energy usage had to be approximated. Moreover, catalyst cost was not included in the simulation as well but simply given as a reference. The electricity usage generated by Aspen was lower than actual as well most probably due to some processing units not being simulated realistically. Additionally many units that were used do not reflect the actual units in terms of separation efficiencies, equipment cost and operating cost. For instance, the Sep units where complete separation was achieved or the RStoic reactors with perfect conversions. Due to these approximations, more end product was generated at a lower cost. The operating cost was also lower than it would be in reality, which in turn led to imprecise results.

On the other hand, the raw material cost or the sellable price of the products might have been overestimated. For instance, fuel price of 5,2 $/gal was assumed. If those conditions could not be met and the oil price would fall below 1,9 $/gal the production would not be profitable under the simulated conditions. Furthermore, if the price of wood would increase similar effects could be observed.

6 Individual unit analysis and design

In this section, closer analysis will be done for the main distillation column SEP-1 and the fractional distillation column PREFLASH for the Co-LTFT case. These units were chosen since they are one of the main units in the process and have the largest impact on the overall equipment and operational cost as well as the overall performance of the processing plant.

6.1 Distillation column

Firstly, sensitivity analysis was done for investigation of more optimal configurations of the current column setup. Secondly, column analysis and detailed design was performed in order to obtain thorough design specifications for the unit.

The original setup for the distillation column was 20 stages with a partial-vapour condenser and a kettle as a reboiler. Calculation type was set to equilibrium, the valid phases were vapour-liquid and the convergence setting was set to standard. The operating specifications were set to 600 kg/hr distillate mass flow rate and a reflux mass ratio of 2. The feed was introduced above the 10th stage while the liquid product stream left the column at the bottom (20th) stage and the vapour at the top (1st) stage. The pressure for the condenser was set to 1 bar, meaning the pressure across the column was constant.

6.1.1 Sensitivity analysis

From the sensitivity analysis for the column setup it was found that the number of stages can be reduced by 4 stages to overall 16 stages and the results for the overall component split remained the same. The stage to which the feed was supplied was simultaneously changed from above the 10th to above the 6th stage.

Better results for the separation could not be obtained regardless any other parameter change. Since all of the feed stream components have already been completely separated in either the LIGHTP or HEAVYOIL stream except for H_2O, which had only 2,27 wt.% of H_2O from the feed stream exiting in the HEAVYOIL stream, this result was not surprising.

Given the decrease in the number of stages the unit equipment cost decreased by over 15%, to 220.300 $.

6.1.2 Column design

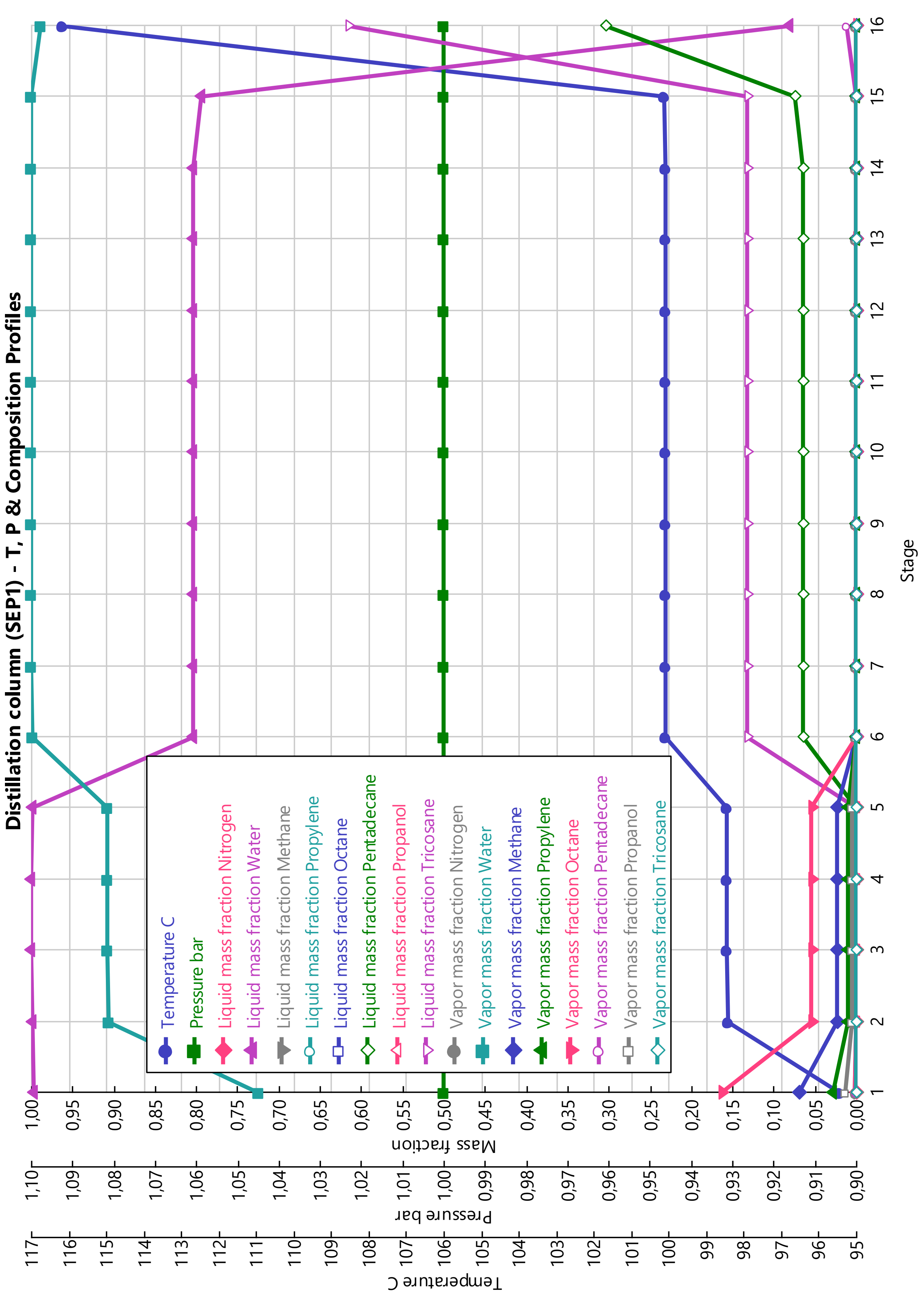

Figure 6.1 - Plot of every component vapour and liquid mass fraction and the pressure and temperature at each stage of the 16-stage distillation column.

From the composition profile plot in *Figure 6.1* the vapour liquid fraction of each component for each stage can be seen. From the look of the figure, it can be said that the distillation column is inefficient, since at most stages the liquid fractions of the components are barely changing therefore little separation is occurring in those stages. To understand why, investigation of the hydraulics plot was performed. In *Figure 6.2* below the hydraulics plot for the second stage is presented. The stages 2-5 essentially have almost identical plots, as can be expected from the results in *Figure 6.1.* Additionally, it is to be expected that when the stage efficiency is improved less stages in the column will be necessary to achieve the desired performance.

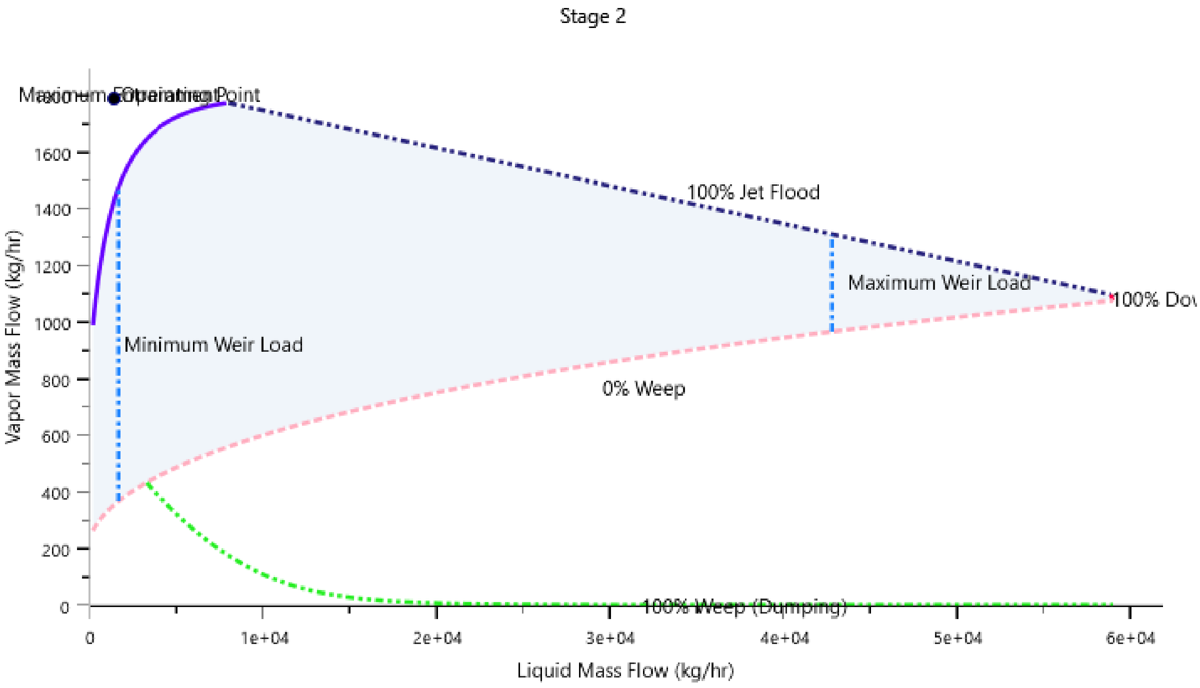

Figure 6.2 – Hydraulics plot for stage 2 of the distillation column

From assessing *Figure 6.2* it can be seen that the vapour mass flow on stage 2-5 is too high. The high flow rate causes jet flooding, meaning that the vapour from the stage below is mixing with the liquid on the stage above. This back mixing causes tray inefficiency as was seen from *Figure 6.1.* From *Figure 6.2* it can also be seen that the weir load is at a minimum, meaning due to little liquid flow on the trays.

In order to decrease the vapour mass flow the tray hole diameter and the column diameter were increased. The liquid mass flow was increased by changing the weir type to a picketed weir. Afterwards the operating point for the stages above the feed was in the optimal zone as presented in *Figure 6.3.*

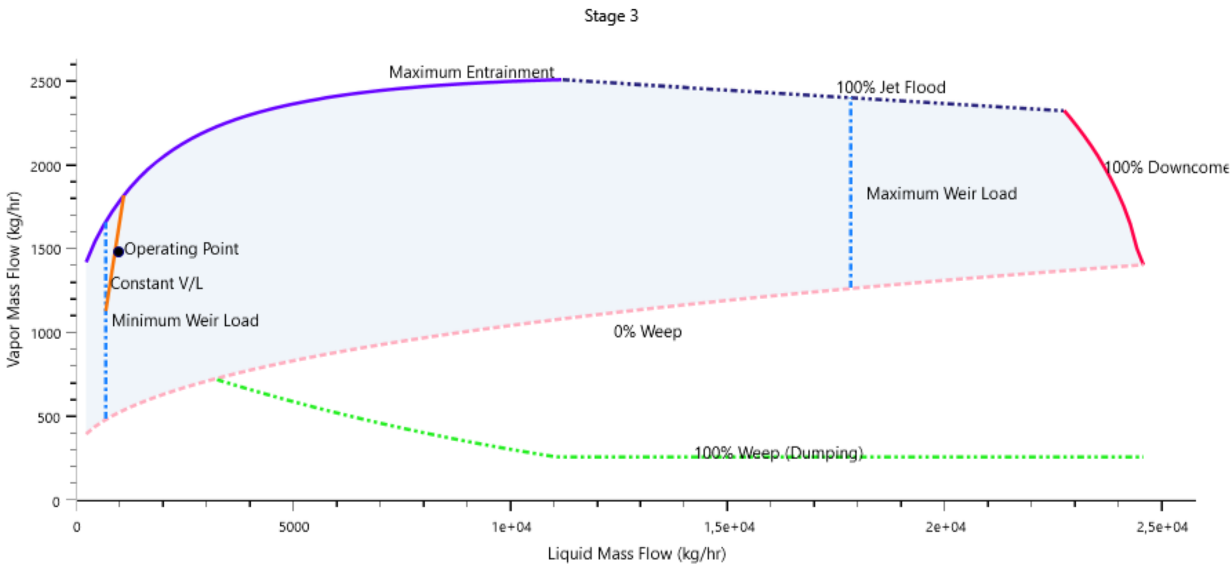

Figure 6.3- Hydraulic plot for stage 2 after design modifications in the column

Afterwards the composition diagram for the components separated in the column was view again but the results remained more or less the same. The reason that component separation barely occurs is probably due to the high water content.

Since there is little separation happening the distillation column stages were further reduced and the obtained results investigated again. The column was reduced to 6 total stages with the most optimal stage of the feed inlet being at the 3rd stage. The obtained differences in the materials streams leaving the column before and after the change are presented in the *Table 6.1* below. The composition profiles for the fractions are presented in *Figure 6.4.*

Table 6.1 – Composition of the distillation column outlet streams for 16 stages, feed – 6th stage (before) and for 6 stages, feed – 3rd stage (after).

Component	**Before**		**After**	
	LIGHTP	**HEAVYOIL**	**LIGHTP**	**HEAVYOIL**
N_2	1	0	1	0
H_2O	0,9773	0,227	0,9773	0,227
CH_4	1	0	1	$1*10^{-13}$
Propylene	1	0	1	$3*10^{-9}$
Octane	1	0	1	0
Pentadecane	0	1	$2*10^{-8}$	1
Propanol	1		1	$1*10^{-7}$
Tricosane	0	1	0	1

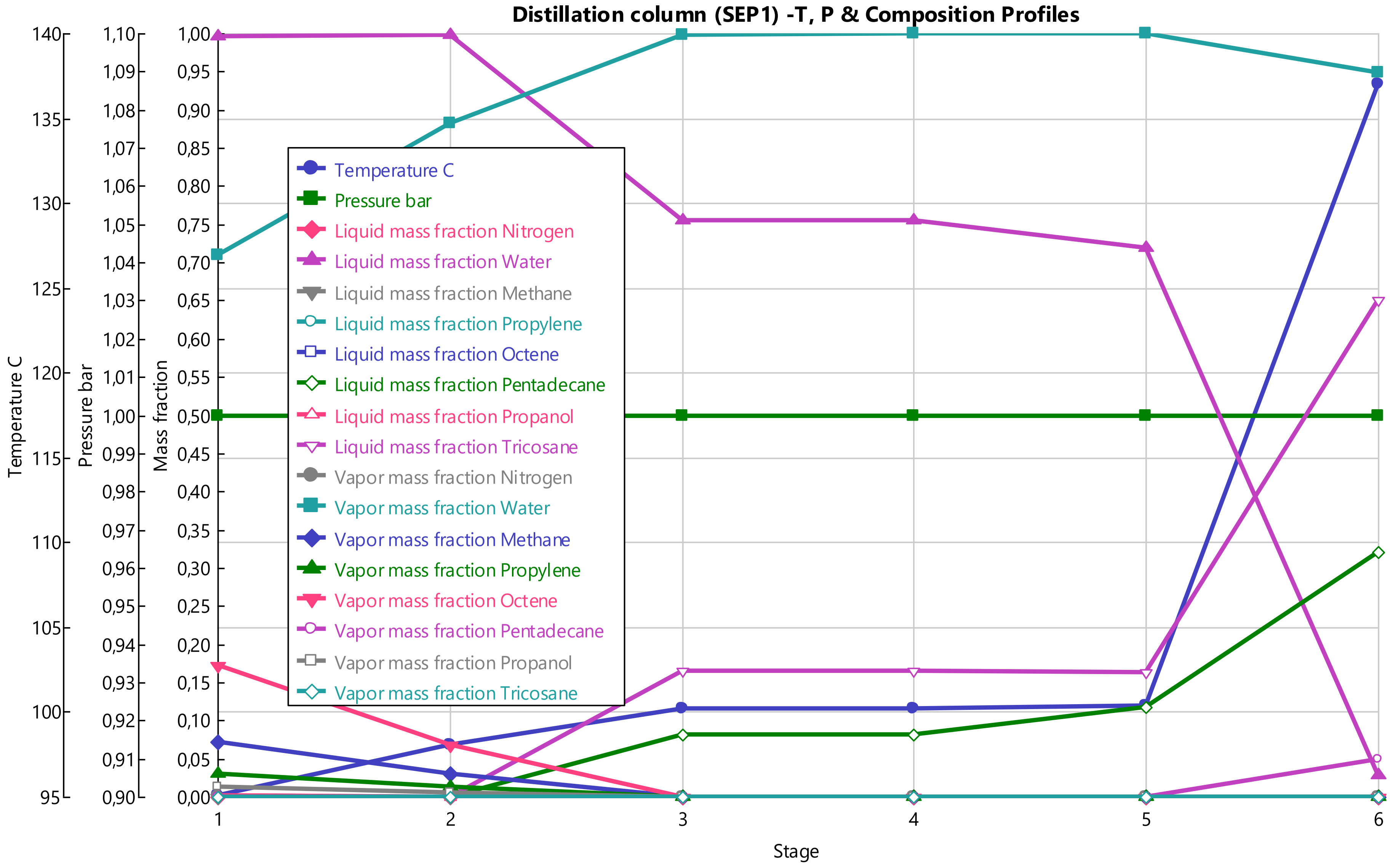

Figure 6.4 - Plot of every component vapour and liquid mass fraction and the pressure and temperature at each stage of the 6-stage distillation column.

From Table 6.1 it can be seen that the difference in the component fraction split before and after the column stage decrease are very small. By decreasing the number of column stages the cost for the column was reduced by over 53% to 100.300$.

6.2 Fractional distillation column

In this section, the optimisation of the fractional distillation column will be described. The composition profiles under the existent column setup are presented in *Figure 6.5* and *Figure 6.6* below.

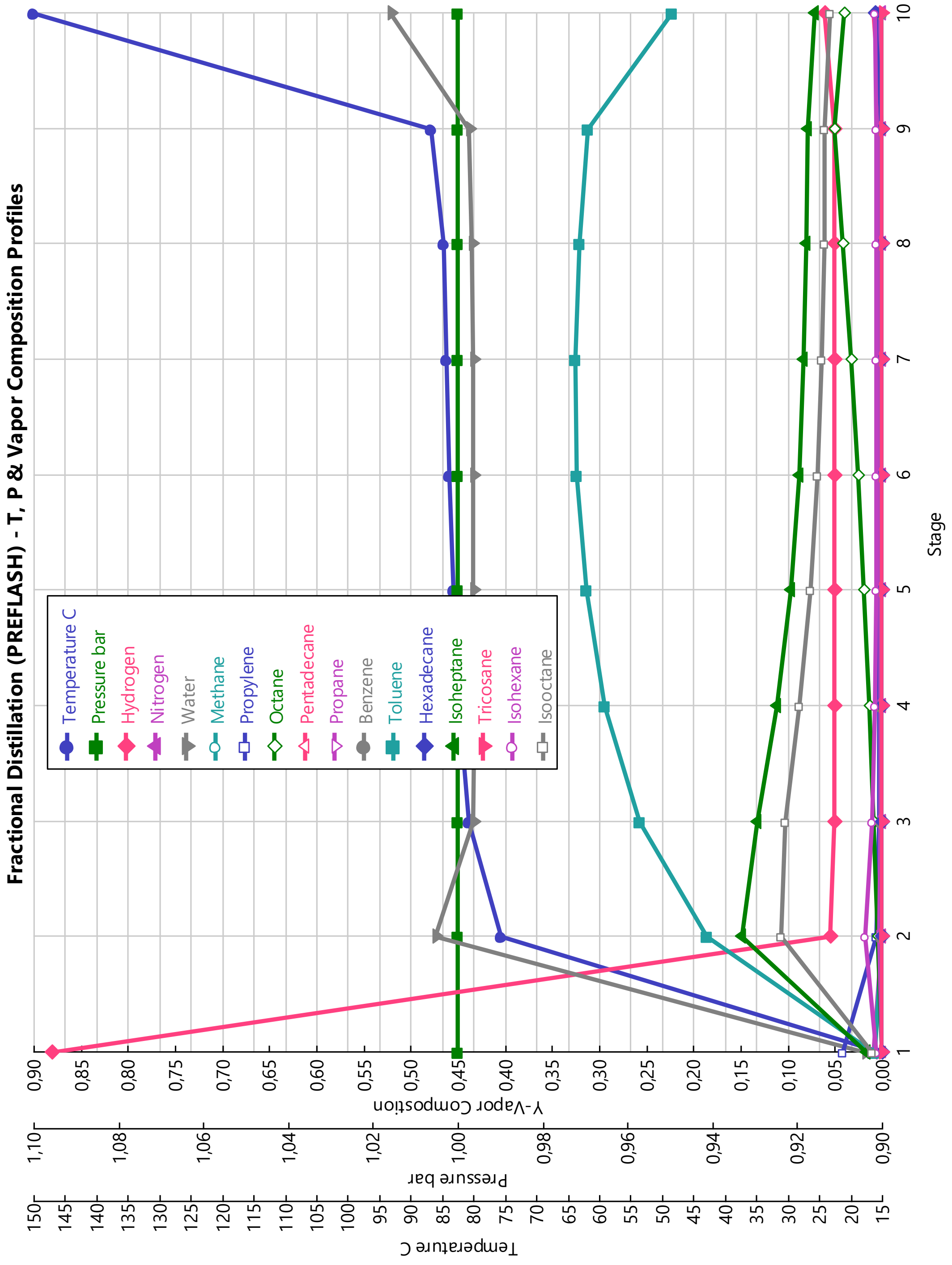

Figure 6.5 - Plot of vapour composition profiles, the pressure and temperature at each stage for the fractional distillation column.

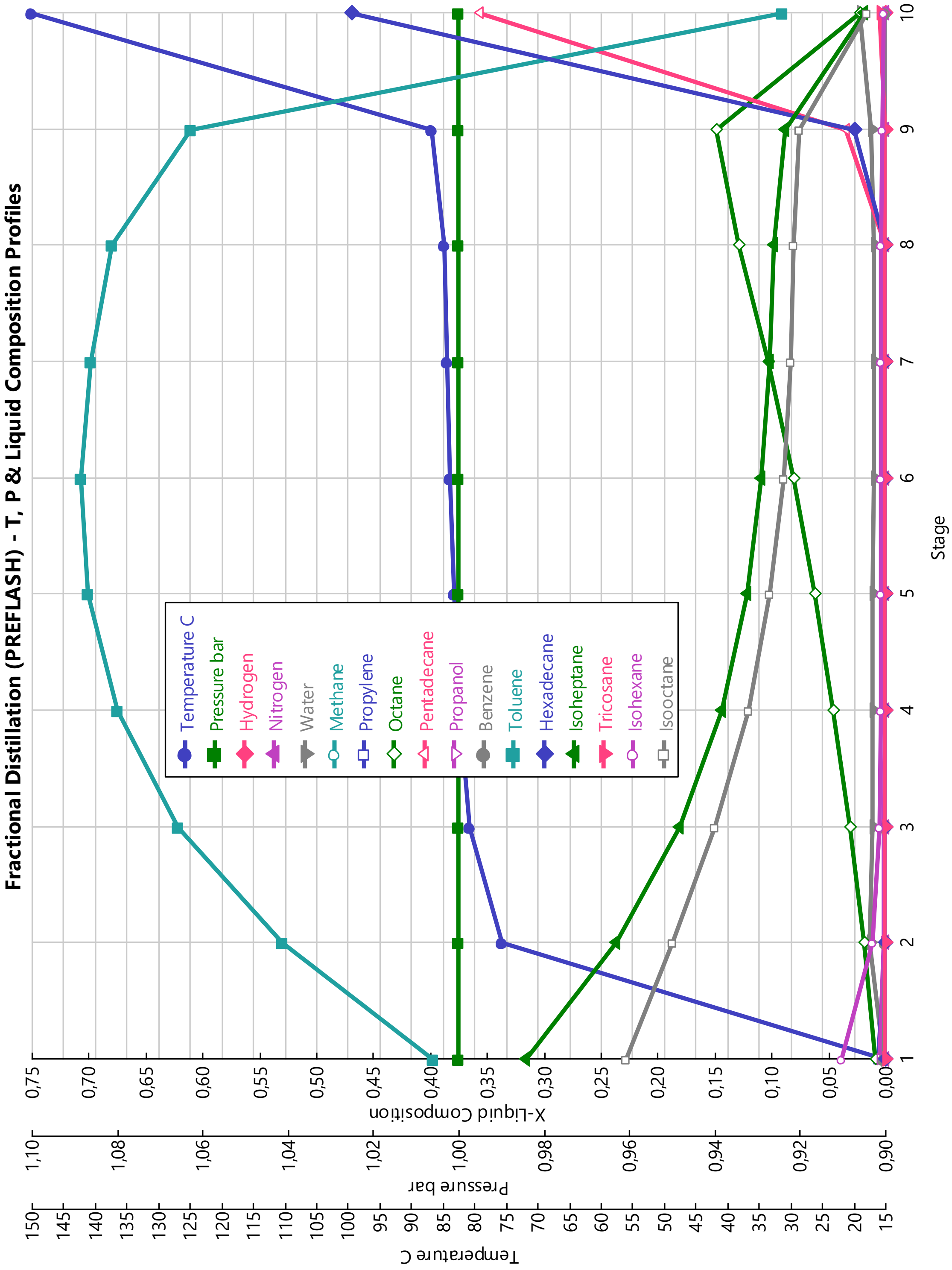

Figure 6.6 - Plot of vapour composition profiles, the pressure and temperature at each stage for the fractional distillation column.

The focus of fractional distillation optimization was to obtain a better separation of the naphtha ranged products from the gaseous stream. By doing so, the separator, which was installed after the fractionation column, could be excluded from the process setup.

The fractionation column's original setup was 10 number of stages with condenser having partial-vapour-liquid phases. Reboiler setting was set to None-Bottom feed and the valid phases were set to Vapor-Liquid-FreeWater. The operating specifications were set to 300 kg/hr for bottoms mass flow rate. The steam and feed stream were introduced in the bottom (10th) stage, while the free water, vapour and light liquids stream left from the top on stage 1. The condenser pressure was set to 1 bar while its temperature was 15°C. The furnace pressure and temperature were 1 bar and 150 °C.

Since most of the components of interest have a high fraction in the liquid phase as seen from *Figure 6.6* the taken approach was to increase the amount of the liquid exiting the 1st column.

The task was accomplished by decreasing the condenser temperature by 10 °C and increasing the condenser pressure to 2 bars. By doing so, the amount of naphtha ranged products in the gaseous stream decreased by an average of 75%. The separator could therefore be excluded from the process and approximately 16.000 $ would be saved for the equipment cost. The overall operating cost would be lower due to the high pressure demand of the separator which operated at 30 bars, while it would be compensated slightly by the higher operating cost from the new setup of the fractionation column.

7 Conclusions

In this thesis the design and simulation of biomass conversion into biofuels has been done. Aspen Plus was used in order to simulate a BtL process through biomass gasification and Fischer-Tropsch synthesis. Several cases were simulated in Aspen. The difference between each case lied in the conditions of FT synthesis. High temperature FT synthesis and low temperature FT synthesis with the use of Fe-based and Co-based catalyst were performed. Afterwards, the evaluation of each case was done and the cases were compared to one another.

Several factors like the equipment and its instalment cost, raw material, utility, labour and maintenance cost were included in the evaluation. The costs were deducted from the approximated fuel profits in order to obtain the net profit from which the final optimal case was obtained. From the comparison, it was found that, the Co-LTFT case lead to the highest amount of produced fuels and had the highest mass conversion rate from the three cases. The highest conversion largely amount due to the most efficient separation processes from all streams.

Overall, the evaluation results were not as expected since overall profit loss was assumed to be the result. The result was likely due to unrealistic simulation approximations like high reactant conversion rates, large separator efficiencies and non-optimal modelling of some included units. On the other hand, the result depends on the prices of the feed and the produced fuel which always change in the market therefore, influencing the final result.

Finally the optimisation of two main unit operations, the main distillation column and the fractionation column, was performed. The distillation column performance remained more or less the same while the number of stages were severely reduced from 20 to 6 stages, leading to significantly lower fixed capital costs for the unit. For the fractionation column better separation between the gaseous and liquid top stage products was achieved which meant no post separation of the gaseous stream was needed and the two phase separator after fractionation could be removed from the process, leading to lower fixed capital as well as operational costs.

8 List of abbreviations

BtL – Biomass to liquid

CFB – Circulating fluidized bed

ECN – Energy research Centre of Netherlands

ESP – Electrostatic precipitator

FT – Fischer-Tropsch

GGE – Gasoline gallon equivalent

GP – Gasoline price

HTFT – High temperature Fischer-Tropsch

LPG – Liquid petroleum gas

LTFT – Low temperature Fischer-Tropsch

OY – Operational year

SAR – Sasol advanced reactor

SNG – Synthetic natural gas

SPA – Solid phosphoric acid

TFBR – Tubular fixed-bed reactor

WGSR – Water gas shift reaction

9 References

[1] "World Energy Consumption Statistics." [Online]. Available: https://yearbook.enerdata.net/total-energy/world-consumption-statistics.html. [Accessed: 27-May-2020].

[2] "Transport Energy Economics." [Online]. Available: https://www.bp.com/en/global/corporate/energy-economics/energy-outlook/demand-by-sector/transport.html. [Accessed: 27-May-2020].

[3] M. Guo, W. Song, and J. Buhain, "Bioenergy and biofuels: History, status, and perspective," *Renew. Sustain. Energy Rev.*, vol. 42, pp. 712–725, 2015, doi: 10.1016/j.rser.2014.10.013.

[4] "The outlook for biogas and biomethane to 2040," 2020. [Online]. Available: https://www.iea.org/reports/outlook-for-biogas-and-biomethane-prospects-for-organic-growth/the-outlook-for-biogas-and-biomethane-to-2040. [Accessed: 27-May-2020].

[5] V. Menon and M. Rao, "Trends in bioconversion of lignocellulose: Biofuels, platform chemicals & biorefinery concept," *Progress in Energy and Combustion Science*, vol. 38, no. 4. Elsevier Ltd, pp. 522–550, 2012, doi: 10.1016/j.pecs.2012.02.002.

[6] M. A. Martin, "First generation biofuels compete," *New Biotechnology*, vol. 27, no. 5. pp. 596–608, 2010, doi: 10.1016/j.nbt.2010.06.010.

[7] E. W. Qian, "Pretreatment and Saccharification of Lignocellulosic Biomass," in *Research Approaches to Sustainable Biomass Systems*, Elsevier Inc., 2013, pp. 181–204.

[8] P. Gonzalez Ibarra, "Synthesis, Simulation and Optimization of Advanced Processes for Biomass-to-liquid Transportation Fuels Production," Ph.D. dissertation, Dept. Chem. Eng., University of Southern Denmark, 2019.

[9] P. T. Martone *et al.*, "Discovery of Lignin in Seaweed Reveals Convergent Evolution of Cell-Wall Architecture," *Curr. Biol.*, vol. 19, no. 2, pp. 169–175, Jan. 2009, doi: 10.1016/j.cub.2008.12.031.

[10] J. Zakzeski, P. C. A. Bruijnincx, A. L. Jongerius, and B. M. Weckhuysen, "The Catalytic

Valorization of Lignin for the Production of Renewable Chemicals," *Chem. Rev.*, vol. 110, no. 6, pp. 3552–3599, Jun. 2010, doi: 10.1021/cr900354u.

[11] A. Nuamah, A. Malmgren, G. Riley, and E. Lester, "Biomass co-firing," in *Comprehensive Renewable Energy*, vol. 5, Elsevier Ltd, 2012, pp. 55–73.

[12] P. Ibarra-Gonzalez and B. G. Rong, "A review of the current state of biofuels production from lignocellulosic biomass using thermochemical conversion routes," *Chinese J. Chem. Eng.*, vol. 27, no. 7, pp. 1523–1535, 2019, doi: 10.1016/j.cjche.2018.09.018.

[13] A. Pandey, C. Larroche, C. G. Dussap, E. Gnansounou, S. K. Khanal, and S. Ricke, *Biofuels: Alternative feedstocks and conversion processes for the production of liquid and gaseous biofuels*. Elsevier, 2019.

[14] "Lecture 2 – Characterisation of Fuels." [Online]. Available: https://nptel.ac.in/content/storage2/courses/113104058/mme_pdf/Lecture2.pdf. [Accessed: 22-Mar-2020].

[15] A. Kraiphanont, B. Nunes, and D. Bennett, "The main criteria of biomass selection for energy generation in Brazil," *IAMOT 2016 - 25th Int. Assoc. Manag. Technol. Conf. Orlando, FL, USA, 15-19 May*, 2016.

[16] N. Forsell *et al.*, "Follow-up study on impacts on resource efficiency of future EU demand for bioenergy (ReceBio follow-up). Final report. Project: ENV.F.1/ETU/2015/Ares(2015)5117224," Luxembourg: Publications Office of the European Union, 2016.

[17] S. Searle and C. Malins, "Availability of cellulosic residues and wastes in the EU," *Int. Counc. Clean Transp. Washington, USA, 1-7 Oct.*, 2013.

[18] I. Hannula and E. Kurkela, "A parametric modelling study for pressurised steam/O 2-blown fluidised-bed gasification of wood with catalytic reforming," *Biomass and Bioenergy*, vol. 38, pp. 58–67, 2012, doi: 10.1016/j.biombioe.2011.02.045.

[19] P. Basu, "Gasification Theory and Modeling of Gasifiers," in *Biomass Gasification and Pyrolysis*, Burlington: Elsevier, 2010, pp. 117–165.

[20] P. Basu, "Design of Biomass Gasifiers," in *Biomass Gasification and Pyrolysis*,

Burlington: Elsevier, 2010, pp. 167–228.

[21] H. Boerrigter, H. P. Calis, D. J. Slor, and H. Bodenstaff, “Gas Cleaning for Integrated Biomass Gasification and Fischer-Tropsch Systems,” *Energy Res. Cent. Netherlands (ECN), Petten, Rep. ECN-C--04-056, December*, 2004, doi: ECN-RX--04-041.

[22] P. Ibarra-Gonzalez and B. G. Rong, “A review of separation technologies in biomass-to-liquid transportation fuels production process,” *Renew. Energy*, p. 26, 2019.

[23] M. Balas *et al.*, “Experience with Hot Gas Moving Bed Filter in Fluidised Bed Biomass Gasification,” *3rd Int. Conf. Biomass Energy, Kyiv, Ukr. 18 - 20 Sept.*, 2016.

[24] H. Boerrigter and R. Rauch, “Syngas production and utilisation,” in *Handbook Biomass Gasification*, H. Knoef, Ed. Biomass Technology Group (BTG), The Netherlands, 2005, pp. 211–230.

[25] H. Hofbauer and K. Ripfel-Nitsche, “Gas Cleaning for Synthesis Applications,” *Inst. Chem. Eng. Univ. Technol. Vienna, Intell. Energy - Eur. Deliv. 2E-3, Oct.*, 2007.

[26] F. Lettner, H. Timmerer, and P. Haselbacher, “Biomass gasification – State of the art description,” *Inst. Therm. Eng. Univ. Technol. Graz, Intell. Energy - Eur. Deliv. 8, December*, 2007.

[27] “Cyclone Separator Design, Components and How it Works.” [Online]. Available: https://savree.com/en/product/cyclone-separator-working-principle-dust-separator/. [Accessed: 14-Apr-2020].

[28] B. Liu, W. Zhou, P. Tan, X. Shan, and Q. Yang, “Dynamic granular bed and its gas–solid separation process,” *Powder Technol.*, vol. 301, pp. 387–395, 2016, doi: 10.1016/j.powtec.2016.06.036.

[29] S. Heidenreich, “Hot gas filtration - A review,” *Fuel*, vol. 104, pp. 83–94, 2013, doi: 10.1016/j.fuel.2012.07.059.

[30] “Electrostatic Precipitator - Working Principle, Types & Applications.” [Online]. Available: https://www.watelectrical.com/electrostatic-precipitator-working-types-applications/. [Accessed: 15-Apr-2020].

[31] G. Y. Chen, C. Liu, W. C. Ma, B. B. Yan, and N. Ji, “Catalytic Cracking of Tar from Biomass Gasification over a HZSM-5-Supported Ni-MgO Catalyst,” *Energy and Fuels*,

vol. 29, no. 12, pp. 7969–7974, 2015, doi: 10.1021/acs.energyfuels.5b00830.

[32] A. van der Drift, B. Coda, H. Boerrigter, K. Hemmes, and M. K. Cieplik, “Entrained flow gasification of biomass,” *Energy Res. Cent. Netherlands (ECN), Petten, Rep. ECN-C--04-039, April*, 2004, doi: 10.1016/j.fuel.2011.10.063.

[33] A. van der Drift, R. van Ree, H. Boerrigter, and K. Hemmes, “Bio-Syngas : Key Intermediate for Large Scale Production of Green Fuels and Chemicals,” *2nd World Conf. Technol. Exhib. Biomass Energy, Ind. Clim. Prot. Rome, Italy, 10-14, May*, 2004.

[34] “What Is A Wet Scrubber?” [Online]. Available: https://www.cecoenviro.com/blog/what-is-a-wet-scrubber. [Accessed: 15-Apr-2020].

[35] T. Phuphuakrat, T. Namioka, and K. Yoshikawa, “Absorptive removal of biomass tar using water and oily materials,” *Bioresour. Technol.*, vol. 102, no. 2, pp. 543–549, 2011, doi: 10.1016/j.biortech.2010.07.073.

[36] W. Zhang *et al.*, “Gas cleaning strategies for biomass gasification product gas,” *Int. J. Low-Carbon Technol.*, vol. 7, no. 2, pp. 69–74, 2012, doi: 10.1093/ijlct/ctr046.

[37] W. Torres, S. S. Pansare, and J. G. Goodwin, “Hot gas removal of tars, ammonia, and hydrogen sulfide from biomass gasification gas,” *Catal. Rev. - Sci. Eng.*, vol. 49, no. 4, pp. 407–456, 2007, doi: 10.1080/01614940701375134.

[38] S. V. Vassilev, D. Baxter, L. K. Andersen, and C. G. Vassileva, “An overview of the chemical composition of biomass,” *Fuel*, vol. 89, no. 5, pp. 913–933, 2010, doi: 10.1016/j.fuel.2009.10.022.

[39] D. Chiche, C. Diverchy, A. Lucquin, F. Porcheron, and F. Defoort, “Synthesis Gas Purification,” *Oil Gas Sci. Technol. - Rev. d’IFP Energies Nouv. Inst. Français du Pétrole*, vol. 68, no. 4, pp. 707–723, 2013, doi: 10.2516/ogst/2013175.

[40] J. Oakey, Ed., *Fuel Flexible Energy Generation : Solid, Liquid and Gaseous Fuels*. Elsevier Science & Technology, 2015.

[41] J. Speight, K. Solange, and B. Mustafa, *The Biofuels Handbook*. Cambridge: The Royal Society of Chemistry, 2011.

[42] H. Deldari, “Suitable catalysts for hydroisomerization of long-chain normal

paraffins," *Appl. Catal. A Gen.*, vol. 293, no. 1–2, pp. 1–10, Sep. 2005, doi: 10.1016/j.apcata.2005.07.008.

[43] "Horizontal Three Phase Separator Part 1 | Oil and Gas Separator." [Online]. Available: http://www.oilngasseparator.info/oil-handling-surfacefacilities/horizontal-three-phase-separator-part-1.html. [Accessed: 29-Apr-2020].

[44] "Basic Equipment and Operation of Distillation Columns." [Online]. Available: https://www.rccostello.com/distil/distileqp.htm. [Accessed: 29-Apr-2020].

[45] "Fractional Distillation - How Oil Refining Works | HowStuffWorks." [Online]. Available: https://science.howstuffworks.com/environmental/energy/oil-refining4.htm. [Accessed: 29-Apr-2020].

[46] "Crude Oil Distillation - Fractional distillation - Wikipedia." [Online]. Available: https://en.wikipedia.org/wiki/Fractional_distillation#/media/File:Crude_Oil_Distillation.png. [Accessed: 29-Apr-2020].

[47] "EU: Fuels: Diesel and Gasoline | Transport Policy." [Online]. Available: https://www.transportpolicy.net/standard/eu-fuels-diesel-and-gasoline/. [Accessed: 08-May-2020].

[48] A. De Klerk, "Fischer-Tropsch fuels refinery design," *Energy Environ. Sci.*, vol. 4, no. 4, pp. 1177–1205, 2011, doi: 10.1039/c0ee00692k.

[49] C. Gable and S. Gable, "Fuel Energy Comparisons: Gasoline Gallon Equivalents." [Online]. Available: http://alternativefuels.about.com/od/resources/a/gge.htm. [Accessed: 25-May-2020].

10 Appendix

Table 10.1 - Generic syncrude composition on a mass basis [48].

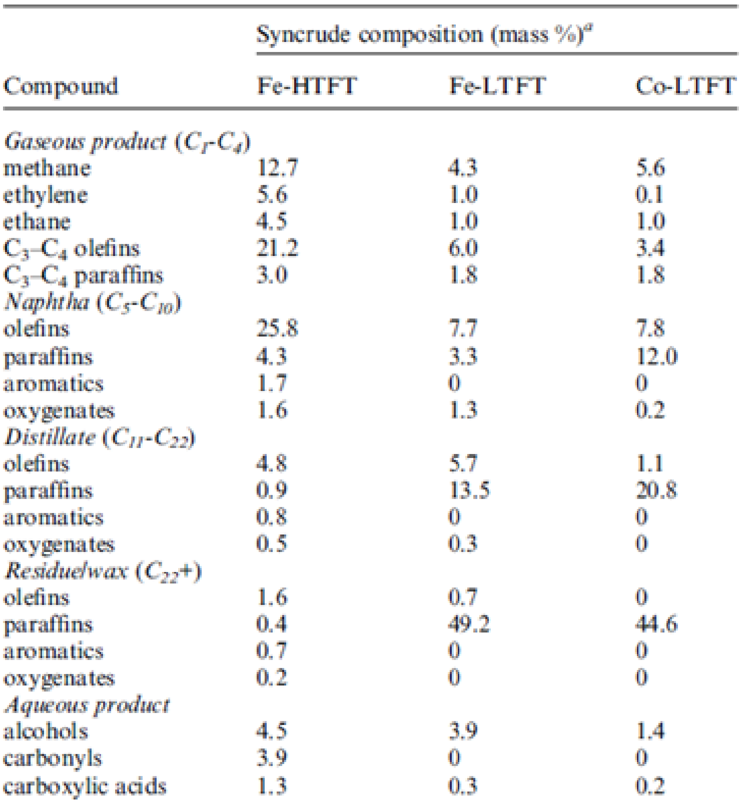

	Syncrude composition (mass %)[a]		
Compound	Fe-HTFT	Fe-LTFT	Co-LTFT
Gaseous product (C_1-C_4)			
methane	12.7	4.3	5.6
ethylene	5.6	1.0	0.1
ethane	4.5	1.0	1.0
C_3–C_4 olefins	21.2	6.0	3.4
C_3–C_4 paraffins	3.0	1.8	1.8
Naphtha (C_5-C_{10})			
olefins	25.8	7.7	7.8
paraffins	4.3	3.3	12.0
aromatics	1.7	0	0
oxygenates	1.6	1.3	0.2
Distillate (C_{11}-C_{22})			
olefins	4.8	5.7	1.1
paraffins	0.9	13.5	20.8
aromatics	0.8	0	0
oxygenates	0.5	0.3	0
Residue/wax (C_{22}+)			
olefins	1.6	0.7	0
paraffins	0.4	49.2	44.6
aromatics	0.7	0	0
oxygenates	0.2	0	0
Aqueous product			
alcohols	4.5	3.9	1.4
carbonyls	3.9	0	0
carboxylic acids	1.3	0.3	0.2

Table 10.2 - Table of unit operation equipment and instalment costs obtained from Aspen Process Economic Analyzer.

Co-LTFT			Fe-LTFT			HTFT		
Unit name	Equipment Cost	Installed Cost	Unit name	Equipment Cost	Installed Cost	Unit name	Equipment Cost	Installed Cost
GRINDER	$ 40.000	$ 195.200	GRINDER	$ 40.000	$ 195.200	GRINDER	$ 40.000	$ 195.200
DRYER	$ 14.300	$ 22.700	DRYER	$ 14.300	$ 22.700	DRYER	$ 14.300	$ 22.700
GASIFIER	$ 61.000	$ 230.500	GASIFIER	$ 61.000	$ 230.500	GASIFIER	$ 61.000	$ 230.500
CYCLON	$ 8.700	$ 25.700	CYCLON	$ 8.700	$ 25.700	CYCLON	$ 8.700	$ 25.700
SCRUBBER	$ 53.200	$ 194.000	SCRUBBER	$ 53.200	$ 194.000	SCRUBBER	$ 53.200	$ 194.000
WGSR	$ 60.300	$ 220.500	WGSR	$ 60.300	$ 220.500	WGSR	$ 60.300	$ 220.500
FTREACT	$ 54.000	$ 230.800	FTREACT	$ 54.000	$ 230.800	FTREACT	$ 54.000	$ 230.800
SEP1	$ 259.500	$ 772.500	SEP1	$ 243.300	$ 750.500	SEP1	$ 218.800	$ 696.500
SEP2	$ 18.500	$ 141.300	SEP2	$ 26.200	$ 156.700	SEP2	$ 25.500	$ 193.400
SEP3	$ 15.300	$ 97.000	SEP3	$ 15.300	$ 97.000	SEP3	$ 15.800	$ 125.500
B3	$ 15.300	$ 97.000	B3	$ 15.300	$ 97.000	B3	$ 18.700	$ 142.800
B4	$ 35.100	$ 236.900	B4	$ 31.800	$ 232.600	B4	$ 15.800	$ 118.300
HYDROC	$ 33.700	$ 233.800	HYDROC	$ 33.300	$ 233.400	HYDROC	$ 21.900	$ 208.500
HYDROTR2	$ 21.400	$ 219.400	HYDROTR2	$ 21.700	$ 219.900	HYDROTR2	$ 28.800	$ 227.900
ISOMER	$ 33.300	$ 221.200	ISOMER	$ 33.300	$ 221.200	ISOMER	$ 21.900	$ 208.500
ISOMER2	$ 21.900	$ 208.500	ISOMER2	$ 21.900	$ 208.500	ISOMER2	$ 24.500	$ 230.500
OLIGOMER	$ 21.700	$ 208.300	OLIGOMER	$ 21.700	$ 153.000	OLIGOMER	$ 21.400	$ 152.600
CATREF	$ 24.200	$ 197.400	CATREF	$ 24.200	$ 197.400	CATREF	$ 42.000	$ 283.100
ALKYL	$ 22.000	$ 151.000	ALKYL	$ 22.000	$ 151.000	ALKYL	$ 18.400	$ 133.200
PREFLASH	$ 116.900	$ 501.200	PREFLASH	$ 95.100	$ 460.100	PREFLASH	$ 88.900	$ 432.600
FLASHY	$ 15.600	$ 85.900	FLASH	$ 15.800	$ 110.500	FLASH	$ 15.800	$ 110.500
HX	$ 13.200	$ 85.600	HX	$ 13.200	$ 85.600	HX	$ 13.200	$ 85.600
HX-1	$ 10.100	$ 107.400	HX-1	$ 10.100	$ 107.400	HX-1	$ 10.100	$ 107.400
HX-2	$ 8.300	$ 73.700	HX-2	$ 8.300	$ 73.700	HX-2	$ 8.300	$ 73.700
HX-3	$ 8.500	$ 60.100	HX-3	$ 8.500	$ 60.100	HX-3	$ 8.500	$ 84.200
HX-4	$ 17.100	$ 87.400	HX-4	$ 17.000	$ 87.300	HX-5	$ 9.400	$ 56.600
HX-5	$ 9.400	$ 56.600	HX-5	$ 9.400	$ 56.600	COOL	$ 7.800	$ 46.400
COOL	$ 7.800	$ 45.800	COOL	$ 7.800	$ 45.800	B2	$ 111.200	$ 488.000
Total sum	$ 1.020.300	$ 5.007.400	Total sum	$ 986.700	$ 4.924.700	B5	$ 15.800	$ 118.300
						HYDROTR	$ 33.000	$ 220.700
						HYDROTRE	$ 21.900	$ 208.500
						Total sum	$ 1.108.900	$ 5.872.700

Table 10.3 - Table of prices for raw materials [8].

Component	Price [$/kg]
Raw materials and intermediate chemicals	
Spruce	0,12
H_2	7,00
Sand	0,01
O_2	0,50
Benzene	1,05
Catalysts	
Cu-Zn-AlO_2 (WGSR)	1,98
Fe_2O_3/Cr_2O_3 (LTFT/HTFT)	2,00
Co-ZrO_2 (LTFT)	2,31
HZSM-5 (Catalytic reforming)	1,10
SPA (Alkylation/ Oligomerization)	1,00
NiMo/Al_2O_3 (Hydrotreating/Hydrocracking/Isomerization)	0,38

Table 10.4 – Table of prices for utilities.

Utilities	**Price [$/hr]**
Electricity [kw]	5,01944
Cooling water [per 1000 m^3/hr]	0,7569797
Steam [100 psi, 1 kg/hr]	0,0615683